ABSTRACT

Title of dissertation: ENTROPY STABLE APPROXIMATIONS
                          OF NONLINEAR CONSERVATION LAWS
                          AND RELATED FLUID EQUATIONS

                          Weigang Zhong
                          Doctor of Philosophy, 2007

Dissertation directed by: Professor Eitan Tadmor
                          Department of Mathematics

We present a systematic study of novel entropy stable approximations for a variety of nonlinear conservation laws, from the scalar Burgers equation to one dimensional Navier-Stokes and two dimensional shallow water equations.

To this end, we construct a new family of second-order entropy stable difference schemes which retain the *precise* entropy decay of the original PDEs. Here we employ the entropy conservative differences of [Tad03] to discretize the convective fluxes, and center differences to discretize the dissipative fluxes. This resulting family of difference schemes are free of artificial numerical viscosity in the sense that their entropy dissipation is then dictated solely by physical dissipation terms. The numerical results of 1D compressible Navier-Stokes equations equations provide us a remarkable evidence for the different roles of viscosity and heat conduction in forming sharp monotone profiles in the immediate neighborhoods of shocks and contacts. Further implementation in 2D shallow water equations is realized dimension by dimension.

ENTROPY STABLE APPROXIMATIONS OF NONLINEAR
CONSERVATIONS LAWS
AND RELATED FLUID EQUATIONS

by

Weigang Zhong

Dissertation submitted to the Faculty of the Graduate School of the
University of Maryland, College Park in partial fulfillment
of the requirements for the degree of
Doctor of Philosophy
2007

Advisory Committee:
Professor Eitan Tadmor, Chair/Advisor
Professor Jian-Guo Liu
Professor Athanasios Tzavaras
Professor Howard Elman
Professor James Baeder

Dedication

To my parents, Chongdong Zhong and Jixin Zhang,

for their everlasting love.

Acknowledgements

I owe tremendous gratitude to many people for making this dissertation possible. I am sure that this enumeration is far from being complete for people I owe thanks to, and for any inadvertent missing I apologize in advance.

First of all, I want to extend my greatest gratitude to a respectful professor, an extraordinary scholar, a knowledgeable advisor, and a lovable friend - Dr. Eitan Tadmor, for his kindness, encouragement, and continuous help that steer me through my Ph.D. studies. In the last three years, I have witnessed and been deeply touched by his passion for mathematics, his expertise in research, his diligence, as well as his sense of humor. I will be forever indebted to him for giving me the opportunity to do research in this interesting area and for taking the time to train me to think critically, to work efficiently, and to communicate effectively.

I also want to thank Dr. Jian-Guo Liu, Dr. Howard Elman, Dr. Athanasios Tzavaras, and Dr. James Baeder for agreeing to serve on my dissertation committee. Especially, I want to extend my gratitude to Dr. Jian-Guo Liu for giving me his advice on many aspects of research and school life, even before I came to Maryland. The numerous conversations we had always gave me new perceptions and ideas. I greatly appreciate the fruitful discussions I had with many other intelligent researchers in the Research Interaction Teams held by Dr. Jian-Guo Liu and Dr. Howard Elman. My thanks also go to Dr. Athanasios Tzavaras for his thought-provoking discussion about my research, and Dr. James Baeder for attending my defense in the busiest time of the year.

I would like to make a grateful acknowledgement to Ms. Agi Alipio and Ms. Alverda McCoy for their generous help in solving the problems in my curricular registration and more importantly, job applications.

I am deeply grateful to my great friends at the University of Maryland with whom I had pleasure to work. They helped me a lot from time to time on either research or everyday life. I would like to extend my special thanks to Ning Jiang who gave me constant care and attention even after he left Maryland. I also want to thank Weiran Sun, Dongming Wei and Bin Cheng for their inspirational discussions. Thanks to Bob Shuttleworth, Aaron Lott, and Purnendu Chakraborty for being such good friends and great fellows in Scientific Computation program from my very first day in Maryland. I will always remember that long night when we struggled together to complete the course project. Thanks to Wenzhi Tan and Shenglan Xuan for being my best roommates for four years. They are like my family here. It is impossible to list all my friends in one page. I want to say that I feel so lucky to have them in Maryland.

My parents are always standing by my side though they are thousands of miles away. Their unlimited love is the greatest support of my endeavors through my graduate studies in America.

Last but not least, I want to thank my graceful wife Hua Wei whose everlasting love and support kept me going through the most frustrating time in my life. Without her help and encouragement, this dissertation would be impossible.

Table of Contents

List of Figures

List of Abbreviations

$1D$	one-dimensional
$2D$	two-dimensional
PDE	Partial differential equations
CFD	Computational fluid dynamics
NSE	Navier-Stoke equations
SWE	Shallow water equations
$RK3$	3-stage Runge-Kutta method
RHS	Right hand side
LHS	Left hand side
AMSC	Applied Mathematics and Scientific Computation
CSCAMM	Center for Scientific Computation and Mathematical Modeling

Chapter 1

Introduction

1.1 Conservation laws

Conservation laws arise from the modeling of balance laws of physical quantities. Specifically, a conservation law asserts the rate of change of the total amount of substance contained in a fixed domain D is equal to the flux of that substance across the boundary of D. Denoting the density functions of N substances by $\mathbf{u} = (u_1, \cdots, u_N)^\top$, and the flux functions by $\mathbf{f}_j = (f_{1j}, \cdots, f_{Nj})^\top$, $1 \leq j \leq M$, the general form of a system of conservation law in M space variables is

$$\frac{d}{dt} \int_D \mathbf{u}\, d\mathbf{x} = -\sum_{j=1}^M \int_{\partial D} \mathbf{f}_j n_j\, dS, \quad \mathbf{x} = (x_1, \cdots, x_M) \in \mathbb{R}^M,\ t > 0. \qquad (1.1.1)$$

Here $\mathbf{n} = (n_1, \cdots, n_M)^\top$ is the outward unit normal vector to D and dS denotes the surface element on ∂D, the boundary of D. Applying the divergence theorem on the RHS of (1.1.1) and moving the time derivative under the integral yields

$$\int_D \left(\frac{\partial \mathbf{u}}{\partial t} + \sum_{j=1}^M \frac{\partial}{\partial x_j} \mathbf{f}_j(\mathbf{u}) \right) dx = 0.$$

Shrinking domain D to a point where all partial derivatives of $\mathbf{u}$ and $\mathbf{f}_j$ are continuous, we obtain the differential *system of conservation laws,*

$$\frac{\partial \mathbf{u}}{\partial t} + \sum_{j=1}^M \frac{\partial}{\partial x_j} \mathbf{f}_j(\mathbf{u}) = 0. \qquad (1.1.2)$$

To study the hyperbolicity of the system (1.1.2), we define in the following way, let $A_j(\mathbf{u}) = \nabla_{\mathbf{u}} \mathbf{f}_j$ be the Jacobian matrix of $\mathbf{f}_j$. The quasi-linear system

$$\frac{\partial \mathbf{u}}{\partial t} + \sum_{j=1}^{M} A_j \frac{\partial \mathbf{u}}{\partial x_j} = 0. \tag{1.1.3}$$

is called *hyperbolic* if, for each $\mathbf{u}$ and unit vector $\boldsymbol{\omega} = (\omega_1, \cdots, \omega_M)^\top$, the matrix $A := \sum_{j=1}^{M} \omega_j A_j(\mathbf{u})$ has N real eigenvalues $\lambda_1(\mathbf{u}, \boldsymbol{\omega}), \cdots, \lambda_N(\mathbf{u}, \boldsymbol{\omega})$ and N linearly independent corresponding eigenvectors $\mathbf{r}_1(\mathbf{u}, \boldsymbol{\omega}), \cdots \mathbf{r}_N(\mathbf{u}, \boldsymbol{\omega})$. If the eigenvalues $\{\lambda_k\}_{k=1}^{N}$ are all distinct, the system (1.1.3) is called *strict hyperbolic.*

Many physical phenomena are dictated by nonlinear hyperbolic systems of conservation laws and related time-dependent problems. Important examples occur in gas dynamics, shallow water theory, nonlinear elasticity, magneto-fluid dynamics, combustion theory, and more. In particular, the driving forces of fluid dynamics are such problems govern by additional dissipative and dispersive forcing terms. In the framework of Newtonian fluids, the central problem is the Navier-Stokes equations, which are derived from the conservation laws of mass, momentum, and total energy for the flow, driven by convection fluxes together with viscous and heat fluxes. We will focus on the convection-dominated problems in this dissertation.

For the systems of conservation laws, we study the Cauchy problems,

$$\begin{cases} \dfrac{\partial \mathbf{u}}{\partial t} + \displaystyle\sum_{j=1}^{M} \dfrac{\partial}{\partial x_j} \mathbf{f}_j(\mathbf{u}) = 0 \\[2mm] \mathbf{u}(\mathbf{x}, 0) = \mathbf{u}_0(\mathbf{x}) \end{cases} \tag{1.1.4}$$

The most distinctive feature of such problems in several dimensions is the formation of shock discontinuities. In general there do not exist classical solutions of (1.1.4) beyond some time interval, even when the initial condition $\mathbf{u}_0$ is very smooth. The

above considerations lead us to consider weak solutions of (1.1.4). A weak solution of (1.1.4) is not necessarily unique. The entropy condition plays an important role in selecting the physically relevant solution among those weak solutions. ([Ole63, Lax73, GR96, Daf00]). It states the additional *entropy inequality*,

$$U(\mathbf{u})_t + \sum_{j=1}^{M} \frac{\partial}{\partial x_j} F_j(\mathbf{u}) \leq 0 \tag{1.1.5}$$

for all admissible entropy U with entropy fluxes F_j satisfying the compatibility relations $(\nabla_{\mathbf{u}} U)^\top \nabla_{\mathbf{u}} \mathbf{f}_j = (\nabla_{\mathbf{u}} F_j)^\top$, $1 \leq j \leq M$. In fact, entropy inequality (1.4.2) characterizes those physically admissible solutions, which are realizable as vanishing viscosity limits,

$$\mathbf{u} = \lim_{\epsilon \downarrow 0} \mathbf{u}^\epsilon, \tag{1.1.6}$$

where

$$\frac{\partial \mathbf{u}^\epsilon}{\partial t} + \sum_{j=1}^{M} \frac{\partial}{\partial x_j} \mathbf{f}_j(\mathbf{u}^\epsilon) = \epsilon \Delta \mathbf{u}^\epsilon. \tag{1.1.7}$$

It follows from the entropy inequality (1.4.2) that the total amount of entropy $\int_{\mathbf{x}} U(\mathbf{u}(\mathbf{x}, t)) \, d\mathbf{x}$ does not increase over time. A canonical example is the second law of thermodynamics, which states that the total entropy decays in an isolated thermodynamical system.

1.2 Entropy-stable and entropy-conservative schemes

When we turn our attention to the numerical framework of the nonlinear conservation laws, entropy stability serves as an essential guideline to seek the physically relevant numerical solutions. Here we restrict ourselves to the system of conservation

laws in one dimensional space,

$$\frac{\partial}{\partial t}\mathbf{u} + \frac{\partial}{\partial x}\mathbf{f}(\mathbf{u}) = 0, \qquad (x, t) \in \mathbb{R} \times [0, \infty) \qquad (1.2.1)$$

while the further extension in multidimensional spaces can be accomplished dimension by dimension. We construct the semi-discrete difference approximations in the general conservative form,

$$\frac{d}{dt}\mathbf{u}_\nu(t) + \frac{\mathbf{f}_{\nu+\frac{1}{2}} - \mathbf{f}_{\nu-\frac{1}{2}}}{\Delta x_\nu} = 0, \qquad (1.2.2)$$

where $\mathbf{u}_\nu(t)$ denotes the solution along the gridline (x_ν, t), and $\mathbf{f}_{\nu+\frac{1}{2}}$ is a consistent numerical flux. The Lax-Wendroff theorem [LW60] states that if the conservative consistent scheme (1.2.2) converges as the grid is refined then it converges to the weak solution of the conservation laws (1.2.1). This theorem does not guarantee that the weak solutions obtained in this manner satisfy the entropy condition, which is necessary in order to single out an unique 'physically relevant' solution among many weak solutions of (1.2.1). To this end, we now consider the conservative schemes (1.2.2) that are *entropy-stable* in the sense of satisfying the discrete entropy inequality,

$$\frac{d}{dt}U(\mathbf{u}_\nu(t)) + \frac{F_{\nu+\frac{1}{2}} - F_{\nu-\frac{1}{2}}}{\Delta x_\nu} \leq 0, \qquad (1.2.3)$$

which is the discrete analogue of the differential entropy inequality

$$U(\mathbf{u})_t + F(\mathbf{u})_x \leq 0,$$

for all admissible entropy pair $(U(\mathbf{u}), F(\mathbf{u}))$. In particular, when equality holds in (1.2.3), we obtain the *entropy-conservative* schemes, which serve as important tools in our entropy stability study through the comparison.

4

In Chapter 2, we start our discussion with the construction of these entropy-stable/conservative schemes. The key ingredient here is the entropy-conservative discretization of the convective fluxes $\mathbf{f}_{\nu+\frac{1}{2}}$ in (1.2.2). The main results of entropy stability/conservation of the numerical schemes were concluded in [Tad87][Theorem 5.2], which states the sufficient condition (sufficient and necessary condition for three-point schemes) of the conservative scheme (1.2.2) being entropy-stable (respectively, entropy-conservative) is

$$\left\langle \mathbf{v}_{\nu+1} - \mathbf{v}_\nu, \, \mathbf{f}_{\nu+\frac{1}{2}} \right\rangle \leq \psi(\mathbf{v}_{\nu+1}) - \psi(\mathbf{v}_\nu), \qquad (1.2.4)$$

and, respectively,

$$\left\langle \mathbf{v}_{\nu+1} - \mathbf{v}_\nu, \, \mathbf{f}_{\nu+\frac{1}{2}} \right\rangle = \psi(\mathbf{v}_{\nu+1}) - \psi(\mathbf{v}_\nu). \qquad (1.2.5)$$

Here, we utilize the *entropy variables* $\mathbf{v} := \nabla_{\mathbf{u}} U$ and the *potential function* $\psi(\mathbf{v}) := \langle \mathbf{v}, \mathbf{f}(\mathbf{v}) \rangle - F(\mathbf{u}(\mathbf{v}))$. The *entropy-conservative numerical fluxes* we want to construct satisfy the condition (1.2.5).

Another important aspect of the construction of such numerical flux is the certain choice of the *integration paths* in phase space of the entropy variable. For the scalar problems, these numerical fluxes are "path-independent", hence the entropy-conservative schemes are unique for a given entropy pair. For the system of equations, the construction of entropy-conservative schemes in terms of numerical fluxes depends on the choices of entropy function and the integration paths. Discussion on different choices of integration paths for one-dimensional systems can be found in [Tad03] and [TZ06]. Specifically, we construct the entropy-stable numerical schemes in terms of a new family of entropy-conservative numerical fluxes subjected to the

choice of a physically relevant integration path in the phase space, then implement such schemes on one-dimensional Navier-Stokes equations for the first time in [TZ06].

We then extend these entropy-conservative approximations to the multidimensional problems by carrying out the same recipe as indicated in the one-dimensional setup dimension by dimension. More discussion on two-dimensional setup of such entropy-stable schemes for 2D shallow water equations can be found in [TZ07].

We focus on the semi-discrete schemes based on the spatial differencing in this dissertation. A general framework of the entropy stability of the fully discrete schemes can be found in [LMR02, Tad03]. We are going to utilize the explicit 3-stage Runge-Kutta method in time discretization for its relatively negligible amount of numerical viscosity and large stability region. Details about the stability properties of multistage Runge-Kutta method can be found on [GST01].

1.3 Burgers equation

One-dimensional Burgers equation serves as a prototype example of the scalar nonlinear conservation law. In Chapter 3, we develop the entropy-conservative schemes for the inviscid Burgers equation,

$$\frac{\partial u}{\partial t} + \frac{\partial}{\partial x} f(u) = 0, \quad f(u) = \frac{1}{2} u^2. \tag{1.3.1}$$

Any convex function $U(u)$ serves as an entropy function for the scalar Burgers equation. Here we consider a family of entropy functions, $U_p(u) = u^{2p} \quad p = 1, 2, \cdots$. Solutions of (1.3.1) satisfy, at the formal level, the additional conservation law of

entropy,

$$\frac{\partial}{\partial t}U_p(u) + \frac{\partial}{\partial x}F_p(u) = 0. \tag{1.3.2}$$

The above entropy equality is balanced by the entropy flux $F_p(u) = 2pu^{2p+1}/(2p+1)$ satisfying the compatibility relation $U_p'(u)f'(u) = F_p'(u)$. Spatial integration then yields the total entropy conservation(ignoring the boundary contributions),

$$\int_x u^{2p}(x,t)\,dx = \int_x u^{2p}(x,0)\,dx. \tag{1.3.3}$$

In the discrete framework, we construct the entropy-conservative discretization

$$\frac{d}{dt}u_\nu(t) + \frac{1}{\Delta x}\left(f^*_{\nu+\frac{1}{2}} - f^*_{\nu-\frac{1}{2}}\right) = 0, \tag{1.3.4a}$$

where $f^*_{\nu+\frac{1}{2}}$ is three-point entropy conservative numerical flux constructed as

$$f_{\nu+\frac{1}{2}} = \frac{2p-1}{2(2p+1)} \cdot \frac{u_{\nu+1}^{2p+1} - u_\nu^{2p+1}}{u_{\nu+1}^{2p-1} - u_\nu^{2p-1}}. \tag{1.3.4b}$$

The resulting scheme (1.3.4a) and (1.3.4b) is entropy conservative in the sense that the discrete analogue of total entropy conservation (1.3.3) is satisfied,

$$\sum_\nu u_\nu^{2p}(t)\,\Delta x = \sum_\nu u_\nu^{2p}(0)\,\Delta x.$$

Different numerical results corresponding to a series of different entropy functions with different p's display the tendency of controlling the $L^\infty-$norm of solutions when the entropy conservation is guaranteed in the numerical approximations.

1.4   One dimensional Navier-Stokes equations

We turn to the system of one-dimensional Navier-Stokes equations governed by additional viscosity and heat fluxes in Chapter 4. We consider the Navier-Stokes

equations governing the density $\rho = \rho(x,t)$, momentum $m = m(x,t)$, and energy $E = E(x,t)$,

$$\frac{\partial}{\partial t}\mathbf{u} + \frac{\partial}{\partial x}\mathbf{f}(\mathbf{u}) = \epsilon\frac{\partial^2}{\partial x^2}\mathbf{d}(\mathbf{u}), \quad \mathbf{u} = [\rho, m, E]^\top. \tag{1.4.1}$$

They are driven by the convective flux $\mathbf{f}(\mathbf{u}) = [m, qm + p, q(E + p)]^\top$, together with the dissipative flux $\epsilon\mathbf{d}(\mathbf{u}) = (\lambda + 2\mu)[0, q, q^2/2]^\top + \kappa[0, 0, \theta]^\top$ which stands for the combined viscous and heat fluxes. Here ϵ denotes the vanishing amplitudes of viscosity and heat conduction. These fluxes involve the velocity $q := m/\rho$, the pressure p and temperature θ which are determined by the polytropic equation of state. Here, the viscosity λ, μ and conductivity κ are fixed.

The viscous and heat fluxes are dissipative terms in the sense that they are responsible for the dissipation of total entropy, $U(\mathbf{u}) = -\rho S$ with the specific entropy $S = \ln(p\rho^{-\gamma})$,

$$\frac{\partial}{\partial t}(-\rho S) + \frac{\partial}{\partial x}(-mS + \kappa(\ln\theta)_x) = -(\lambda + 2\mu)\frac{q_x^2}{\theta} - \kappa\left(\frac{\theta_x}{\theta}\right)^2 \leq 0. \tag{1.4.2}$$

Spatial integration of (1.4.2) then yields the second law of thermodynamics,

$$\frac{d}{dt}\int_x(-\rho S)\,dx = -(\lambda + 2\mu)\int_x\frac{q_x^2}{\theta}dx - \kappa\int_x\left(\frac{\theta_x}{\theta}\right)^2 dx \leq 0. \tag{1.4.3}$$

In fact, the total entropy balance statement (1.4.3) specifies the precise entropy decay rate. In the case of the Euler equations without viscous and heat fluxes, $\lambda = \mu = \kappa = 0$, total entropy is precisely conserved, $\int_x -\rho S(x,t)\,dx = \int_x -\rho S(x,0)\,dx$. Indeed, the entropy-stable solutions of the Euler equations are realized as the vanishing Navier-Stokes limits, which is analogous to the vanishing viscosity limit (1.1.6) we mentioned in the previous section.

8

Discretize the Navier-Stokes equations (4.4.6a) in space,

$$\frac{d}{dt}\mathbf{u}_\nu(t) + \frac{1}{\Delta x}\left(\mathbf{f}^*_{\nu+\frac{1}{2}} - \mathbf{f}^*_{\nu-\frac{1}{2}}\right) = \frac{\epsilon}{(\Delta x)^2}\left(\mathbf{d}(\mathbf{u}_{\nu+1}) - 2\mathbf{d}(\mathbf{u}_\nu) + \mathbf{d}(\mathbf{u}_{\nu-1})\right). \qquad (1.4.4)$$

As in Burgers equation, we seek entropy conservative numerical flux $\mathbf{f}^*_{\nu+\frac{1}{2}}$, so that the numerical entropy decay will be dictated solely by viscous and heat fluxes in the Navier-Stokes equations. Different from the numerical fluxes outlined in [Tad87] which are integrated along straight line paths in phase space, $\mathbf{f}^*_{\nu+\frac{1}{2}}$ are constructed along a piecewise-constant path in phase space directed by an arbitrary set of 3 linear independent vectors $\{\mathbf{r}^j\}_{j=1}^{j=3}$ and its orthogonal set $\{\boldsymbol{\ell}^j\}_{j=1}^{j=3}$. In our computation, a "physically relevant" choice is a Riemann path connecting two neighboring gridpoints. Our approach is to construct the Roe-path in $\mathbf{u}$-space, then project it back to $\mathbf{v}$-space to obtain $\{\mathbf{r}^j\}$ and $\{\boldsymbol{\ell}^j\}$. These new entropy-conservative numerical fluxes admit an explicit and closed-form expression, and enable us to enforce the entropy stability by fine-tuning the amount of numerical viscosity along each sub-path carrying different intermediate waves. The resulting entropy-stable difference schemes (1.4.4) contain no artificial numerical viscosity in the sense that their entropy dissipation is dictated solely by viscous and heat fluxes. Equipped with this new family of difference schemes, we are able to recover the *precise* entropy decay of the Navier-Stokes equations.

Our prototype result about the Navier-Stokes equations is the following.

Theorem 1.4.1. *Consider the Navier-Stokes equations (4.4.6a),*

$$\frac{\partial}{\partial t}\mathbf{u} + \frac{\partial}{\partial x}\mathbf{f}(\mathbf{u}) = \epsilon\frac{\partial^2}{\partial x^2}\mathbf{d}(\mathbf{u}).$$

Here, $\mathbf{u} = [\rho, m, E]^\top$ is the vector of conservative variables, $\mathbf{f}(\mathbf{u})$ is the corresponding 3-vector of fluxes $\mathbf{f}(\mathbf{u}) = [m, qm + p, q(E + p)]^\top$, and $\epsilon \mathbf{d}(\mathbf{u})$ stands for the combined viscous and heat fluxes,

$$\epsilon \mathbf{d}(\mathbf{u}) = (\lambda + 2\mu)[0, q, q^2/2]^\top + \kappa[0, 0, \theta]^\top$$

where ϵ signals the vanishing amplitudes of viscosity λ, μ and heat conductivity κ.

We approximate these Navier-Stokes equations by a semi-discrete scheme of the form

$$\frac{d}{dt}\mathbf{u}_\nu(t) + \frac{1}{\Delta x_\nu}\left(\mathbf{f}^*_{\nu+\frac{1}{2}} - \mathbf{f}^*_{\nu-\frac{1}{2}}\right) = \frac{\epsilon}{\Delta x_\nu}\left(\frac{\mathbf{d}(\mathbf{u}_{\nu+1}) - \mathbf{d}(\mathbf{u}_\nu)}{\Delta x_{\nu+\frac{1}{2}}} - \frac{\mathbf{d}(\mathbf{u}_\nu) - \mathbf{d}(\mathbf{u}_{\nu-1})}{\Delta x_{\nu-\frac{1}{2}}}\right).$$

$$\text{(1.4.5a)}$$

Let $\mathbf{f}^*_{\nu+\frac{1}{2}} = \mathbf{f}^*(\mathbf{u}_\nu, \mathbf{u}_{\nu+1})$ is the numerical flux given the by the explicit formula,

$$\mathbf{f}^*_{\nu+\frac{1}{2}} = (\gamma - 1)\sum_{j=1}^3 \frac{m^{j+1} - m^j}{\langle \boldsymbol{\ell}^j, \mathbf{v}_{\nu+1} - \mathbf{v}_\nu \rangle}\boldsymbol{\ell}^j, \qquad \mathbf{v} = \mathbf{v}(\mathbf{u}) := \left[-\frac{E}{e} - S + \gamma + 1, \frac{q}{\theta}, -\frac{1}{\theta}\right]^\top.$$

$$\text{(1.4.5b)}$$

Here, $\{\boldsymbol{\ell}^j = \boldsymbol{\ell}^j_{\nu+\frac{1}{2}}\}_{j=1}^3$ are three linearly independent directions in $\mathbf{v}$-space at our disposal (consult examples 2.2.1, 2.2.2 and 2.2.3 below); $\{\mathbf{r}^j = \mathbf{r}^j_{\nu+\frac{1}{2}}\}_{j=1}^3$ is the corresponding orthogonal system and $\{m^j = m^j_{\nu+\frac{1}{2}}\}_{j=1}^4$ are the intermediate values of the momentum specified along the corresponding path, $\mathbf{v}^{j+1} = \mathbf{v}^j + \langle \boldsymbol{\ell}^j, \mathbf{v}_{\nu+1} - \mathbf{v}_\nu \rangle \mathbf{r}^j$, starting with $\mathbf{v}^1 = \mathbf{v}_\nu$ and ending with $\mathbf{v}^4 = \mathbf{v}_{\nu+1}$. Then, the resulting scheme (1.4.5a),(1.4.5b) is entropy stable and the following discrete entropy balance holds[1]

$$\frac{d}{dt}\sum_\nu (-\rho_\nu S_\nu)\Delta x_\nu = -(\lambda + 2\mu)\sum_\nu \left(\frac{\Delta q_{\nu+\frac{1}{2}}}{\Delta x_{\nu+\frac{1}{2}}}\right)^2 \widehat{(1/\theta)}_{\nu+\frac{1}{2}}\Delta x_{\nu+\frac{1}{2}}$$

$$-\kappa\sum_\nu \left(\frac{\Delta \theta_{\nu+\frac{1}{2}}}{\Delta x_{\nu+\frac{1}{2}}}\right)^2 \widetilde{(1/\theta)}^2_{\nu+\frac{1}{2}}\Delta x_{\nu+\frac{1}{2}} \leq 0. \qquad \text{(1.4.6)}$$

---

[1] We let $\widehat{z}_{\nu+\frac{1}{2}}$ and $\widetilde{z}_{\nu+\frac{1}{2}}$ denote the arithmetic and geometric means, $\widehat{z}_{\nu+\frac{1}{2}} = (z_\nu + z_{\nu+1})/2$ and $\widetilde{z}_{\nu+\frac{1}{2}} = \sqrt{z_\nu z_{\nu+1}}$.

The entropy balance (1.4.6) is a precise discrete analogue of (1.4.3). The scheme (1.4.5a),(1.4.5b) contains no artificial numerical viscosity in the sense that entropy dissipation is driven solely by the viscous and heat fluxes. In the particular case that viscosity and the heat conduction are absent, $\kappa = \lambda = \mu = 0$, then the entropy balance (1.4.2) is reduced to the formal entropy *equality* of the Euler equations without viscous and heat fluxes,

$$\frac{\partial}{\partial t}\big(-\rho S\big) + \frac{\partial}{\partial x}\big(-mS\big) = 0, \tag{1.4.7}$$

which in turn, implies the entropy conservation $\int_x (-\rho S)(\cdot, t)\, dx = \int_x (-\rho S)(\cdot, 0)\, dx$. Similarly, setting $\epsilon \mathbf{d} = 0$ we omit the dissipative terms in Navier-Stokes equations, and the difference scheme (1.4.5a) becomes *entropy conservative*,

$$\sum (-\rho_\nu S_\nu)(t)\Delta x_\nu = \sum (-\rho_\nu S_\nu)(0)\Delta x_\nu.$$

Entropy conservative schemes are studied in section 4.4, following [Tad03]. The key ingredient here is the construction of their entropy conservative fluxes, such as $\mathbf{f}^*_{\nu+\frac{1}{2}}$ in (1.4.5b). These fluxes employ the so called *entropy variables*, $\mathbf{v} = \mathbf{v}(\mathbf{u})$, which are discussed in section 2.1. The main results are then summarized in theorems 2.2.2 and 4.4.1. Finally, in section 4.5 we present a series of numerical simulations with the new schemes. The entropy conservative approximations of Euler equations are 'purely dispersive' and as such, their solutions experience dispersive oscillations, interesting for their own sake, consult [Lax86, HFM86, Tad86, LLV93, LL96, LR00] and the references therein. Turning to the Navier-Stokes equations, our simulations provide a remarkable evidence for the different roles that viscosity and heat conduction have in removing the dispersive oscillations, to yield sharp monotone profiles of

well-resolved shock and contact layers. No limiters were added, but instead, the viscous and heat conduction terms in Navier-Stokes equations are found to serve as accurate edge detectors. See [TZ06] for the first implementation of this new family of entropy-stable schemes on 1D Navier-Stokes equations.

Remark 1.4.1. The viscous Navier-Stokes equations dissipate a general family of entropies, $-\rho h(S)$, where $h(S)$ is an arbitrary increasing function . Indeed, arguing along the above lines we multiply the continuity equation by $h(S)$ and adding it to (4.2.2)$\times$ $h'(S)$ to find

$$
\frac{\partial}{\partial t}\big(-\rho h(S)\big) + \frac{\partial}{\partial x}\Big(-mh(S) + \kappa(\ln\theta)_x h'(S)\Big) =
$$
$$
= \kappa h''(S)S_x\frac{\theta_x}{\theta} - h'(S)\left((\lambda+2\mu)\frac{q_x^2}{\theta} + \kappa\left(\frac{\theta_x}{\theta}\right)^2\right). \quad (1.4.8)
$$

In the case that the heat conduction is absent, the first term on the RHS of (1.4.8) vanishes, and we are left with

$$
\frac{d}{dt}\int_x\big(-\rho h(S)\big)dx = -(\lambda+2\mu)\int_x\frac{q_x^2}{\theta}h'(S)dx. \quad (1.4.9)
$$

Thus, the viscous Navier-Stokes equations imply the dissipation of a family of entropies, $\int_x(-\rho h(S))\,dx$ for all $h'(S) > 0$; consult [Har83]. Each one of these entropies carries its own entropy conservative flux $\mathbf{f}^*_{\nu+\frac{1}{2}}$. The explicit construction of such fluxes is outlined in theorem 2.2.2 below. Combining these entropy conservative fluxes together with centered differencing of the additional viscous terms, $(\lambda+2\mu)[0, q, q^2/2]^\top$, yield a generalization of Theorem 1.4.1 which recovers the precise entropy balance (1.4.9).

We note in passing that when heat conduction is present, however, the negativity of the first term on the right of (1.4.8) requires $h''(S) = 0$, so that we

12

are left with one canonical entropy, $h(S) \sim S$ discussed in theorem 1.4.1; consult [HFM86, HMM86, HM86a, HM86b]. The above characterizations of the general entropy function of the Navier-Stokes equations satisfy the Harten's convexity condition in [HLLM98].

1.5   Two-dimensional shallow water equations

It is straightforward to generalize the recipe for 'faithful' entropy stable approximations of *multidimensional* problems. The extension is carried out dimension by dimension and as indicated in the one-dimensional setup of theorem 1.4.1, one has the freedom of choosing different paths in phase space.

In Chapter 5, we extend our discussion to the two-dimensional shallow water equations.

$$\frac{\partial}{\partial t}\mathbf{u} + \frac{\partial}{\partial x}\mathbf{f}(\mathbf{u}) + \frac{\partial}{\partial y}\mathbf{g}(\mathbf{u}) = \varsigma\frac{\partial}{\partial x}\left(h\frac{\partial}{\partial x}\mathbf{d}(\mathbf{u})\right) + \varsigma\frac{\partial}{\partial y}\left(h\frac{\partial}{\partial y}\mathbf{d}(\mathbf{u})\right), \qquad (1.5.1)$$

with $\mathbf{u} = [h,\, uh,\, vh]^\top$ being the vector of conserved variables balanced by the flux vectors $\mathbf{f} = [uh,\, u^2h + gh^2/2,\, uvh]^\top$, $\mathbf{g} = [vh,\, uvh,\, v^2h + gh^2/2]^\top$, and the viscous flux vector $\mathbf{d} = [0,\, u,\, v]^\top$. Here, $h = h(x,t)$ is the total water height, $(u(x,t), v(x,t))$ are the depth-averaged velocities along x and y direction. Finally, g is the constant acceleration due to gravity, and $\varsigma > 0$ is the constant eddy viscosity which models the turbulence stress in the flow.

The total energy $U(\mathbf{u}) = (gh^2 + u^2h + v^2h)/2$ serves as an entropy function,

$$\frac{\partial}{\partial t}U(\mathbf{u}) + \frac{\partial}{\partial x}F(\mathbf{u}) + \frac{\partial}{\partial y}G(\mathbf{u}) = -\eta h(u_x^2 + u_y^2 + v_x^2 + v_y^2), \qquad (1.5.2)$$

13

where $F(\mathbf{u}) = guh^2 + \frac{u^3 h + uv^2 h}{2} - huu_x - hvv_x$ and $G(\mathbf{u}) = gvh^2 + \frac{u^2 vh + v^3 h}{2} - huu_y - hvv_y$

are the entropy fluxes. Spatial integration of (1.5.2) yields

$$\frac{d}{dt} \int_y \int_x U(\mathbf{u})\, dx dy = -\varsigma \int_y \int_x h(u_x^2 + u_y^2 + v_x^2 + v_y^2)\, dx dy. \qquad (1.5.3)$$

For the inviscid case ($\varsigma = 0$), the total energy is preserved,

$$\int_y \int_x U(\mathbf{u}(x,t))\, dx dy = \int_y \int_x U(\mathbf{u}(x,0))\, dx dy.$$

Arguing along the same line as the above NSE dimension by dimension, we obtain the entropy/energy-stable semi-discrete schemes (recall $\widehat{z_{\nu+\frac{1}{2}}} := (z_{\nu+1} + z_\nu)/2$)

$$\frac{d}{dt}\mathbf{u}_{\nu,\mu}(t) + \frac{1}{\Delta x}(\mathbf{f}^*_{\nu+\frac{1}{2},\mu} - \mathbf{f}^*_{\nu-\frac{1}{2},\mu}) + \frac{1}{\Delta y}(\mathbf{g}^*_{\nu,\mu+\frac{1}{2}} - \mathbf{g}^*_{\nu,\mu-\frac{1}{2}}) =$$

$$\frac{\eta}{\Delta x}(\widehat{h_{\nu+\frac{1}{2},\mu}}\frac{\mathbf{d}_{\nu+1,\mu} - \mathbf{d}_{\nu,\mu}}{\Delta x} - \widehat{h_{\nu-\frac{1}{2},\mu}}\frac{\mathbf{d}_{\nu,\mu} - \mathbf{d}_{\nu-1,\mu}}{\Delta x})$$

$$+ \frac{\eta}{\Delta y}(\widehat{h_{\nu,\mu+\frac{1}{2}}}\frac{\mathbf{d}_{\nu,\mu+1} - \mathbf{d}_{\nu,\mu}}{\Delta x} - \widehat{h_{\nu,\mu-\frac{1}{2}}}\frac{\mathbf{d}_{\nu,\mu} - \mathbf{d}_{\nu,\mu-1}}{\Delta x}), \quad (1.5.4a)$$

with the entropy-conservative fluxes $\mathbf{f}^*_{\nu+\frac{1}{2},\mu}$ and $\mathbf{g}^*_{\nu,\mu+\frac{1}{2}}$ constructed as indicated in one-dimensional case,

$$\mathbf{f}^*_{\nu+\frac{1}{2},\mu} = \frac{g}{2}\sum_{j=1}^{3} \frac{(h^{j+1}_{\nu+\frac{1}{2},\mu})^2 u^{j+1}_{\nu+\frac{1}{2},\mu} - (h^j_{\nu+\frac{1}{2},\mu})^2 u^j_{\nu+\frac{1}{2},\mu}}{\left\langle \boldsymbol{\ell}^{x^j}_{\nu+\frac{1}{2},\mu}, \Delta\mathbf{v}_{\nu+\frac{1}{2},\mu} \right\rangle} \boldsymbol{\ell}^{x^j}_{\nu+\frac{1}{2},\mu}, \qquad (1.5.4b)$$

$$\mathbf{g}^*_{\nu,\mu+\frac{1}{2}} = \frac{g}{2}\sum_{j=1}^{3} \frac{(h^{j+1}_{\nu,\mu+\frac{1}{2}})^2 u^{j+1}_{\nu,\mu+\frac{1}{2}} - (h^j_{\nu,\mu+\frac{1}{2}})^2 v^j_{\nu,\mu+\frac{1}{2}}}{\left\langle \boldsymbol{\ell}^{y^j}_{\nu,\mu+\frac{1}{2}}, \Delta\mathbf{v}_{\nu,\mu+\frac{1}{2}} \right\rangle} \boldsymbol{\ell}^{y^j}_{\nu,\mu+\frac{1}{2}}, \qquad (1.5.4c)$$

Here, $u_{\nu,\mu}(t)$ denotes the discrete solution at the grid point (x_ν, y_ν, t), $\mathbf{d}_{\nu,\mu} := \mathbf{d}(\mathbf{u}_{\nu,\mu})$, and $\mathbf{v} := U_\mathbf{u} = [gh - \frac{1}{2}(u^2 + v^2), u, v]^\top$ is the entropy variable. Numerical flux $\mathbf{f}^*$ and $\mathbf{g}^*$ are constructed separately along two different phase pathes dictated by two sets of vectors $\{\boldsymbol{\ell}^{x^j}\}$ and $\{\boldsymbol{\ell}^{y^j}\}$. $\{h^j\}$ and $\{u^j\}$ are intermediate values of height and velocity along the path. The above difference scheme (1.5.4a)-(1.5.4c)

14

is an entropy/energy stable scheme with no artificial viscosity in the sense that the following discrete entropy/energy balance is satisfied,

$$\frac{d}{dt}\sum_{\nu,\mu}U(\mathbf{u}_{\nu,\mu}(t))\Delta x\Delta y = -\eta\sum_{\nu,\mu}\left\{\widehat{h_{\nu+\frac{1}{2},\mu}}\left[\left(\frac{\Delta\mathbf{u}_{\nu+\frac{1}{2},\mu}}{\Delta x}\right)^2 + \left(\frac{\Delta\mathbf{v}_{\nu+\frac{1}{2},\mu}}{\Delta x}\right)^2\right]\right.$$
$$\left. +\widehat{h_{\nu,\mu+\frac{1}{2}}}\left[\left(\frac{\Delta\mathbf{u}_{\nu,\mu+\frac{1}{2}}}{\Delta y}\right)^2 + \left(\frac{\Delta\mathbf{v}_{\nu,\mu+\frac{1}{2}}}{\Delta y}\right)^2\right]\right\}\Delta x\Delta y. \quad (1.5.5)$$

(1.5.5) is a discrete analogue of the entropy balance statement (1.5.3).

To illustrate the performance of the above generalization of the entropy/energy-stable schemes, we test two dimensional partial-dam-break problem. The numerical results, especially those of the fine mesh, successfully simulate both the circular shock water wave propagations and the vortices formed on the both sides of the breach. The physical undershoots are also developed near sharp corners of the remanent dam. This implementation for 2D shallow water equations was done in [TZ07] for the first time.

There are many other successful energy-preserving numerical schemes constructed for two-dimensional flows. In [Ara97], Arakawa constructed finite-difference Jacobians that maintain important integral constraints on the continuous Jacobian. When applied to the vorticity equation governing two-dimensional incompressible inviscid flow by Arakawa and Lamb in [AL81], maintaining these constraints guarantees conservation of energy and enstrophy in the discrete system. Our energy-preserving schemes show advantage of simplicity over Arakawa schemes in terms of avoid using the staggered grid.

The purpose of this dissertation is to present a systematic study of the novel entropy stable approximate methods of nonlinear conservation laws with no artificial viscosity. The resulting numerical schemes respect the precise entropy balance statements of the original systems. Numerical implementations have been done for a series of fluid equations as prototypes of scalar problems, one-dimensional and two-dimensional systems of conservation laws, specifically, the Burgers equation, the 1D Navier-Stokes equations, and the 2D shallow water equations. Our simulations demonstrate the genuine roles of physical dissipation terms in removing spurious numerical oscillations.

Chapter 2

Entropy Variables and Entropy-Conservative Schemes

2.1 Entropy dissipation

Let Ω be an open subset of $\mathbb{R}^N$. We consider general form of systems of conservation laws in one space variable,

$$\frac{\partial}{\partial t}\mathbf{u} + \frac{\partial}{\partial x}\mathbf{f}(\mathbf{u}) = 0, \qquad (x,t) \in \mathbb{R} \times [0,\infty), \qquad (2.1.1)$$

governing the N-vector of conserved variables, $\mathbf{u} = [u_1, \cdots, u_N]^\top \in \Omega$. Here the functions $\mathbf{f}(\mathbf{u}) = [f_1, \cdots, f_N]^\top$ are called the flux function. Formally the system (2.1.1) expresses the conservation of N quantities $u_1, u_2, \cdots, u_N$. In fact, if we ignore the boundary contributions, it follows from (2.1.1) that

$$\frac{d}{dt}\int_x \mathbf{u}\,\Delta x = 0.$$

This balance statement means the time invariance of $\int_x \mathbf{u}\,\Delta x$.

The system (2.1.1) is called *hyperbolic* if for any $\mathbf{u} \in \Omega$, the matrix $A(\mathbf{u}) = \mathbf{f_u}$ has N real eigenvalues $\lambda_1(\mathbf{u}) \leq \lambda_2(\mathbf{u}) \leq \cdots \leq \lambda_N(\mathbf{u})$ and N linearly independent corresponding eigenvectors $\mathbf{r}_1(\mathbf{u}), \cdots, \mathbf{r}_N(\mathbf{u})$, i.e.

$$A(\mathbf{u})\mathbf{r}_k(\mathbf{u}) = \lambda_k(\mathbf{u})\mathbf{r}_k(\mathbf{u}), \quad k = 1, 2, \cdots, N.$$

In addition, if $\lambda_k(\mathbf{u})$ are all distinct, the system (2.1.1) is called *strict hyperbolic*. Hyperbolicity expresses the well-posedness of the linearization of system (2.1.1)

about the constant solution with value $\mathbf{u}$, and hence constitute a necessary condition for the well-posedness of the full system for initial data with values near $\mathbf{u}$.

We assume that the hyperbolic system (2.1.1) obeys an additional conservation law where a admissible entropy function $U(\mathbf{u})$ is balanced by entropy fluxes $F(\mathbf{u})$ and $G(\mathbf{u})$.

$$\frac{\partial}{\partial t}U(\mathbf{u}) + \frac{\partial}{\partial x}F(\mathbf{u}) = 0. \tag{2.1.2}$$

Here U and F are sufficiently smooth functions from Ω into $\mathbb{R}$. We may restrict ourselves to *convex* entropy functions due to the fundamental connection between hyperbolicity and the strict convexity of entropy function [God61, Moc80]. Specifically, an entropy function $U(\mathbf{u})$ is said to be strictly convex entropy function associated with the system (2.1.1) if the Hessian matrix $U_{\mathbf{uu}}$ is positive definite, and this Hessian matrix symmetrizes the system (2.1.1) upon multiplication 'on the right', [FL71]

$$\mathbf{f_u}(U_{\mathbf{uu}})^{-1} = \left[\mathbf{f_u}(U_{\mathbf{uu}})^{-1}\right]^{\top}. \tag{2.1.3}$$

Alternatively, this symmetrization can also be carried out by multiplication 'on the left', where (2.1.3) is replaced by the equivalent statement,

$$U_{\mathbf{uu}}\mathbf{f_u} = [U_{\mathbf{uu}}\mathbf{f_u}]^{\top}.$$

The Euler equations (4.1.5) of gas dynamics are viewed as a prototype example for such systems, with the three conservative variables $\mathbf{u} = \left[\rho, m, E\right]^{\top}$ balanced by the flux $\mathbf{f} = \left[m, qm + p, q(E + p)\right]^{\top}$ and endowed with entropy pairs $(U, F) = \left(-\rho h(S), -mh(S)\right)$. We now briefly recall the circle of ideas linking the dissipation of the total entropy, $\int_x U(\mathbf{u}(\cdot, t))dx$, and the realization of $\mathbf{u}$ as a vanishing viscosity

limit, in analogy to the vanishing Navier-Stokes limits and their relation to entropic solutions of the Euler equations. We refer to e.g., [Liu91] and [Daf00], for a more comprehensive discussion.

Let $(U(\mathbf{u}), F(\mathbf{u}))$ be a given entropy pair associated with (2.1.1). Note that $U(\mathbf{u})$ satisfies the entropy equality (2.1.2) if and only if it is linked to an entropy flux function $F(\mathbf{u})$ through the compatibility relation

$$U_{\mathbf{u}}^{\top} \mathbf{f_u} = F_{\mathbf{u}}^{\top}. \tag{2.1.4}$$

Indeed, multiplying (2.1.1) by $U_{\mathbf{u}}^{\top}$ on the left, one recovers the equivalence between (2.1.2) and (2.1.4) for all $\mathbf{u}$'s solving (2.1.1). Of course, these formal manipulations are valid only under the smooth regime. To justify these steps in the presence of shock discontinuities, the conservation law (2.1.1) is realized by appropriate vanishing viscosity limits. To this end, we define the *entropy variables* $\mathbf{v}(\mathbf{u}) := U_{\mathbf{u}}(\mathbf{u})$. Because of the additional assumption that the entropy $U(\mathbf{u})$ is strictly *convex*, the nonlinear mapping $\mathbf{u} \mapsto \mathbf{v}$ is a one-to-one. Following, [God61, Moc80], we claim that the change of variables, $\mathbf{u} = \mathbf{u}(\mathbf{v})$, puts the system (2.1.1) into the equivalent *symmetric* form,

$$\frac{\partial}{\partial t}\mathbf{u}(\mathbf{v}) + \frac{\partial}{\partial x}\mathbf{f}(\mathbf{u}(\mathbf{v})) = 0. \tag{2.1.5}$$

The system (2.1.5) is symmetric in the sense that the Jacobian matrices of fluxes

are symmetric, namely[1],

$$\mathbf{u_v}(\mathbf{v}) = \big(\mathbf{u_v}(\mathbf{v})\big)^\top \quad \text{and} \quad \mathbf{f_v}(\mathbf{v}) = \big(\mathbf{f_v}(\mathbf{v})\big)^\top. \tag{2.1.6}$$

Indeed, a straightforward computation utilizing the compatibility relation (2.1.4), shows that $\mathbf{u}(\mathbf{v})$ and $\mathbf{f}(\mathbf{v})$ are, respectively, the gradients of the corresponding potential functions, ϕ and ψ,

$$\mathbf{u}(\mathbf{v}) = \phi_\mathbf{v}(\mathbf{v}), \quad \phi(\mathbf{v}) := \langle \mathbf{v}, \mathbf{u}(\mathbf{v}) \rangle - U(\mathbf{u}(\mathbf{v})), \tag{2.1.7}$$

$$\mathbf{f}(\mathbf{v}) = \psi_\mathbf{v}(\mathbf{v}), \quad \psi(\mathbf{v}) := \langle \mathbf{v}, \mathbf{f}(\mathbf{v}) \rangle - F(\mathbf{u}(\mathbf{v})). \tag{2.1.8}$$

Hence the Jacobian matrices $H(\mathbf{v}) := \mathbf{u_v}(\mathbf{v})$ and $B(\mathbf{v}) := \mathbf{f_v}(\mathbf{v})$ in (2.1.6) are symmetric, being Hessians of the potentials $\phi(\mathbf{v})$ and $\psi(\mathbf{v})$. Moreover, the convexity of $U(\cdot)$ implies that H is positive definite, $H = (U_{\mathbf{uu}})^{-1} > 0$.

Physically relevant solutions of (2.1.1) are postulated as limits of the vanishing viscosity solutions $\mathbf{u}^\epsilon$, as ϵ tends to zero,

$$\frac{\partial}{\partial t}\mathbf{u}^\epsilon + \frac{\partial}{\partial x}\mathbf{f}(\mathbf{u}^\epsilon) = \epsilon \frac{\partial^2}{\partial x^2}\mathbf{d}(\mathbf{u}^\epsilon), \tag{2.1.9}$$

where $\mathbf{d}(\mathbf{u})$ is any *admissible* dissipative flux, and $\epsilon \downarrow 0$ stands for vanishing amplitudes such as the viscosity coefficients λ, μ, the heat conductivity κ, etc. Here, the admissibility of the dissipative flux requires the Jacobian $\mathbf{d_u}$ to be H-symmetric positive-definite, that is,

$$\mathbf{d}_H = (\mathbf{d}_H)^\top \geq 0, \quad \mathbf{d}_H := \mathbf{d_u}H. \tag{2.1.10}$$

---

[1]For brevity of notation we often write $\mathbf{f}(\mathbf{v})$ for $\mathbf{f}(\mathbf{u}(\mathbf{v}))$ whenever the different dependence of $\mathbf{f}(\mathbf{u})$ and $\mathbf{f}(\mathbf{v})$ is made clear by the distinction between the conservative variables $\mathbf{u}$ and entropy variables $\mathbf{v}$.

If we express the dissipation flux in terms of the entropy variables, $\mathbf{d}(\mathbf{v}) = \mathbf{d}(\mathbf{u}(\mathbf{v}))$, then admissibility requires that the $\mathbf{v}$-Jacobian of this flux will be positive symmetric, $\mathbf{d}_H = \mathbf{d_v}(\mathbf{v}) = \mathbf{d_v^\top}(\mathbf{v}) \geq 0$. Thus, in this case (2.1.9) reads

$$\frac{\partial}{\partial t}\mathbf{u}(\mathbf{v}^\epsilon) + \frac{\partial}{\partial x}\mathbf{f}(\mathbf{v}^\epsilon) = \epsilon\frac{\partial^2}{\partial x^2}\mathbf{d}(\mathbf{v}^\epsilon),$$

and all $\mathbf{v}$-dependent fluxes — the temporal, spatial and the dissipation flux have symmetric Jacobains.

We now integrate (2.1.9) against $\mathbf{v}^\top = U_\mathbf{u}^\top$, employ the compatibility relation $U_\mathbf{u}^\top \mathbf{f}_x = F_x^\top$ and use 'differentiation by parts' on the admissible dissipation on the right hand side to find

$$\frac{\partial}{\partial t}U(\mathbf{u}^\epsilon) + \frac{\partial}{\partial x}\left(F^\epsilon(\mathbf{u}^\epsilon) - \epsilon\langle\mathbf{v}^\epsilon, \mathbf{d}(\mathbf{u}^\epsilon)_x\rangle\right) = -\epsilon\langle\mathbf{v}_x^\epsilon, \mathbf{d_v}\mathbf{v}_x^\epsilon\rangle \leq 0. \qquad (2.1.11)$$

Letting $\epsilon \downarrow 0$, we obtain that $\mathbf{u}$ will also satisfy, in the sense of distributions, the *entropy inequality*, [Lax73]

$$\frac{\partial}{\partial t}U(\mathbf{u}) + \frac{\partial}{\partial x}F(\mathbf{u}) \leq 0. \qquad (2.1.12)$$

Here, the passage $\mathbf{u}^\epsilon \to \mathbf{u}$ is required to be strong. In fact, statement (2.1.12) is the generalization of the entropy decay statements in the second law of thermodynamics.

2.2 Entropy conservative schemes

Let's consider the Cauchy problem for a general hyperbolic system of conservation laws (2.1.1),

$$\begin{cases} \dfrac{\partial\mathbf{u}}{\partial t} + \dfrac{\partial}{\partial x}\mathbf{f}(\mathbf{u}) = 0 \quad , \quad x \in \mathbb{R},\ t > 0 \\[2mm] u(x, 0) = u_0(x) \end{cases}$$

21

We turn our attention to consistent approximations of (2.1.1), based on semi-discrete conservative schemes of the form

$$\frac{d}{dt}\mathbf{u}_\nu(t) = -\frac{1}{\Delta x_\nu}\left(\mathbf{f}_{\nu+\frac{1}{2}} - \mathbf{f}_{\nu-\frac{1}{2}}\right). \qquad (2.2.1)$$

Here, $\mathbf{u}_\nu(t)$ denotes the discrete solution along the grid line (x_ν, t), $\Delta x_\nu := \frac{x_{\nu+1} - x_{\nu-1}}{2}$ is the possibly variable mesh spacing and $\mathbf{f}_{\nu+\frac{1}{2}}$ is the Lipschitz-continuous numerical flux which occupies a stencil of $2p$-gridvalues,

$$\mathbf{f}_{\nu+\frac{1}{2}} = \mathbf{f}(\mathbf{u}_{\nu-p+1}, \cdots, \mathbf{u}_{\nu+p}).$$

The scheme is said to be consistent with the system (2.1.1) if $\mathbf{f}$ satisfies

$$\mathbf{f}(\mathbf{u}, \mathbf{u}, \cdots, \mathbf{u}) = \mathbf{f}(\mathbf{u}), \quad \forall \mathbf{u} \in \mathbb{R}^N.$$

By making the changes of variables $\mathbf{u}_\nu = \mathbf{u}(\mathbf{v}_\nu)$, we obtain the equivalent form of (2.2.1)

$$\frac{d}{dt}\mathbf{u}(\mathbf{v}_\nu(t)) = -\frac{1}{\Delta x_\nu}\left(\mathbf{f}_{\nu+\frac{1}{2}} - \mathbf{f}_{\nu-\frac{1}{2}}\right). \qquad (2.2.2)$$

The essential difference lies with the numerical flux, $\mathbf{f}_{\nu+\frac{1}{2}}$, which is now expressed in terms of the entropy variables,

$$\mathbf{f}_{\nu+\frac{1}{2}} = \mathbf{f}\left(\mathbf{v}_{\nu-p+1}, \cdots, \mathbf{v}_{\nu+p}\right) := \mathbf{f}\left(\mathbf{u}\left(\mathbf{v}_{\nu-p+1}\right), \cdots, \mathbf{u}\left(\mathbf{v}_{\nu+p}\right)\right),$$

consistent with the differential flux,

$$\mathbf{f}(\mathbf{v}, \mathbf{v}, \cdots, \mathbf{v}) = \mathbf{f}(\mathbf{v}) \equiv \mathbf{f}(\mathbf{u}(\mathbf{v})). \qquad (2.2.3)$$

The semi-discrete schemes (2.2.1) and (2.2.2) are completely identical. It proved useful, however, to work with the entropy variables rather than the usual conservative ones, since system (2.1.1) is symmetrized with respect to these entropy

variables. The entropy variables-based formula (2.2.2) has the advantage that it provides a natural ordering of symmetric matrices, which in turn enables us to *compare* the numerical viscosities of different schemes, consult [Tad84b, Tad87] for details. In particular, we will be able to utilize the entropy conservative discretization of [Tad03] for the convective part of the system of conservation laws eq(2.1.1), and thus recover the precise entropy balance dictated by physical dissipative terms in the original systems.

Let (U, F) be a given entropy pair associated with the system (2.1.1). Physical relevance of numerical solutions requires that the scheme (2.2.1) is *entropy-stable* with respect to such a entropy pair, in the sense of satisfying a discrete entropy inequality analogous to (2.1.12), that is

$$\frac{d}{dt}U(\mathbf{u}_\nu(t)) + \frac{1}{\Delta x_\nu}(F_{\nu+\frac{1}{2}} - F_{\nu-\frac{1}{2}}) \leq 0. \tag{2.2.4}$$

In particular, when equality holds in (2.2.4), the scheme (2.2.1) is *entropy-conservative.* Here we proceed with the construction of an entropy conservative scheme, in the sense of satisfying a discrete *entropy equality* analogous to (2.1.2),

$$\frac{d}{dt}U(\mathbf{u}_\nu(t)) + \frac{1}{\Delta x_\nu}\left(F_{\nu+\frac{1}{2}} - F_{\nu-\frac{1}{2}}\right) = 0. \tag{2.2.5}$$

Here, $F_{\nu+\frac{1}{2}} = F(\mathbf{u}_{\nu-p+1}, \cdots, \mathbf{u}_{\nu+p})$ is a consistent numerical entropy flux, such that $F(\mathbf{u}, \mathbf{u}, \cdots, \mathbf{u}) = F(\mathbf{u})$, $\forall \mathbf{u} \in \mathbb{R}^N$. The numerical flux of such entropy conservative schemes will play an essential role in the construction of entropy stable schemes, by adding a judicious amount of physical viscosity. The results of entropy-stability of the numerical schemes were concluded in [Tad87][Theorem 5.2], which states,

Theorem 2.2.1 (Tadmor1987, Theorem 5.2). *The conservative scheme* (2.2.1) *is entropy-stable (respectively, entropy-conservative) if, and for three-point schemes* ($p = 1$) *only if,*

$$\left\langle \Delta \mathbf{v}_{\nu+\frac{1}{2}}, \mathbf{f}_{\nu+\frac{1}{2}} \right\rangle \leq \Delta \psi_{\nu+\frac{1}{2}}, \tag{2.2.6}$$

and, respectively,

$$\left\langle \Delta \mathbf{v}_{\nu+\frac{1}{2}}, \mathbf{f}_{\nu+\frac{1}{2}} \right\rangle = \Delta \psi_{\nu+\frac{1}{2}}. \tag{2.2.7}$$

Here, $\Delta \mathbf{v}_{\nu+\frac{1}{2}} := \mathbf{v}_{\nu+1} - \mathbf{v}_\nu$ *and* $\Delta \psi_{\nu+\frac{1}{2}} := \psi(\mathbf{v}_{\nu+1}) - \psi(\mathbf{v}_\nu)$ *denote the differences of entropy variable and entropy flux potential respectively.*

Sketch of the Proof. The proof is based on the identity

$$\frac{d}{dt} U(\mathbf{u}_\nu(t)) + \frac{1}{\Delta x_\nu}(F_{\nu+\frac{1}{2}} - F_{\nu-\frac{1}{2}}) = \frac{1}{2}\left[\left\langle \Delta \mathbf{v}_{\nu+\frac{1}{2}}, \mathbf{f}_{\nu+\frac{1}{2}} \right\rangle - \Delta \psi_{\nu+\frac{1}{2}}\right]$$
$$+ \frac{1}{2}\left[\left\langle \Delta \mathbf{v}_{\nu-\frac{1}{2}}, \mathbf{f}_{\nu-\frac{1}{2}} \right\rangle - \Delta \psi_{\nu-\frac{1}{2}}\right], \tag{2.2.8}$$

where the consistent entropy flux is defined in the following,

$$F_{\nu+\frac{1}{2}} := \frac{1}{2}\left\langle [\mathbf{v}_\nu + \mathbf{v}_{\nu+1}], \mathbf{f}_{\nu+\frac{1}{2}} \right\rangle - \frac{1}{2}\left[\psi(\mathbf{v}_\nu) - \psi(\mathbf{v}_{\nu+1})\right].$$

□

In the scalar case, entropy-conservative schemes are unique with respect to a given entropy pair. For the systems, there are various choices for the entropy conservative numerical fluxes which meet the entropy-conservative requirement (2.2.7). The key step in the construction of entropy conservative schemes for the systems of conservation laws is the choice of an *arbitrary* piecewise-constant path in phase space of the entropy variable $\mathbf{v}$, connecting two neighboring gridvalues $\mathbf{v}_\nu$ and $\mathbf{v}_{\nu+1}$ through

24

the intermediate states $\{\mathbf{v}_{\nu+\frac{1}{2}}^j\}_{j=1}^N$ at the spatial cell $[x_\nu, x_{\nu+1}]$. Let $\{\mathbf{r}_{\nu+\frac{1}{2}}^j\}_{j=1}^N$ be an arbitrary set of N linearly independent N-vectors, and let $\{\boldsymbol{\ell}_{\nu+\frac{1}{2}}^j\}_{j=1}^N$ be the corresponding orthogonal set. We introduce the intermediate gridvalues $\{\mathbf{v}_{\nu+\frac{1}{2}}^j\}_{j=1}^N$, which define a piecewise constant path in phase space

$$
\begin{cases}
\mathbf{v}_{\nu+\frac{1}{2}}^1 = \mathbf{v}_\nu \\[2mm]
\mathbf{v}_{\nu+\frac{1}{2}}^{j+1} = \mathbf{v}_{\nu+\frac{1}{2}}^j + \left\langle \boldsymbol{\ell}_{\nu+\frac{1}{2}}^j, \Delta\mathbf{v}_{\nu+\frac{1}{2}} \right\rangle \mathbf{r}_{\nu+\frac{1}{2}}^j, \quad j = 1, 2, \cdots, N-1, \cdot \\[2mm]
\mathbf{v}_{\nu+\frac{1}{2}}^{N+1} = \mathbf{v}_{\nu+1}
\end{cases}
\tag{2.2.9}
$$

Theorem 2.2.2 (Tadmor2004, Theorem 6.1). *Consider the system of conservation laws (2.1.1). Given the entropy pair (U, F), then the conservative scheme*

$$
\frac{d}{dt}\mathbf{u}_\nu(t) = -\frac{1}{\Delta x_\nu}\left(\mathbf{f}_{\nu+\frac{1}{2}}^* - \mathbf{f}_{\nu-\frac{1}{2}}^*\right)
\tag{2.2.10}
$$

with a numerical flux $\mathbf{f}_{\nu+\frac{1}{2}}^*$

$$
\mathbf{f}_{\nu+\frac{1}{2}}^* = \sum_{j=1}^N \frac{\psi\left(\mathbf{v}_{\nu+\frac{1}{2}}^{j+1}\right) - \psi\left(\mathbf{v}_{\nu+\frac{1}{2}}^j\right)}{\left\langle \boldsymbol{\ell}_{\nu+\frac{1}{2}}^j, \Delta\mathbf{v}_{\nu+\frac{1}{2}} \right\rangle}\boldsymbol{\ell}_{\nu+\frac{1}{2}}^j
\tag{2.2.11}
$$

is an entropy-conservative approximation, consistent with (2.1.1),(2.1.2). Here, $\mathbf{v}$ are the entropy variables, $\mathbf{v} = U_{\mathbf{u}}(\mathbf{u})$ and $\psi(\mathbf{v})$ is the entropy potential (2.1.8)

$\psi(\mathbf{v}) = \langle \mathbf{v}, \mathbf{f}(\mathbf{u}(\mathbf{v})) \rangle - F(\mathbf{u}(\mathbf{v}))$.

The proof is based on the requirement of entropy conservation in (2.2.7),

$$
\left\langle \Delta\mathbf{v}_{\nu+\frac{1}{2}}, \mathbf{f}_{\nu+\frac{1}{2}}^* \right\rangle = \Delta\psi_{\nu+\frac{1}{2}}.
\tag{2.2.12}
$$

The numerical flux (2.2.11) satisfies this entropy conservation requirement, for

$$
\left\langle \Delta\mathbf{v}_{\nu+\frac{1}{2}}, \mathbf{f}_{\nu+\frac{1}{2}}^* \right\rangle = \sum_{j=1}^N \frac{\psi\left(\mathbf{v}_{\nu+\frac{1}{2}}^{j+1}\right) - \psi\left(\mathbf{v}_{\nu+\frac{1}{2}}^j\right)}{\left\langle \boldsymbol{\ell}_{\nu+\frac{1}{2}}^j, \Delta\mathbf{v}_{\nu+\frac{1}{2}} \right\rangle}\left\langle \boldsymbol{\ell}_{\nu+\frac{1}{2}}^j, \Delta\mathbf{v}_{\nu+\frac{1}{2}} \right\rangle
$$

$$
= \sum_{j=1}^N \psi\left(\mathbf{v}_{\nu+\frac{1}{2}}^{j+1}\right) - \psi\left(\mathbf{v}_{\nu+\frac{1}{2}}^j\right) = \psi\left(\mathbf{v}_{\nu+\frac{1}{2}}^{N+1}\right) - \psi\left(\mathbf{v}_{\nu+\frac{1}{2}}^1\right) = \Delta\psi_{\nu+\frac{1}{2}}.
$$

In addition, $\mathbf{f}^*_{\nu+\frac{1}{2}}$ is a consistent flux satisfying (2.2.3). Indeed, if we let $\mathbf{v}^{j+\frac{1}{2}}_{\nu+\frac{1}{2}}(\xi)$ denote intermediate path, $\mathbf{v}^{j+\frac{1}{2}}_{\nu+\frac{1}{2}}(\xi) := \left(\mathbf{v}^j_{\nu+\frac{1}{2}} + \mathbf{v}^{j+1}_{\nu+\frac{1}{2}}\right)/2 + \xi\left\langle \boldsymbol{\ell}^j_{\nu+\frac{1}{2}}, \Delta\mathbf{v}_{\nu+\frac{1}{2}}\right\rangle \mathbf{r}^j_{\nu+\frac{1}{2}}$ connecting $\mathbf{v}^j_{\nu+\frac{1}{2}}$ and $\mathbf{v}^{j+1}_{\nu+\frac{1}{2}}$, then by (2.1.8), we have

$$\psi\left(\mathbf{v}^{j+1}_{\nu+\frac{1}{2}}\right) - \psi\left(\mathbf{v}^j_{\nu+\frac{1}{2}}\right) = \int_{\xi=-\frac{1}{2}}^{\frac{1}{2}} \frac{d}{d\xi}\psi\left(\mathbf{v}^{j+\frac{1}{2}}_{\nu+\frac{1}{2}}(\xi)\right)\,d\xi$$

$$= \left\langle \int_{\xi=-\frac{1}{2}}^{\frac{1}{2}} \mathbf{f}\left(\mathbf{v}^{j+\frac{1}{2}}_{\nu+\frac{1}{2}}(\xi)\right)\,d\xi, \mathbf{r}^j_{\nu+\frac{1}{2}}\right\rangle \left\langle\boldsymbol{\ell}^j_{\nu+\frac{1}{2}}, \Delta\mathbf{v}_{\nu+\frac{1}{2}}\right\rangle.$$

Inserted into (2.2.11), we can rewrite the entropy-conservative flux (2.2.11) in the equivalent form

$$\mathbf{f}^*_{\nu+\frac{1}{2}} = \sum_{j=1}^N \left\langle \int_{\xi=-\frac{1}{2}}^{\frac{1}{2}} \mathbf{f}\left(\mathbf{v}^{j+\frac{1}{2}}_{\nu+\frac{1}{2}}(\xi)\right)\,d\xi, \mathbf{r}^j_{\nu+\frac{1}{2}}\right\rangle \boldsymbol{\ell}^j_{\nu+\frac{1}{2}}, \qquad (2.2.13)$$

and the consistency relation (2.2.3) now follows,

$$\mathbf{f}^*(\mathbf{v}, \mathbf{v}) = \sum_{j=1}^N \left\langle \mathbf{f}(\mathbf{v}), \mathbf{r}^j_{\nu+\frac{1}{2}}\right\rangle \boldsymbol{\ell}^j_{\nu+\frac{1}{2}} = \mathbf{f}(\mathbf{v}).\square$$

We emphasize that the recipe for construction entropy-conservative fluxes in (2.2.11) allows an *arbitrary* choice of a path in phase space. We demonstrate this recipe with three examples.

Example 2.2.1. Set $\{\mathbf{r}^j\}$ along the standard Cartesian coordinates, $\mathbf{r}^j_{\nu+\frac{1}{2}} = \mathbf{e}_j$, $j = 1, 2, \ldots, N$. In this case we have

$$\mathbf{v}^j_{\nu+\frac{1}{2}} = \left[(\mathbf{v}_{\nu+1})_1, \ldots, (\mathbf{v}_{\nu+1})_{j-1}, (\mathbf{v}_\nu)_j, \ldots, (\mathbf{v}_\nu)_N\right], \quad j = 2, 3, \ldots, N-1,$$

and the entropy conservative flux (2.2.11) is given by the particularly simple explicit formula

$$\mathbf{f}^*_{\nu+\frac{1}{2}} = \left[\frac{\psi\big(\mathbf{v}^2_{\nu+\frac{1}{2}}\big) - \psi\big(\mathbf{v}_\nu\big)}{\big(\mathbf{v}_{\nu+1}\big)_1 - \big(\mathbf{v}_\nu\big)_1}, \ldots, \frac{\psi\big(\mathbf{v}^{j+1}_{\nu+\frac{1}{2}}\big) - \psi\big(\mathbf{v}^j_{\nu+\frac{1}{2}}\big)}{\big(\mathbf{v}_{\nu+1}\big)_j - \big(\mathbf{v}_\nu\big)_j}, \ldots, \frac{\psi\big(\mathbf{v}_{\nu+1}\big) - \psi\big(\mathbf{v}^N_{\nu+\frac{1}{2}}\big)}{\big(\mathbf{v}_{\nu+1}\big)_N - \big(\mathbf{v}_\nu\big)_N} \right]^\top .$$

$$(2.2.14)$$

We carried out numerical experiments with these fluxes for the approximate solution of Euler and Navier-Stokes equations. The formulation is particularly simple though the computed intermediate values might lie outside the physical space $\rho, p > 0$.

Example 2.2.2. A more 'physically relevant' choice than the Cartesian path is offered by a Riemann path which consists of $\{\mathbf{u}^j_{\nu+\frac{1}{2}}\}^N_{j=1}$, stationed along an (approximate) set of right eigenvectors, $\{\widehat{\mathbf{r}}^j_{\nu+\frac{1}{2}}\}$, of the Jacobian $\mathbf{f}_\mathbf{u}(\mathbf{u}_{\nu+\frac{1}{2}})$. Set $\mathbf{v}^j_{\nu+\frac{1}{2}} = \mathbf{v}(\mathbf{u}^j_{\nu+\frac{1}{2}})$, $j = 1, 2, \ldots, N$, and let $\boldsymbol{\ell}^j$'s be the orthogonal system to $\{\mathbf{v}^{j+1} - \mathbf{v}^j\}^N_{j=1}$. This will be our choice of a path for computing entropy stable approximations of Navier-Stokes equations in section 4.4.1 below. The resulting flux, mixing conservative and entropy variables, admits the somewhat simpler form

$$\mathbf{f}^*_{\nu+\frac{1}{2}} = \sum_{j=1}^N \frac{\psi\left(\mathbf{u}^{j+1}_{\nu+\frac{1}{2}}\right) - \psi\left(\mathbf{u}^j_{\nu+\frac{1}{2}}\right)}{\left\langle \boldsymbol{\ell}^j_{\nu+\frac{1}{2}}, \Delta\mathbf{v}_{\nu+\frac{1}{2}} \right\rangle} \boldsymbol{\ell}^j_{\nu+\frac{1}{2}} \quad \text{where} \quad \psi(\mathbf{u}) = U_\mathbf{u}^\top \mathbf{f}(\mathbf{u})\rangle - F(\mathbf{u}) \quad (2.2.15)$$

Example 2.2.3. If all $\mathbf{r}^j$'s are chosen to approach the same direction of $\Delta\mathbf{v}_{\nu+\frac{1}{2}}$, then by (2.2.13) the flux (2.2.13) 'collapses' to the entropy-conservative flux

$$\mathbf{f}^*_{\nu+\frac{1}{2}} = \int_{\xi=-\frac{1}{2}}^{\frac{1}{2}} \mathbf{f}\left(\mathbf{v}_{\nu+\frac{1}{2}}(\xi)\right) d\xi, \quad \mathbf{v}_{\nu+\frac{1}{2}}(\xi) := \frac{1}{2}(\mathbf{v}_\nu + \mathbf{v}_{\nu+1}) + \xi\Delta\mathbf{v}_{\nu+\frac{1}{2}}. \quad (2.2.16)$$

The resulting flux (2.2.16) was introduced in [Tad86] and was the forerunner for the family of entropy conservative fluxes outlined in theorem 2.2.2. It has the drawback, however, that its evaluation requires a nonlinear integration in phase space. Thus,

27

with the loss of linear independence, we lose here the *explicit* evaluation of the entropy conservative flux offered in (2.2.11) and demonstrated in the previous two examples.

Chapter 3

The Burgers' Equation

3.1   Entropy conservative schemes

Burgers' equation([Bur48]) is a fundamental first-order nonlinear partial differential equation from fluid mechanics. Though very simple, it provides a model of wave processes in acoustics and hydrodynamics. Burgers equation is a prototype of the equations whose solutions can develop discontinuities. Due to its simplicity and predictable dynamics, Burgers equation is often used as the test case for numerical methods.

We begin with the inviscid Burgers' equation as a prototype of the nonlinear scalar conservation law,

$$\frac{\partial u}{\partial t} + \frac{\partial}{\partial x} f(u) = 0, \quad f(u) = \frac{1}{2} u^2. \tag{3.1.1}$$

(3.1.1) describes the evolution of the field $u = u(x, t)$ under the nonlinear advection. Any convex function $U(u)$ serves as an entropy function for the scalar Burgers equation. Here we consider a family of entropy functions,

$$U_p(u) = u^{2p} \quad p = 1, 2, \cdots, \tag{3.1.2}$$

so that solutions of (3.1.1) satisfy, at the *formal* level,

$$\frac{\partial}{\partial t} U_p(u) + \frac{\partial}{\partial x} F_p(u) = 0. \tag{3.1.3}$$

29

These are additional conservation laws balanced by the corresponding entropy flux functions $F_p(u) = 2pu^{2p+1}/(2p+1)$ satisfying the compatibility relation $U_p'f' = F_p'$. Spatial integration then yields the total entropy conservation (ignoring boundary contributions)

$$\int_x u^{2p}(x,t)\,dx = \int_x u^{2p}(x,0)\,dx. \qquad (3.1.4)$$

We now turn to the discrete framework. Discretization in space yields the semi-discrete scheme,

$$\frac{d}{dt}u_\nu(t) + \frac{1}{\Delta x}\left(f_{\nu+\frac{1}{2}} - f_{\nu-\frac{1}{2}}\right) = 0. \qquad (3.1.5)$$

Here, $u_\nu(t)$ denotes the discrete solution along the gridline $(x_\nu,\, t)$ with $x_\nu := \nu\Delta x$, Δx being the uniform meshsize, and $f_{\nu+\frac{1}{2}}$ is a consistent numerical flux based on a stencil of $2r+1$ neighboring grid values, that is

$$f_{\nu+\frac{1}{2}} := f(u_{\nu-r+1}, \cdots, u_{\nu+r}), \quad f(u, u, \cdots, u) = f(u).$$

This numerical flux makes (3.1.5) conservative in the sense that

$$\sum_\nu u_\nu(t)\Delta x = \sum_\nu u_\nu(0)\Delta x.$$

Fix p. We seek a semi-discrete scheme that conserves the entropy $U_p(u) = u^{2p}$ in the sense of satisfying the discrete analogue of (3.1.3),

$$\frac{d}{dt}U_p(u_\nu(t)) + \frac{1}{\Delta x}(F_{\nu+\frac{1}{2}} - F_{\nu-\frac{1}{2}}) = 0.$$

Here, $F_{\nu+\frac{1}{2}}$ is a consistent numerical entropy flux,

$$F_{\nu+\frac{1}{2}} := F(u_{\nu-r+1}, \cdots, u_{\nu+r}), \quad F(u, u, \cdots, u) = F(u).$$

According to (2.2.7), such 3-point scalar *entropy conservative* schemes are uniquely determined by the entropy conservative numerical flux $f_{\nu+\frac{1}{2}} = f^*_{\nu+\frac{1}{2}}$ given by,

$$f_{\nu+\frac{1}{2}} = f^*_{\nu+\frac{1}{2}} := \frac{\psi(u_{\nu+1}) - \psi(u_\nu)}{v(u_{\nu+1}) - v(u_\nu)} = \frac{2p-1}{2(2p+1)} \cdot u_\nu^2 \cdot \frac{(u_{\nu+1}/u_\nu)^{2p+1} - 1}{(u_{\nu+1}/u_\nu)^{2p-1} - 1}. \qquad (3.1.6)$$

Recall that $v(u) := U'(u) = 2pu^{2p-1}$ is the entropy variable associated with the entropy $U(u) = u^{2p}$, and $\psi(u) := v(u)f(u) - F(u) = \frac{p(2p-1)}{2p+1}u^{2p+1}$ is the potential function of the flux $f(u(v))$. The resulting scheme (3.1.5), (3.1.6) is entropy conservative in the sense that the discrete analogue of total entropy conservation (3.1.4) is satisfied,

$$\sum_\nu u_\nu^{2p}(t)\,\Delta x = \sum_\nu u_\nu^{2p}(0)\,\Delta x.$$

Indeed, we multiply the scheme (3.1.5) by entropy variable $v_\nu = U'_p(u_\nu) = 2pu_\nu^{2p-1}$, then sum up all spatial cells to get the total entropy balance statement,

$$\frac{d}{dt}\sum_\nu U_\nu(t)\Delta x + \sum_\nu v_\nu(f^*_{\nu+\frac{1}{2}} - f^*_{\nu-\frac{1}{2}}) = 0. \qquad (3.1.7)$$

Since $f^*_{\nu+\frac{1}{2}}$ are chosen to be the entropy conservative numerical fluxes, the second term on the left becomes the perfect conservative difference which will vanish after the summation over all spatial cells. Indeed, a straightforward manipulation on the entropy conservation requirement (2.2.7) yields the conservative difference,

$$v_\nu(f^*_{\nu+\frac{1}{2}} - f^*_{\nu-\frac{1}{2}}) = F_{\nu+\frac{1}{2}} - F_{\nu-\frac{1}{2}} \qquad (3.1.8)$$

where $F_{\nu+\frac{1}{2}} = (v_\nu + v_{\nu+1})f^*_{\nu+\frac{1}{2}} - (\psi_\nu + \psi_{\nu+1})$ is the discrete entropy flux. Of course, all the above manipulations are at the formal level.

To recover the physical relevant *entropy inequality*, that is

$$\partial_t U_p(u) + \partial_x F_p(u) \leq 0,$$

31

one can add numerical dissipation,

$$\frac{d}{dt}u_\nu(t) + \frac{1}{\Delta x}\left(f^*_{\nu+\frac{1}{2}} - f^*_{\nu-\frac{1}{2}}\right) = \frac{\epsilon}{(\Delta x)^2}\left(d(u_{\nu+1}) - 2d(u_\nu) + d(u_{\nu-1})\right), \quad \epsilon > 0.$$

(3.1.9)

This serves as an approximation to the vanishing viscosity regularization

$$u_t + f(u)_x = \epsilon d(u)_{xx}, \quad d'(u) > 0, \ \epsilon > 0.$$

Sum this scheme (3.1.9) against the entropy variable v_ν,

$$\frac{d}{dt}\sum_\nu U_p(u_\nu(t))\Delta x + \sum_\nu v_\nu\left(f^*_{\nu+\frac{1}{2}} - f^*_{\nu-\frac{1}{2}}\right) = \epsilon\sum_\nu v_\nu\frac{d(u_{\nu+1}) - 2d(u_\nu) + d(u_{\nu-1})}{\Delta x}.$$

(3.1.10)

Due to the same reason indicated in (3.1.8), the second term on the left of (3.1.10) vanishes. The summation by parts on the RHS of (3.1.10) yields

$$\epsilon\sum_\nu v_\nu\frac{d(u_{\nu+1}) - 2d(u_\nu) + d(u_{\nu-1})}{\Delta x} = -\frac{\epsilon}{\Delta x}\sum_\nu (v_{\nu+1} - v_\nu)(d(u_{\nu+1}) - d(u_\nu))$$

$$= -\frac{\epsilon}{\Delta x}\sum_\nu (\Delta v_{\nu+\frac{1}{2}})^2\frac{\Delta d_{\nu+\frac{1}{2}}}{\Delta v_{\nu+\frac{1}{2}}} \leq 0,$$

since $\frac{\Delta d_{\nu+\frac{1}{2}}}{\Delta v_{\nu+\frac{1}{2}}} := \frac{d(u_{\nu+1}) - d(u_\nu)}{v_{\nu+1} - v_\nu} > 0$ for $d'(u) > 0$. The resulting entropy balance that follows reads,

$$\frac{d}{dt}\sum_\nu U_p(u_\nu(t))\Delta x = -\frac{\epsilon}{\Delta x}\sum_\nu \frac{\Delta d_{\nu+\frac{1}{2}}}{\Delta v_{\nu+\frac{1}{2}}}(\Delta v_{\nu+\frac{1}{2}})^2 \leq 0.$$

(3.1.11)

The above entropy decay statement is the discrete analogue of the entropy balance statement (2.1.11) indeed. Observe that the amount of entropy dissipation on the right is completely determined by the dissipation term $\epsilon d(u)$. No artificial viscosity is introduced by the convective term. If we exclude any dissipative mechanism

($\epsilon = 0$), the entropy conservative solutions admit dispersive oscillations interesting for their own sake, consult [Lax86, LL96].

Remark 3.1.1. As I will show you in the following numerical results, these entropy conservative schemes work better in terms of oscillations for large p. In fact, as $p \uparrow \infty$, the limit of these schemes is the first order Engquist-Osher scheme [EO80] which is independent of the different choices of entropy variables. As a matter of fact, when p increases, the control of a constant entropy,

$$U_p = \left[\sum_\nu u_\nu^{2p}(t) \, \Delta x \right]^{\frac{1}{2p}} \tag{3.1.12}$$

approaches the control of L^∞-norm of the solutions.

3.2 Time discretization

To complete the computation of a semi-discrete scheme, the semi-discrete entropy conservative scheme (3.1.5),(3.1.6) needs to be augmented with a proper time discretization. To enable a large time-stability region and maintain simplicity, the explicit three-stage third-order Runge-Kutta (RK3) method will be used, consult [GST01],

$$\begin{cases} u^{(1)} & = u^n + \Delta t L(u^n) \\[2mm] u^{(2)} & = \frac{3}{4}u^n + \frac{1}{4}u^{(1)} + \frac{1}{4}\Delta t L(u^{(1)}) \\[2mm] u^{n+1} & = \frac{1}{3}u^n + \frac{2}{3}u^{(2)} + \frac{2}{3}\Delta t L(u^{(2)}) \end{cases} \tag{3.2.1}$$

where

$$[L(u)]_\nu = -\frac{1}{\Delta x}(f^*_{\nu+\frac{1}{2}} - f^*_{\nu-\frac{1}{2}}) \tag{3.2.2}$$

33

.

We note that this explicit RK3 time discretization produces a negligible amount of entropy dissipation. For a general framework of entropy conservative fully discrete schemes, consult [LMR02].

3.3   Numerical experiments

3.3.1   Continuous initial condition

We first solve the inviscid Burgers equation (3.1.1) in the domain $x \in [0, 1]$ with the sine initial condition,

$$u(0, x) = \sin(2\pi x), \quad x \in [0, 1]$$

and periodic boundary enforced by replacing the value at the right most grid point by the value at the left most one,

$$u(t, 1) = u(t, 0).$$

In **Fig.**3.3.1, we display the numerical solutions for (3.2.1)-(3.2.2) with the numerical flux (3.1.6) for different choices of p. For small values of p, the dispersive oscillations become noticeable after the shock is generated in the middle of the figure due to the absence of any dissipative mechanism in the entropy-conservative scheme. As p increases, the amplitude of the spurious dispersive oscillations decreases, that indeed demonstrates the control of L^∞-norm through the control of the constant entropy function (3.1.12).

(a) p=1

(b) p=4

(c) p=8

(d) p=15

(e) p=25

(f) p=40
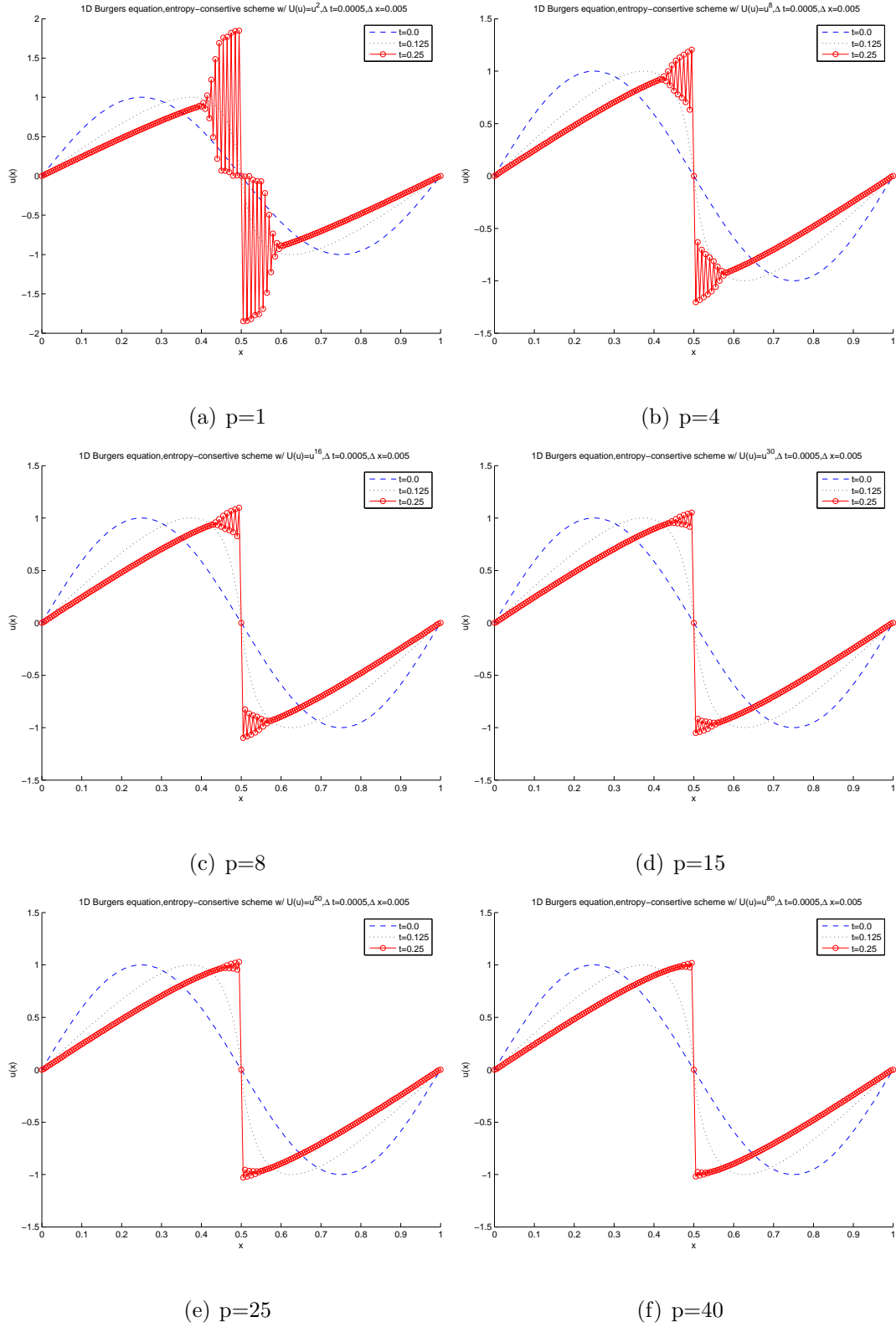
Figure 3.3.1: 1D Burger's equation, sine initial condition, entropy-conservative schemes, 200 spatial grids, $U(u) = u^{2p}$

3.3.2   Shock initial condition

We solve the 1D inviscid Burgers equation (3.1.1) in the domain $x \in [0, 1]$ with the shock initial condition,

$$
u(0, x) = \begin{cases} 2, & x \in [0,\ 0.5] \\[2mm] 1, & x \in (0.5,\ 1] \end{cases}
$$

The boundary values are extrapolated from the interior points. Actually, we are only interested in the propagation of the shock wave in the computational domain [0, 1]. Within certain period of time, the boundary values do not vary at all. In **Fig.**3.3.2, we display the numerical solutions for (3.2.1)-(3.2.2) with the numerical flux (3.1.6) for different choices of p. Those solutions show the same pattern as the sine initial condition case. Diminishing amplitude of the dispersive oscillations demonstrates the control of the L^∞-norm of the solution.
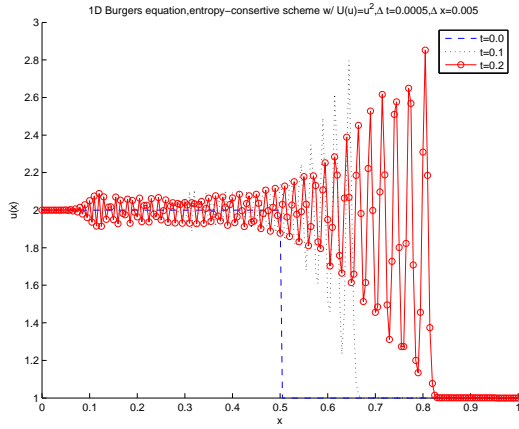
(a) p=1 (b) p=4
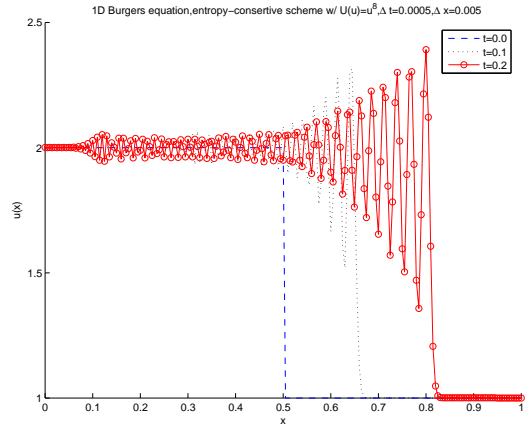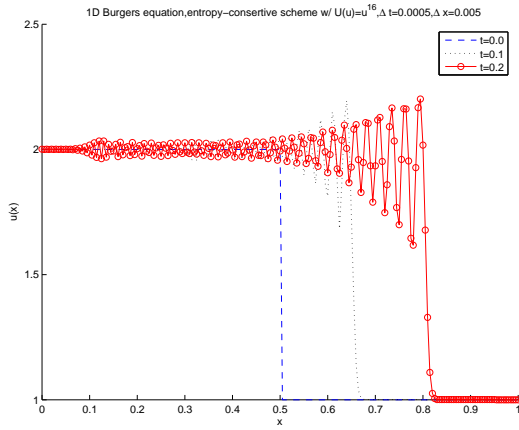
(c) p=8 (d) p=15
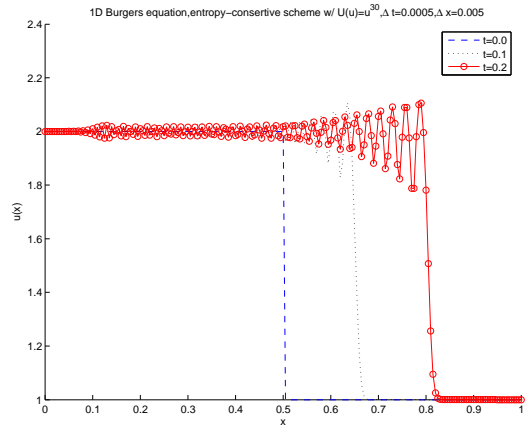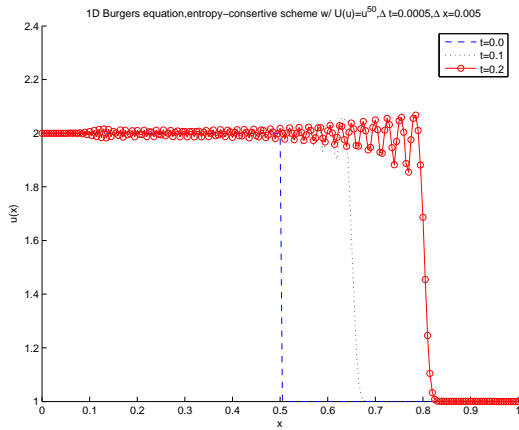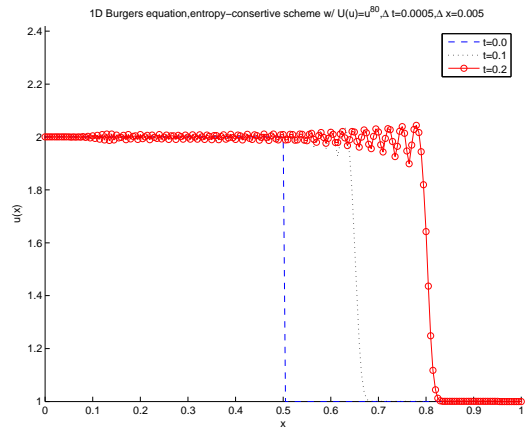
(e) p=25 (f) p=40

Figure 3.3.2: 1D Burger's equation, shock initial condition, entropy-conservative schemes, 200 spatial grids, $U(u) = u^{2p}$

Chapter 4

One-Dimensional Navier-Stokes Equations

4.1   Governing equations

The fundamental basis of fluid dynamics is the Navier-Stoke equations, which characterize any single-phase fluid flow. Based on the assumption that the fluid, at the scale of interest, is continuum, the Navier-Stokes equations describe the motion of viscous fluid substances such as liquids and gases through the conservation laws of mass, momentum, and total energy at any given region of fluid. This set of equations are widely used to model water flow in a pipe, ocean currents, air flow around the wing, blood flow, and lots of other problems in hydrodynamics. Some further applications of the Navier-Stoke equations in magnetohydrodynamics can be realized by coupling them with Maxwell's equations.

The Navier-Stokes equations can be simplified by removing the viscous term to yield the Euler equations, which describe the inviscid fluid flow. From compressibility point of view, the Navier-Stokes equations can be simplified to a good degree by making the incompressibility assumption. In reality, all materials are compressible to some extent, but it is often very useful to assume liquids are incompressible, i.e. the density of the fluid does not change.

Here we consider the full Navier-Stokes equations for compressible viscous

flows in one-space dimension,

$$
\frac{\partial}{\partial t}
\begin{bmatrix} \rho \\ m \\ E \end{bmatrix}
+ \frac{\partial}{\partial x}
\begin{bmatrix} m \\ qm + p \\ q(E + p) \end{bmatrix}
= (\lambda + 2\mu)\frac{\partial^2}{\partial x^2}
\begin{bmatrix} 0 \\ q \\ q^2/2 \end{bmatrix}
+ \kappa \frac{\partial^2}{\partial x^2}
\begin{bmatrix} 0 \\ 0 \\ \theta \end{bmatrix}. \quad (4.1.1)
$$

Here, $\rho = \rho(x,t)$ is the density of the flow, $m = m(x,t)$ is the momentum and $E = E(x,t)$ stands for the total energy per unit volume. The three equations express, respectively, conservation laws of mass, momentum and total energy for the flow, driven by convective fluxes on the left together with viscous and heat fluxes on the right. These fluxes involve the velocity $q := m/\rho$, the pressure $p = p(x,t)$ which is determined by an ideal polytropic equation of state,

$$
p = (\gamma - 1)e, \quad e := E - \frac{m^2}{2\rho}, \quad (4.1.2)
$$

and the absolute temperature, $\theta = \theta(x,t) > 0$, such that $C_v \rho \theta = e$. The constant $\gamma > 1$ is the specific heat ratio and $e = e(x,t)$ is the internal energy. On the RHS of (4.1.1) we have the viscous and heat fluxes, depending on the constant Lamé coefficients of the viscosity $\lambda, \mu > 0$ and the constant conductivity $\kappa > 0$. Finally, $C_v > 0$ is the specific heat at constant volume; for simplicity, we set $C_v = 1$ while rescaling $\kappa \mapsto \kappa/C_v$.

If the heat flux is excluded from the full Navier-Stokes equations, i.e. $\kappa = 0$, we obtain the viscous Navier-Stokes equations

$$
\frac{\partial}{\partial t}
\begin{bmatrix} \rho \\ m \\ E \end{bmatrix}
+ \frac{\partial}{\partial x}
\begin{bmatrix} m \\ qm + p \\ q(E + p) \end{bmatrix}
= (\lambda + 2\mu)\frac{\partial^2}{\partial x^2}
\begin{bmatrix} 0 \\ q \\ q^2/2 \end{bmatrix}. \quad (4.1.3)
$$

On the other hand, if we turn off the viscosity, i.e. $\lambda = \mu = 0$, then the Navier-Stokes equations amount to

$$\frac{\partial}{\partial t}\begin{bmatrix} \rho \\ m \\ E \end{bmatrix} + \frac{\partial}{\partial x}\begin{bmatrix} m \\ qm + p \\ q(E + p) \end{bmatrix} = \kappa \frac{\partial^2}{\partial x^2}\begin{bmatrix} 0 \\ 0 \\ \theta \end{bmatrix}. \qquad (4.1.4)$$

If the heat flux and viscosity are both taken away, the system (4.1.1) is reduced to the compressible Euler equations,

$$\frac{\partial}{\partial t}\begin{bmatrix} \rho \\ m \\ E \end{bmatrix} + \frac{\partial}{\partial x}\begin{bmatrix} m \\ qm + p \\ q(E + p) \end{bmatrix} = 0. \qquad (4.1.5)$$

4.2 Physical entropy balance

The additional viscous and heat flux terms on the RHS of the various Navier-Stokes equations (4.1.1), (4.1.3) or (4.1.4), are dissipative terms in the sense that they are responsible for the dissipation of the total *entropy*. To this end, we now discuss the entropy balance associated with the above equations. We begin with the specific entropy $S := \ln\left(p\rho^{-\gamma}\right)$. A straightforward manipulation on (4.1.1), (4.1.2) yields the transport equation,

$$S_t + qS_x = \frac{\kappa}{\rho}(\ln\theta)_{xx} + (\lambda + 2\mu)\frac{q_x^2}{e} + \frac{\kappa}{\rho}\left(\frac{\theta_x}{\theta}\right)^2. \qquad (4.2.1)$$

Multiplied by ρ, (4.2.1) becomes

$$\rho S_t + mS_x = \kappa(\ln\theta)_{xx} + (\lambda + 2\mu)\frac{q_x^2}{\theta} + \kappa\left(\frac{\theta_x}{\theta}\right)^2. \qquad (4.2.2)$$

40

On the other hand, pre-multiplying the continuity equation, $\rho_t + m_x = 0$, by S and adding it to (4.2.2),

$$\frac{\partial}{\partial t}\left(-\rho S\right) + \frac{\partial}{\partial x}\left(-mS + \kappa(\ln\theta)_x\right) = -(\lambda + 2\mu)\frac{q_x^2}{\theta} - \kappa\left(\frac{\theta_x}{\theta}\right)^2. \qquad (4.2.3)$$

Spatial integration of (4.2.3) then yields

$$\frac{d}{dt}\int_x\left(-\rho S\right) dx = -(\lambda + 2\mu)\int_x q_x^2 \cdot \frac{1}{\theta}\, dx - \kappa\int_x \theta_x{}^2\left(\frac{1}{\theta}\right)^2 dx. \qquad (4.2.4)$$

Since the expression on the right is negative, we conclude that the total entropy, $\int_x(-\rho S)\, dx$, is decreasing in time, thus recovering the second law of thermodynamics, e.g., [dGM84]. In fact, equation (4.2.4) specifies the precise entropy decay rate, which is dictated by the viscous and heat fluxes through their dependence on the nonnegative κ, λ, and μ.

We are going to develop a new family of difference schemes which respect the above entropy dissipation statements. The typical approach by practitioners in the field of Computational Fluid Dynamics is to address the general issue of entropy stability by adding 'enough' artificial numerical viscosity — often an excessive amount of it, in order to mask various discretizations errors and enforce the decay of the total entropy $\int_x(-\rho S)\, dx$. Our aim here is to construct more 'faithful' approximations of the Navier-Stokes equations, with a discrete analogue for the precise entropy decay statement in (4.2.4).

4.3 Entropy pairs for Navier-Stokes equations

As shown in Remark 1.4.1, the Navier-Stokes equations admit the family of convex entropy pairs

$$U(\mathbf{u}) = -\rho h(S), \quad F(\mathbf{u}) = -mh(S), \qquad h'(\cdot) \geq 0. \tag{4.3.1}$$

Here $S = \ln(p\rho^{-\gamma})$ is the specific entropy and the convexity of the corresponding $U(\mathbf{u})$'s as functions of $\mathbf{u} = (\rho, m, E)^\top$ holds iff $h'(S) - \gamma h''(S) > 0$, [Har83]. We consider two prototype examples.

Example 4.3.1. The simplest choice of $h(S)$ is the specific entropy S itself,

$$h(S) = S = \ln\left(p\rho^{-\gamma}\right). \tag{4.3.2}$$

Straightforward computation gives us the following entropy pair, entropy variables, and potentials.

- Entropy pair $U(\mathbf{u}) = -\rho S$ and $F(\mathbf{u}) = -mS$;

- Entropy variable (consult [Har83])

$$\mathbf{v}(\mathbf{u}) = \begin{bmatrix} -E/e - S + \gamma + 1 \\ q/\theta \\ -1/\theta \end{bmatrix} \tag{4.3.3}$$

with the inverse mapping

$$\mathbf{u}(\mathbf{v}) = \frac{p}{\gamma - 1} \begin{bmatrix} -v_3 \\ v_2 \\ 1 - \frac{v_2^2}{2v_3} \end{bmatrix} = w \begin{bmatrix} -v_3 \\ v_2 \\ 1 - \frac{v_2^2}{2v_3} \end{bmatrix},$$

42

where $w = \left(\frac{\gamma-1}{(-v_3)^\gamma}\right)^{\frac{1}{\gamma-1}} e^{\left(\frac{-S}{\gamma-1}\right)}$, $S = \gamma - v_1 + \frac{v_2^2}{2v_3}$;

- Potential pair $\phi = (\gamma - 1)\rho$ and $\psi = (\gamma - 1)m$.

In this case, the general statement of entropy balance in (2.1.11) with the entropy pair $(U, F) = (-\rho S, -mS)$ amounts to the one we have in (4.2.4),

$$\frac{d}{dt}\int_x -(\rho S)\,dx = -\epsilon \int_x \langle \mathbf{v}_x^\epsilon, \mathbf{d_v v}_x^\epsilon \rangle\,dx = -(\lambda + 2\mu)\int_x \frac{q_x^2}{\theta}dx - \kappa \int_x \frac{\theta_x^2}{\theta^2}dx \leq 0. \quad (4.3.4)$$

Example 4.3.2. A particularly convenient form of entropy variables is associated the entropy function (consult [Har83, Tad03]),

$$U(\mathbf{u}) = -\rho h(S) \text{ with } h(S) = \frac{\gamma+1}{\gamma-1}e^{\frac{S}{\gamma+1}}, \quad (4.3.5)$$

where we have the following.

- Entropy pair $U(\mathbf{u}) = \frac{1+\gamma}{1-\gamma}(\rho p)^{\frac{1}{1+\gamma}}$ and $F(\mathbf{u}) = \frac{1+\gamma}{1-\gamma}q(\rho p)^{\frac{1}{1+\gamma}}$;

- Entropy variable $\mathbf{v}(\mathbf{u}) = \nabla_\mathbf{u}U(\mathbf{u}) = -(\rho p)^{-\frac{\gamma}{1+\gamma}}\begin{bmatrix} E \\ -m \\ \rho \end{bmatrix}$

  with the inverse mapping

  $$\mathbf{u}(\mathbf{v}) = -(\rho p)^{\frac{\gamma}{\gamma+1}}\begin{bmatrix} v_3 \\ -v_2 \\ v_1 \end{bmatrix} = -\left[(\gamma-1)\left(v_1 v_3 - \frac{v_2^2}{2}\right)\right]^{\frac{\gamma}{1-\gamma}}\begin{bmatrix} v_3 \\ -v_2 \\ v_1 \end{bmatrix};$$

- Potential pair $(\phi, \psi) = \left((\rho p)^{\frac{1}{\gamma+1}}, m(p\rho^{-\gamma})^{\frac{1}{\gamma+1}}\right)$

In case that the heat conduction is absent ($\kappa = 0$), we apply the general statement of entropy balance (2.1.11) with the entropy pair, $(U, F) = \frac{1+\gamma}{1-\gamma}\left((\rho p)^{\frac{1}{1+\gamma}}, q(\rho p)^{\frac{1}{1+\gamma}}\right)$,

43

obtaining

$$\frac{d}{dt}\int_x -(\rho p)^{\frac{1}{1+\gamma}}dx = -\epsilon\int_x \langle \mathbf{v}_x^\epsilon, \mathbf{d_v}\mathbf{v}_x^\epsilon\rangle\,dx$$

$$\equiv -(\lambda + 2\mu)\int_x \frac{(\gamma-1)h'(S)q_x^2}{(1+\gamma)\theta}dx = -\frac{\lambda+2\mu}{1+\gamma}\int_x \frac{e^{S/(1+\gamma)}q_x^2}{\theta}dx \le 0.$$

$$(4.3.6)$$

Remark 4.3.1. As noted in [Har83], the flux $\mathbf{f}(\mathbf{v})$ is a homogeneous function of degree $\eta =: (1+\gamma)/(1-\gamma)$, $\mathbf{f}(\alpha\mathbf{v}) = \alpha^\eta \mathbf{f}(\mathbf{v})$, $\forall\,\alpha\in\mathbb{R}$. Homogeneity implies that $\mathbf{f_v}(\mathbf{v})\mathbf{v} = \eta\mathbf{f}(\mathbf{v})$ which in turn, enables us to rewrite the spatial flux in (2.1.1) in a skew-adjoint form, $\mathbf{f}(\mathbf{u})_x = \big(\mathbf{f_v}\mathbf{v}_x + (\mathbf{f_v}\mathbf{v})_x\big)/(\eta+1)$; consult [Tad84a].

4.4 Entropy stable schemes for Navier-Stokes equations

4.4.1 Entropy stable semi-discrete schemes for Navier-Stokes equations

4.4.1.1 The compressible Euler equations

Let (U, F) be an admissible entropy pair associated with the Euler equations (4.1.5), let $\mathbf{v} = \mathbf{v}(\mathbf{u})$ denote the corresponding entropy variables outlined in examples 4.3.1 and 4.3.2 above. To conserve the total entropy $\int_x U(\mathbf{u}(\cdot, t))dx$, we appeal to the semi-discrete scheme (2.2.10) with the entropy-conservative numerical flux (2.2.11),

$$\mathbf{f}_{\nu+\frac{1}{2}}^* = \sum_{j=1}^3 \frac{\psi\left(\mathbf{v}_{\nu+\frac{1}{2}}^{j+1}\right) - \psi\left(\mathbf{v}_{\nu+\frac{1}{2}}^j\right)}{\left\langle \boldsymbol{\ell}_{\nu+\frac{1}{2}}^j, \Delta\mathbf{v}_{\nu+\frac{1}{2}}\right\rangle}\boldsymbol{\ell}_{\nu+\frac{1}{2}}^j.$$

To compute $\mathbf{f}^*_{\nu+\frac{1}{2}}$, we distinguish between two cases. If $\mathbf{v}_\nu = \mathbf{v}_{\nu+1}$, we employ the equivalent form of the numerical flux in (2.2.13),

$$
\mathbf{f}^*_{\nu+\frac{1}{2}} = \sum_{j=1}^{3} \left\langle \int_{\xi=-\frac{1}{2}}^{\frac{1}{2}} \mathbf{f}\left(\mathbf{v}^{j+\frac{1}{2}}_{\nu+\frac{1}{2}}(\xi)\right) d\xi, \mathbf{r}^j_{\nu+\frac{1}{2}} \right\rangle \boldsymbol{\ell}^j_{\nu+\frac{1}{2}},
$$

which implies that all the intermediate gridvalues coincide, $\mathbf{v}_\nu = \mathbf{v}^1_{\nu+\frac{1}{2}} = \mathbf{v}^2_{\nu+\frac{1}{2}} = \mathbf{v}^3_{\nu+\frac{1}{2}} = \mathbf{v}^4_{\nu+\frac{1}{2}} = \mathbf{v}_{\nu+1}$ and the entropy-conservative flux amounts to $\mathbf{f}^*_{\nu+\frac{1}{2}} = \mathbf{f}_\nu = \mathbf{f}_{\nu+1}$. Otherwise, if $\mathbf{v}_\nu \neq \mathbf{v}_{\nu+1}$, we choose to work along the path which is dictated by an (approximate) Riemann solver. Specifically, we use the eigensystem of the Roe matrix, [Roe81],

$$
\begin{bmatrix}
0 & 1 & 0 \\[2mm]
\frac{\gamma-3}{2}\bar{q}^2_{\nu+\frac{1}{2}} & (3-\gamma)\bar{q}_{\nu+\frac{1}{2}} & \gamma-1 \\[2mm]
\frac{\gamma-1}{2}\bar{q}^3_{\nu+\frac{1}{2}} - \bar{q}_{\nu+\frac{1}{2}}\bar{G}_{\nu+\frac{1}{2}} & \bar{G}_{\nu+\frac{1}{2}} - (\gamma-1)\bar{q}^2_{\nu+\frac{1}{2}} & \gamma\bar{q}_{\nu+\frac{1}{2}}
\end{bmatrix}.
\tag{4.4.1a}
$$

Here $\bar{q}$ and $\bar{G}$ are the average values of the velocity q and total enthalpy $G = (E+p)/\rho$ at Roe-average state,

$$
\bar{q}_{\nu+\frac{1}{2}} = \frac{q_\nu\sqrt{\rho_\nu} + q_{\nu+1}\sqrt{\rho_{\nu+1}}}{\sqrt{\rho_\nu} + \sqrt{\rho_{\nu+1}}}, \quad \bar{G}_{\nu+\frac{1}{2}} = \frac{G_\nu\sqrt{\rho_\nu} + G_{\nu+1}\sqrt{\rho_{\nu+1}}}{\sqrt{\rho_\nu} + \sqrt{\rho_{\nu+1}}}.
\tag{4.4.1b}
$$

The $\mathbf{r}^j$'s are the right eigenvectors $\{\widehat{\mathbf{r}}^j \equiv \widehat{\mathbf{r}}^j_{\nu+\frac{1}{2}}\}_{j=1}^{3}$ of the Roe matrix (4.4.1a) given by (omitting the subscript $(\cdot)_{\nu+\frac{1}{2}}$ of all averaged variables)

$$
\widehat{\mathbf{r}}^1 = \begin{bmatrix} 1 \\ \bar{q} - \bar{c} \\ \bar{G} - \bar{q}\bar{c} \end{bmatrix}, \quad \widehat{\mathbf{r}}^2 = \begin{bmatrix} 1 \\ \bar{q} \\ \bar{q}^2/2 \end{bmatrix}, \quad \widehat{\mathbf{r}}^3 = \begin{bmatrix} 1 \\ \bar{q} + \bar{c} \\ \bar{G} + \bar{q}\bar{c} \end{bmatrix},
\tag{4.4.1c}
$$

45

with the corresponding left eigenvector set $\{\widehat{\boldsymbol{\ell}}^j \equiv \widehat{\boldsymbol{\ell}}_{\nu+\frac{1}{2}}^j\}_{j=1}^3$ given by

$$\widehat{\boldsymbol{\ell}}^1 = \begin{bmatrix} (2+\delta)/(4(\gamma-1)) \\ -(1+\delta)/(2\bar{c}) \\ (\gamma-1)/(2\bar{c}^2) \end{bmatrix}, \widehat{\boldsymbol{\ell}}^2 = \begin{bmatrix} 1-\delta^2/(2(\gamma-1)) \\ \delta/\bar{c} \\ -(\gamma-1)/\bar{c}^2 \end{bmatrix}, \quad (4.4.1\text{d})$$

$$\widehat{\boldsymbol{\ell}}^3 = \begin{bmatrix} -(2-\delta)/(4(\gamma-1)) \\ (1-\delta)/(2\bar{c}) \\ (\gamma-1)/(2\bar{c}^2) \end{bmatrix}.$$

Here $\delta := (\gamma-1)\bar{q}/\bar{c}$, and $\bar{c}$ is the average sound speed given by $\bar{c}^2 = (\gamma-1)\left(\bar{G} - \frac{\bar{q}^2}{2}\right)$.

We are now able to form the intermediate path in $\mathbf{u}$−space as in $(2.2.9)$

$$\mathbf{u}^{j+1} = \mathbf{u}^j + \left\langle \widehat{\boldsymbol{\ell}}^j, \Delta\mathbf{u} \right\rangle \widehat{\mathbf{r}}^j, \quad j = 1, 2, 3. \quad (4.4.2)$$

Since the mapping between $\mathbf{u}$ and $\mathbf{v}$ is one-to-one, then these intermediate gridvalues in $\mathbf{u}$−space, $\{\mathbf{u}^j\}_{j=1}^4$, correspond to intermediate gridvalues $\{\mathbf{v}^j\}_{j=1}^4$ in $\mathbf{v}$−space. We let $\{\mathbf{r}^j\}_{j=1}^3$ be the (right) vectors connecting these $\mathbf{v}$-values, $\mathbf{r}^j := \mathbf{v}^{j+1} - \mathbf{v}^j$, and let $\{\boldsymbol{\ell}^j\}_{j=1}^3$ be the corresponding (left) orthogonal set. We summarize the algorithm of computing the entropy-conservative flux $\mathbf{f}_{\nu+\frac{1}{2}}^*$ in the following.

Algorithm 4.4.1. If $\quad \mathbf{u}_\nu = \mathbf{u}_{\nu+1}$ then $\quad \mathbf{f}_{\nu+\frac{1}{2}}^* = \mathbf{f}(\mathbf{v}_\nu)$; **else**

- Set $\mathbf{u}_{\nu+\frac{1}{2}}^1 := \mathbf{u}_\nu$ and compute recursively the intermediate states,

$$\mathbf{u}_{\nu+\frac{1}{2}}^{j+1} = \mathbf{u}_{\nu+\frac{1}{2}}^j + \left\langle \widehat{\boldsymbol{\ell}}_{\nu+\frac{1}{2}}^j, \Delta\mathbf{u}_{\nu+\frac{1}{2}} \right\rangle \widehat{\mathbf{r}}_{\nu+\frac{1}{2}}^j, \quad j = 1, 2, 3. \quad (4.4.3)$$

Here, $\{\widehat{\boldsymbol{\ell}}_{\nu+\frac{1}{2}}^j\}$ and $\{\widehat{\mathbf{r}}_{\nu+\frac{1}{2}}^j\}$ are the left and right eigensystems of the Roe matrix in $(4.4.1\text{c})$, $(4.4.1\text{d})$.

- Set $\mathbf{r}^j_{\nu+\frac{1}{2}} = \mathbf{v}(\mathbf{u}^{j+1}_{\nu+\frac{1}{2}}) - \mathbf{v}(\mathbf{u}^j_{\nu+\frac{1}{2}})$ and compute $\{\boldsymbol{\ell}^j\}^3_{j=1}$ as the corresponding orthogonal system,

$$\left\langle \boldsymbol{\ell}^j_{\nu+\frac{1}{2}}, \mathbf{r}^k_{\nu+\frac{1}{2}} \right\rangle = \delta_{jk}, \qquad \mathbf{r}^j_{\nu+\frac{1}{2}} := \mathbf{v}^{j+1}_{\nu+\frac{1}{2}} - \mathbf{v}^j_{\nu+\frac{1}{2}} \tag{4.4.4}$$

- Compute the entropy-conservative numerical flux,

$$\mathbf{f}^*_{\nu+\frac{1}{2}} = \sum_{j=1}^3 \frac{\psi\left(\mathbf{v}^{j+1}_{\nu+\frac{1}{2}}\right) - \psi\left(\mathbf{v}^j_{\nu+\frac{1}{2}}\right)}{\left\langle \boldsymbol{\ell}^j_{\nu+\frac{1}{2}}, \Delta\mathbf{v}_{\nu+\frac{1}{2}} \right\rangle} \boldsymbol{\ell}^j_{\nu+\frac{1}{2}} \tag{4.4.5}$$

Remark 4.4.1. Observe that if $\{\mathbf{u}^{j+1}_{\nu+\frac{1}{2}} - \mathbf{u}^j_{\nu+\frac{1}{2}}\}^3_{j=1}$ are linearly independent then, since $\mathbf{u_v}$ is symmetric positive definite, the corresponding set of directions in $\mathbf{v}$-phase space, $\{\mathbf{v}^{j+1}_{\nu+\frac{1}{2}} - \mathbf{v}^j_{\nu+\frac{1}{2}}\}^3_{j=1}$ are also linearly independent, at least when $\mathbf{u}_{\nu+1}$ is in a small neighborhood of $\mathbf{u}_\nu$. It guarantees the existence of the orthogonal set $\{\boldsymbol{\ell}^j_{\nu+\frac{1}{2}}\}^3_{j=1}$. But what happens when $\left\langle \boldsymbol{\ell}^j_{\nu+\frac{1}{2}}, \Delta\mathbf{v}_{\nu+\frac{1}{2}} \right\rangle = 0$ for certain j's? For example, if $\mathbf{u}_\nu$ is connected to $\mathbf{u}_{\nu+1}$ through a k-shock. then the Roe matrix $[A]_{\nu+\frac{1}{2}}$ retains the perfect resolution of such a shock by enforcing $\left\langle \boldsymbol{\ell}^j_{\nu+\frac{1}{2}}, \Delta\mathbf{v}_{\nu+\frac{1}{2}} \right\rangle = 0$, $\forall j \neq k$ and we can omit the contribution of these sub-paths to the conservative flux $\mathbf{f}^*$. The general approach is to construct a precise mirror image of the Roe-path in $\mathbf{v}$-phase space in terms of the right and left orthogonal systems,

$$\mathbf{r}^j_{\nu+\frac{1}{2}} := [H]^{-1}_{\nu+\frac{1}{2}} \widehat{\mathbf{r}}^j, \quad \boldsymbol{\ell}^j_{\nu+\frac{1}{2}} := [H]_{\nu+\frac{1}{2}} \widehat{\boldsymbol{\ell}}^j, \qquad j = 1, 2, \cdots,$$

where $[H]_{\nu+\frac{1}{2}}$ denotes an averaged symmetrizer such that $\Delta\mathbf{u}_{\nu+\frac{1}{2}} = [H]_{\nu+\frac{1}{2}} \Delta\mathbf{v}_{\nu+\frac{1}{2}}$ (and there are many different such averages). Then, $\{\mathbf{r}^j_{\nu+\frac{1}{2}}\}^3_{j=1}$ forms the path in $\mathbf{v}$-phase space, $\mathbf{v}^{j+1}_{\nu+\frac{1}{2}} = \mathbf{v}^j_{\nu+\frac{1}{2}} + \left\langle \boldsymbol{\ell}^j_{\nu+\frac{1}{2}}, \Delta\mathbf{v}_{\nu+\frac{1}{2}} \right\rangle \mathbf{r}^j_{\nu+\frac{1}{2}}$, which retains the desired Roe property of perfect resolution of shocks. Indeed, if $\Delta\mathbf{u}$ is a k-shock with speed s

then it satisfies $\Delta \mathbf{f}_{\nu+\frac{1}{2}} = s\Delta\mathbf{u}_{\nu+\frac{1}{2}} = s[H]_{\nu+\frac{1}{2}}\Delta\mathbf{v}_{\nu+\frac{1}{2}}$. But the Roe matrix in (4.4.1a) is constructed so that $\Delta\mathbf{f}_{\nu+\frac{1}{2}} = [A]\Delta\mathbf{u}_{\nu+\frac{1}{2}} = [A][H]_{\nu+\frac{1}{2}}\Delta\mathbf{v}_{\nu+\frac{1}{2}}$ (consult [Roe81]), and we conclude that $\Delta\mathbf{v}_{\nu+\frac{1}{2}} = \mathbf{r}^k_{\nu+\frac{1}{2}}$. Thus, $\left\langle \boldsymbol{\ell}^j_{\nu+\frac{1}{2}}, \Delta\mathbf{v}_{\nu+\frac{1}{2}} \right\rangle = 0, \ \forall j \neq k$. The corresponding entropy conservative numerical flux reads

$$\mathbf{f}^*_{\nu+\frac{1}{2}} = \sum_{\{j|\xi^j \neq 0\}} \frac{\psi(\mathbf{v}^j_{\nu+\frac{1}{2}} + \xi^j \mathbf{r}^j_{\nu+\frac{1}{2}}) - \psi(\mathbf{v}^j_{\nu+\frac{1}{2}})}{\xi^j} \boldsymbol{\ell}^j_{\nu+\frac{1}{2}}, \quad \xi^j = \left\langle \boldsymbol{\ell}^j_{\nu+\frac{1}{2}}, \Delta\mathbf{v}_{\nu+\frac{1}{2}} \right\rangle.$$

4.4.1.2 The Navier-Stokes equations

We turn to the construction of entropy-stable schemes for the full Navier-Stokes equations (4.1.1). To this end, we rewrite the equation as a system of conservation laws

$$\frac{\partial}{\partial t}\mathbf{u} + \frac{\partial}{\partial x}\mathbf{f}(\mathbf{u}) = \epsilon \frac{\partial^2}{\partial x^2}\mathbf{d}(\mathbf{u}), \quad \mathbf{u} = \begin{bmatrix} \rho \\ m \\ E \end{bmatrix}, \ \mathbf{f}(\mathbf{u}) = \begin{bmatrix} m \\ qm + p \\ q(E + p) \end{bmatrix}, \quad (4.4.6a)$$

with additional diffusive terms

$$\epsilon \mathbf{d}(\mathbf{u}) := (\lambda + 2\mu) \begin{bmatrix} 0 \\ q \\ q^2/2 \end{bmatrix} + \kappa \begin{bmatrix} 0 \\ 0 \\ \theta \end{bmatrix}. \quad (4.4.6b)$$

For the convection part on the LHS, we use the same entropy-conservative differencing used for the Euler equations. For the dissipative terms on the RHS, we employ standard centered differences. We arrive at our main result of one dimensional Navier-Stokes equations.

Theorem 4.4.1. *Let (U, F) be a given entropy pair of the Navier-Stokes equations (4.4.6a),(4.4.6b), which respect the entropy inequality (2.1.11). Consider the semi-discrete approximation*

$$\frac{d}{dt}\mathbf{u}_\nu(t) + \frac{1}{\Delta x_\nu}\left(\mathbf{f}^*_{\nu+\frac{1}{2}} - \mathbf{f}^*_{\nu-\frac{1}{2}}\right) = \frac{\epsilon}{\Delta x_\nu}\left(\frac{\mathbf{d}_{\nu+1} - \mathbf{d}_\nu}{\Delta x_{\nu+\frac{1}{2}}} - \frac{\mathbf{d}_\nu - \mathbf{d}_{\nu-1}}{\Delta x_{\nu-\frac{1}{2}}}\right). \qquad (4.4.7a)$$

Here $\mathbf{f}^*_{\nu+\frac{1}{2}}$ is an entropy conservative numerical flux (2.2.11),

$$\mathbf{f}^*_{\nu+\frac{1}{2}} = \sum_{j=1}^{3}\frac{\psi\left(\mathbf{v}^{j+1}_{\nu+\frac{1}{2}}\right) - \psi\left(\mathbf{v}^j_{\nu+\frac{1}{2}}\right)}{\left\langle\boldsymbol{\ell}^j_{\nu+\frac{1}{2}}, \Delta\mathbf{v}_{\nu+\frac{1}{2}}\right\rangle}\boldsymbol{\ell}^j_{\nu+\frac{1}{2}}, \qquad (4.4.7b)$$

which is outlined in algorithm 4.4.1 above.

{i} The resulting scheme (4.4.7a),(4.4.7b) is entropy-dissipative in the sense that

$$\frac{d}{dt}\sum_\nu U_\nu(t)\,\Delta x_\nu = -\sum_\nu\frac{\epsilon}{\Delta x_{\nu+\frac{1}{2}}}\left\langle\Delta\mathbf{v}_{\nu+\frac{1}{2}}, \frac{\Delta\mathbf{d}_{\nu+\frac{1}{2}}}{\Delta\mathbf{v}_{\nu+\frac{1}{2}}}\Delta\mathbf{v}_{\nu+\frac{1}{2}}\right\rangle \le 0. \qquad (4.4.8)$$

This entropy balance is a discrete analogue of the entropy balance statements (4.3.4) and (4.3.6).

{ii} In the specific case of the canonical entropy pair $(U, F) = (-\rho S, -mS)$, the entropy decay (4.4.8) amounts to (1.4.6)

$$\frac{d}{dt}\sum_\nu U_\nu(t)\,\Delta x_\nu = -(\lambda + 2\mu)\sum_\nu\left(\frac{\Delta q_{\nu+\frac{1}{2}}}{\Delta x_{\nu+\frac{1}{2}}}\right)^2\left(\widetilde{1/\theta}\right)_{\nu+\frac{1}{2}}\Delta x_{\nu+\frac{1}{2}}$$

$$-\kappa\sum_\nu\left(\frac{\Delta\theta_{\nu+\frac{1}{2}}}{\Delta x_{\nu+\frac{1}{2}}}\right)^2\left(\widetilde{1/\theta}\right)^2_{\nu+\frac{1}{2}}\Delta x_{\nu+\frac{1}{2}} \le 0. \qquad (4.4.9)$$

Proof. We multiply (4.4.7a) by $[U_\mathbf{u}]^\top_\nu = \mathbf{v}^\top_\nu$, then sum up all spatial cells to get the balance of the total entropy,

$$\frac{d}{dt}\sum_\nu U_\nu(t)\,\Delta x_\nu + \sum_\nu\left\langle\mathbf{v}_\nu, \mathbf{f}^*_{\nu+\frac{1}{2}} - \mathbf{f}^*_{\nu-\frac{1}{2}}\right\rangle = \epsilon\sum_\nu\left\langle\mathbf{v}_\nu, \frac{\mathbf{d}_{\nu+1} - \mathbf{d}_\nu}{\Delta x_{\nu+\frac{1}{2}}} - \frac{\mathbf{d}_\nu - \mathbf{d}_{\nu-1}}{\Delta x_{\nu-\frac{1}{2}}}\right\rangle.$$

$$(4.4.10)$$

Since we chose $\mathbf{f}^*_{\nu+\frac{1}{2}}$ as the entropy conservative flux, a straightforward manipulation on the entropy conservation requirement (2.2.12) yields the conservative difference,

$$\left\langle \mathbf{v}_\nu, \mathbf{f}^*_{\nu+\frac{1}{2}} - \mathbf{f}^*_{\nu-\frac{1}{2}} \right\rangle = F_{\nu+\frac{1}{2}} - F_{\nu-\frac{1}{2}}, \tag{4.4.11}$$

where $2F_{\nu+\frac{1}{2}} = \left\langle (\mathbf{v}_\nu + \mathbf{v}_{\nu+1}), \mathbf{f}_{\nu+\frac{1}{2}} \right\rangle - (\psi(\mathbf{v}_\nu) + \psi(\mathbf{v}_{\nu+1}))$. On the other hand, summation by parts on the RHS of (4.4.10) yields

$$\epsilon \sum_\nu \left\langle \mathbf{v}_\nu, \frac{\mathbf{d}_{\nu+1} - \mathbf{d}_\nu}{\Delta x_{\nu+\frac{1}{2}}} - \frac{\mathbf{d}_\nu - \mathbf{d}_{\nu-1}}{\Delta x_{\nu-\frac{1}{2}}} \right\rangle = -\sum_\nu \frac{\epsilon}{\Delta x_{\nu+\frac{1}{2}}} \left\langle \mathbf{v}_{\nu+1} - \mathbf{v}_\nu, \mathbf{d}_{\nu+1} - \mathbf{d}_\nu \right\rangle$$

$$= -\sum_\nu \frac{\epsilon}{\Delta x_{\nu+\frac{1}{2}}} \left\langle \Delta \mathbf{v}_{\nu+\frac{1}{2}}, \Delta \mathbf{d}_{\nu+\frac{1}{2}} \right\rangle \tag{4.4.12a}$$

$$= -\sum_\nu \frac{\epsilon}{\Delta x_{\nu+\frac{1}{2}}} \left\langle \Delta \mathbf{v}_{\nu+\frac{1}{2}}, \frac{\Delta \mathbf{d}_{\nu+\frac{1}{2}}}{\Delta \mathbf{v}_{\nu+\frac{1}{2}}} \Delta \mathbf{v}_{\nu+\frac{1}{2}} \right\rangle. \tag{4.4.12b}$$

By (4.4.11) and (4.4.12b), the semi-discrete entropy balance amounts to

$$\frac{d}{dt} \sum_\nu U_\nu(t) \Delta x_\nu = -\sum_\nu \frac{\epsilon}{\Delta x_{\nu+\frac{1}{2}}} \left\langle \Delta \mathbf{v}_{\nu+\frac{1}{2}}, \frac{\Delta \mathbf{d}_{\nu+\frac{1}{2}}}{\Delta \mathbf{v}_{\nu+\frac{1}{2}}} \Delta \mathbf{v}_{\nu+\frac{1}{2}} \right\rangle. \tag{4.4.13}$$

Here

$$\frac{\Delta \mathbf{d}_{\nu+\frac{1}{2}}}{\Delta \mathbf{v}_{\nu+\frac{1}{2}}} = \int_{\xi=-\frac{1}{2}}^{\frac{1}{2}} \mathbf{d_v}\left(\mathbf{v}_{\nu+\frac{1}{2}}(\xi)\right) d\xi,$$

where $\mathbf{v}_{\nu+\frac{1}{2}}(\xi)$ is given by (2.2.16). By the admissibility of the dissipative Navier-Stokes fluxes $\mathbf{d_v} \geq 0$ and the RHS of (4.4.13) is indeed non-positive. Thus, the semi-discrete scheme (4.4.7a) guarantees the total entropy dissipation.

In the specific case of the entropy pair $(U, F) = (-\rho S, -mS)$, the entropy variables are found in (4.3.3), and we explicitly compute the inner products in

(4.4.12a) as (omitting all subscripts),

$$-\sum_\nu \frac{\epsilon}{\Delta x}\left\langle \Delta\mathbf{v}, \Delta\mathbf{d}\right\rangle$$

$$= -\sum_\nu \frac{1}{\Delta x}\left\{(\lambda + 2\mu)\,\Delta\left(\frac{q}{\theta}\right)\Delta q - \frac{\lambda + 2\mu}{2}\,\Delta\left(\frac{1}{\theta}\right)\Delta\left(q^2\right) - \kappa\,\Delta\left(\frac{1}{\theta}\right)\Delta\theta\right\}$$

$$= -(\lambda + 2\mu)\sum_\nu \frac{1}{\Delta x}(\Delta q)^2\frac{1}{2}\left(\frac{1}{\theta_{\nu+1}} + \frac{1}{\theta_\nu}\right) - \kappa\sum_\nu \frac{1}{\Delta x}\Delta\left(\frac{1}{\theta}\right)\Delta\theta$$

$$= -(\lambda + 2\mu)\sum_\nu \left(\frac{\Delta q}{\Delta x}\right)^2\frac{1}{2}\left(\frac{1}{\theta_{\nu+1}} + \frac{1}{\theta_\nu}\right)\Delta x - \kappa\sum_\nu \left(\frac{\Delta\theta}{\Delta x}\right)^2\frac{1}{\theta_{\nu+1}\theta_\nu}\Delta x \leq 0.$$

The discrete entropy balance (1.4.6) now follows. □

We emphasize the main point made here, namely, we introduce no excessive entropy dissipation due to spurious, *artificial* numerical viscosity: by (4.4.8), the semi-discrete scheme contains the precise amount of numerical viscosity to enforce the correct entropy dissipation dictated by the Navier-Stokes equations.

4.4.2 Time discretization

Similar to the time integration of the Burgers equation, the semi-discrete entropy conservative scheme (4.4.7a) and (4.4.7b) of 1D Navier-Stokes equations is integrated with the explicit three-stage third-order Runge-Kutta (RK3) method (3.2.1), due to the high-order accuracy, large stability region and simplicity of this method. Consult [GST01],

$$\begin{cases} \mathbf{u}^{(1)} &= \mathbf{u}^n + \Delta t L(\mathbf{u}^n) \\[2mm] \mathbf{u}^{(2)} &= \dfrac{3}{4}\mathbf{u}^n + \dfrac{1}{4}\mathbf{u}^{(1)} + \dfrac{1}{4}\Delta t L(\mathbf{u}^{(1)}) \\[2mm] \mathbf{u}^{n+1} &= \dfrac{1}{3}\mathbf{u}^n + \dfrac{2}{3}\mathbf{u}^{(2)} + \dfrac{2}{3}\Delta t L(\mathbf{u}^{(2)}) \end{cases}$$

where

$$[L(\mathbf{u})]_\nu = -\frac{1}{\Delta x_\nu}(\mathbf{f}^*_{\nu+\frac{1}{2}} - \mathbf{f}^*_{\nu-\frac{1}{2}}) + \frac{\epsilon}{\Delta x_\nu}\left(\frac{\mathbf{d}_{\nu+1} - \mathbf{d}_\nu}{\Delta x_{\nu+\frac{1}{2}}} - \frac{\mathbf{d}_\nu - \mathbf{d}_{\nu-1}}{\Delta x_{\nu-\frac{1}{2}}}\right)$$

.

We note in passing that though the fully explicit RK3 time discretization need not conserve the entropy, it introduces a negligible amount of entropy dissipation; for a general framework of entropy-conservative fully discrete schemes consult [LMR02].

4.5 Numerical experiments

We consider ideal polytropic gas equations as an approximation of air with

$$\gamma = 1.4, \quad C_v = 716, \quad \kappa = 0.03, \quad \lambda + 2\mu = 2.28 \times 10^{-5}$$

We simulate the Sod's shocktube problem, [Sod78], where the Euler and Navier-Stokes equations are solved over the interval $[0, 1]$ subject to Riemann initial conditions

$$(\rho, m, E)_{t=0} = \begin{cases} (1.0,\ 0.0,\ 2.5) & 0 < x \le 0.5 \\ (0.125,\ 0.0,\ 0.25) & 0.5 < x < 1. \end{cases}$$

The resulting fully-discrete schemes (4.4.14) has a spatial stencil involving three-point gridvalues, with one boundary value on the left boundary and one boundary value on the right required to close the system. For simplicity, Dirichlet boundary conditions are used in our computation. As a matter of fact, we are only interested in the shock propagation within the given finite domain here. The treatments on the boundaries do not concern us in this numerical experiment.

Due to the small scale of the computation of one dimensional problems, numerical tests of the Sod problem for Navier-Stokes equations are done in Matlab. The Matlab program runs for 1-2 hours on a PC with Intel Pentium 4 3.0GHz CPU to get the following results. In the following figures, we display the numerical solutions for the fully discrete scheme (4.4.14) with the numerical flux (2.2.11), or in its equivalent yet simpler form (2.2.15). Uniform space and time grid sizes, Δx and Δt, are used. Both viscous and inviscid cases are explored. We use different spatial resolutions for the same problem, and adjust time step according to the CFL condition. Different choices of entropy function are also tested in the numerical experiments. We group our results into four sets.

1. Euler equations. The first four sets of figures are devoted to the Euler equations with zero viscous and heat fluxes (4.1.5).

With the choice of the entropy pair

$$(U(\mathbf{u}),\, F(\mathbf{u})) = \left(\frac{1+\gamma}{1-\gamma}(\rho p)^{\frac{1}{1+\gamma}},\, \frac{1+\gamma}{1-\gamma} q(\rho p)^{\frac{1}{1+\gamma}} \right), \qquad (4.5.1)$$

Figure 4.5.1 depicts the density, velocity, and pressure fields at $t = 0.05$ and $t = 0.1$; here we use $\Delta x = 0.001$ and $\frac{\Delta t}{\Delta x} = 0.025$. Comparing these to the corresponding results of the canonical entropy pair

$$(U(\mathbf{u}),\, F(\mathbf{u})) = \left(-\rho \ln(p\rho^{-\gamma}),\, -m \ln(p\rho^{-\gamma}) \right), \qquad (4.5.2)$$

in figure 4.5.2, we see that the different choices of entropies do not affect the behavior of the numerical solutions. Figures 4.5.1(d) and 4.5.2(d) demonstrate the conservation of the total entropies: the negligible amount of entropy decay $\sim 10^{-4}$ is introduced by the RK3 time discretization.

Next, we make the same comparison for the refined the spatial mesh, taking $\Delta x = 0.00025$, $\frac{\Delta t}{\Delta x} = 0.1$. Figure 4.5.3 presents the computed solutions of density, velocity, and pressure fields at $t = 0.05$ and $t = 0.1$ with the entropy pair (4.5.1) while figure 4.5.4 depicts the solutions with the canonical entropy pair (4.5.2). The total entropy is shown in figures 4.5.3(d) and 4.5.4(d).

The above results demonstrate the purely dispersive character of the entropy conservative schemes. Dispersive oscillations on the mesh scale are observed in shocks and contact regions, due to the absence of any dissipation mechanism, consult [Lax86, LL96]. The numerical solutions do *not* blow up. Actually, as we refine the mesh, these dispersive oscillations approach a modulated wave envelope. The study of these modulated waves in the conservative Euler equations would be an extremely challenging task. A similar entropy conservative *Lagrangian formulation* of Euler equations of [TT61] motivated the discussion in [Lax86].

2 Navier-Stokes equations with heat flux. We solve the Navier-Stokes equations (4.1.4). The results are summarized in the next three sets of figures 4.5.5–4.5.7. We follow the same pattern of plotting density, velocity, pressure and total entropy. As before, the choice of entropy pairs (4.5.1) in figures 4.5.5 and 4.5.6 are very similar.

The presence of heat flux causes the oscillations to be dramatically reduced around the contact discontinuity. Furthermore, oscillations are significantly damped around the shock; when the mesh is well-refined, figure 4.5.7 shows that heat conduction causes these oscillations to be well localized in the immediate neighborhood

of the shocks. If the mesh is underresolved, a small portion of dispersive oscillations persist in the neighborhood of shocks.

3. Navier-stokes equations with viscosity and no heat flux. We solve the viscous Navier-Stokes equations (4.1.3). The results are summarized in figures 4.5.8–4.5.9. Since the results are essentially independent of the choice of entropy, we chose to quote here only the results for the canonical pair (4.5.2).

The viscosity in Navier-Stokes equations is doing a better job than heat flux in damping oscillations around the shock discontinuity. The plots of total entropy, reveal a greater entropy decay than the Navier-Stokes equations with heat conduction. On the other hand, we still observe an oscillatory behavior around the contact discontinuity, even with the refined mesh in figure 4.5.9.

4. Full Navier-stokes equations with viscous and heat fluxes. In figures 4.5.10–4.5.11 we record the results for the full Navier-Stokes equations (4.1.1). As before, the difference due to different entropy functions is undetectable and we chose to record here only the canonical entropy.

As expected, these numerical solutions are the smoothest ones found in our numerical experiments. especially in very fine meshes, depicted in figure 4.5.11. Small oscillations remain with underresolved meshes.

Not only the oscillations around the shocks are damped out by viscosity, but the oscillations around the contact discontinuity are significantly reduced due to the heat flux. Compared with the results of Navier-Stokes equations with heat conduction (4.1.4) in figures 4.5.6–4.5.7, oscillations in the neighborhood of the

shock are better damped here thanks to the viscosity terms. The remaining sharp "spike" at the tip of shock discontinuity is due to the relatively small viscosity coefficient of air.
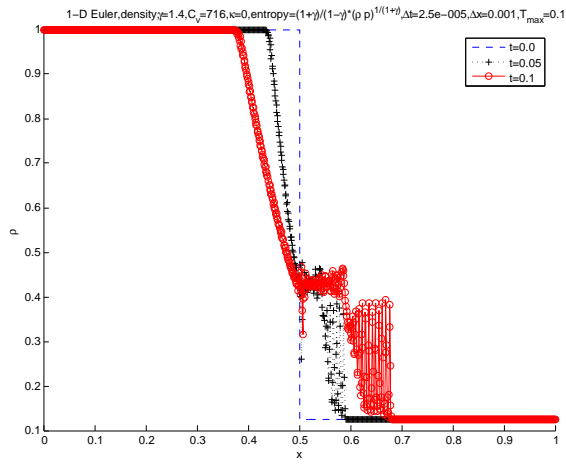
(a) Density
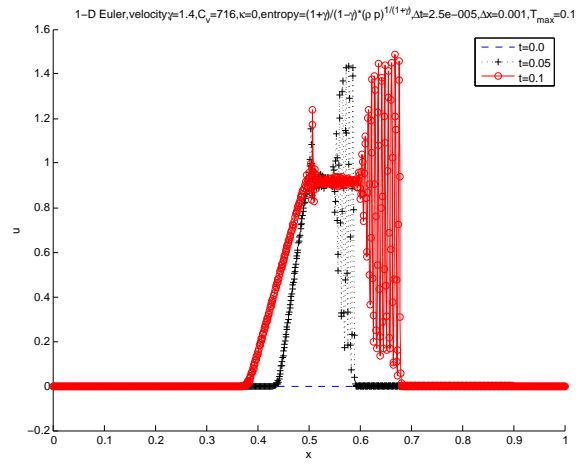
(b) Velocity
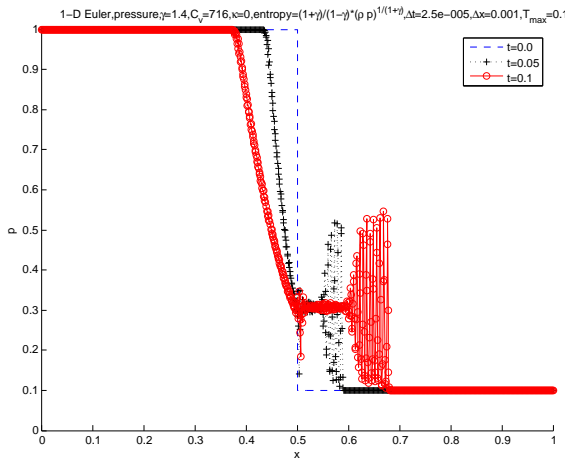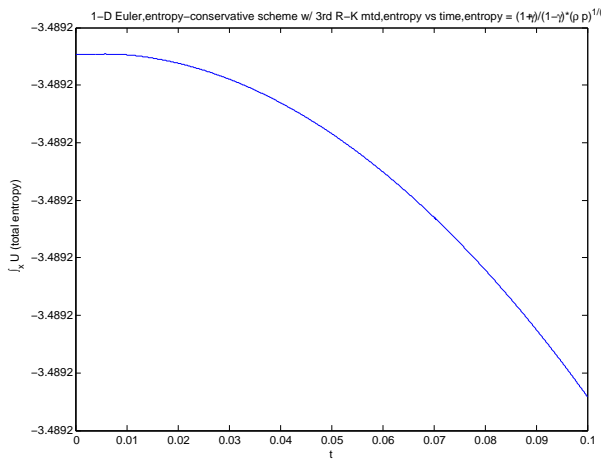
(c) Pressure

(d) Total entropy v.s. time

Figure 4.5.1: Euler equations with 1000 spatial gridpoints, $U(\mathbf{u}) = \frac{1+\gamma}{1-\gamma} \cdot (p\rho)^{\frac{1}{1+\gamma}}$, $\Delta t = 2.5 \times 10^{-5}$, $\Delta x = 10^{-3}$
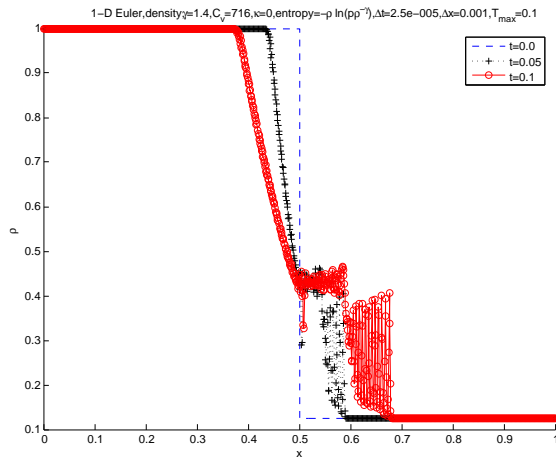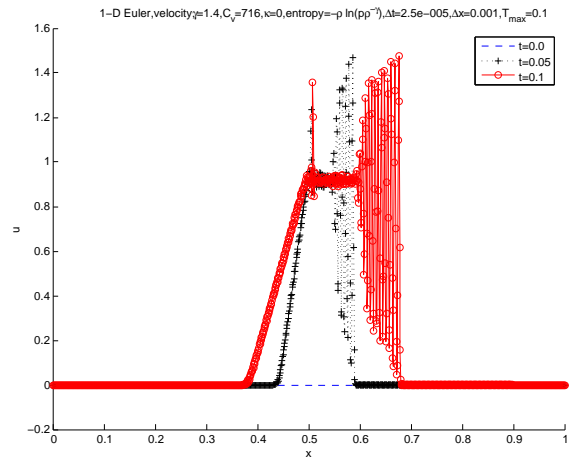
(a) Density
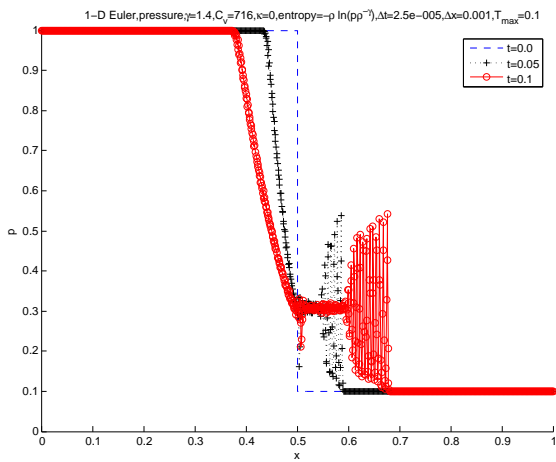
(b) Velocity
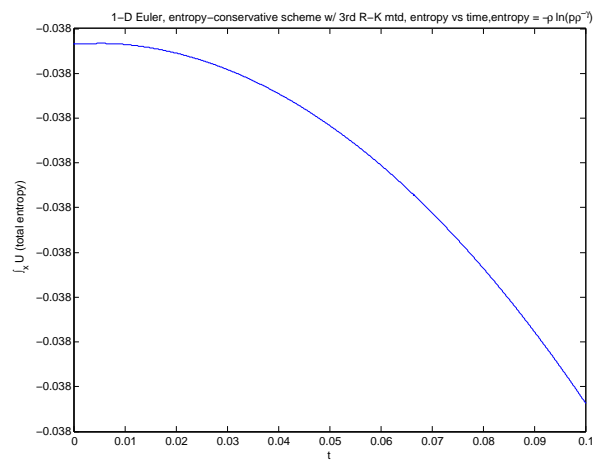
(c) Pressure

(d) Total entropy v.s. time

Figure 4.5.2: Euler equations with 1000 spatial gridpoints, $U(\mathbf{u}) = -\rho \ln \left(p\rho^{-\gamma} \right)$ and same Δt and Δx as figure 4.5.1
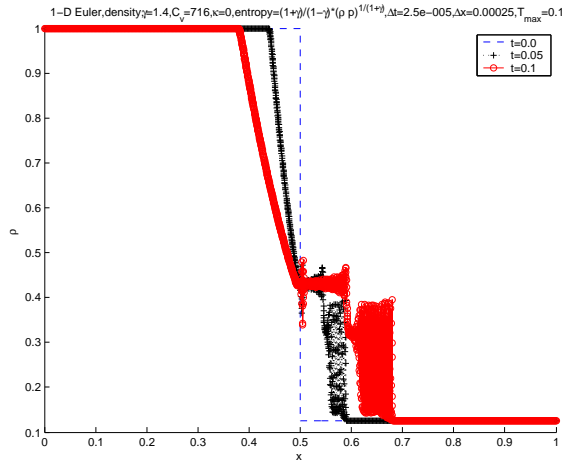
(a) Density
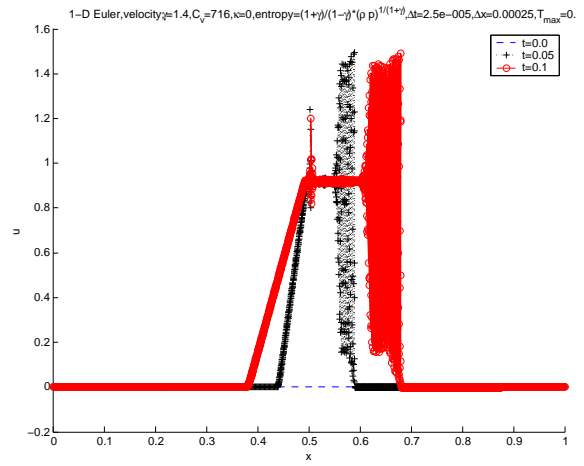
(b) Velocity
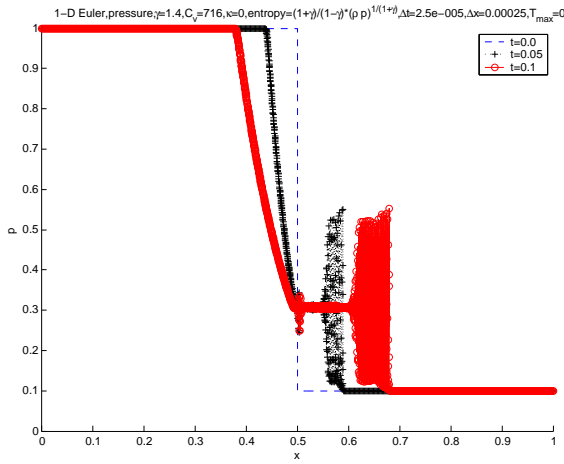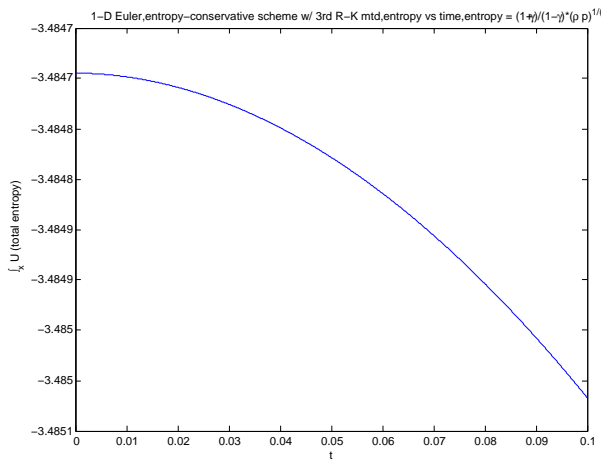
(c) Pressure

(d) Total entropy v.s. time

Figure 4.5.3: Euler equations with 4000 spatial gridpoints, $U(\mathbf{u}) = \frac{1+\gamma}{1-\gamma} \cdot (p\rho)^{\frac{1}{1+\gamma}}$, $\Delta t = 2.5 \times 10^{-5}$, $\Delta x = 2.5 \times 10^{-4}$
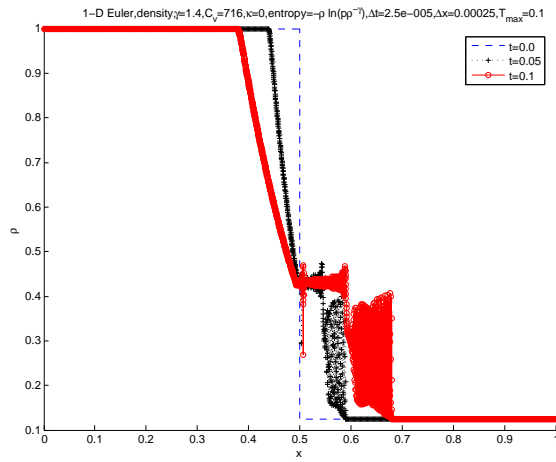
(a) Density
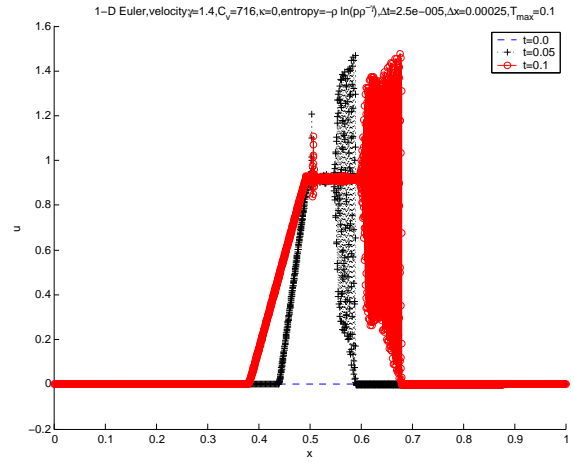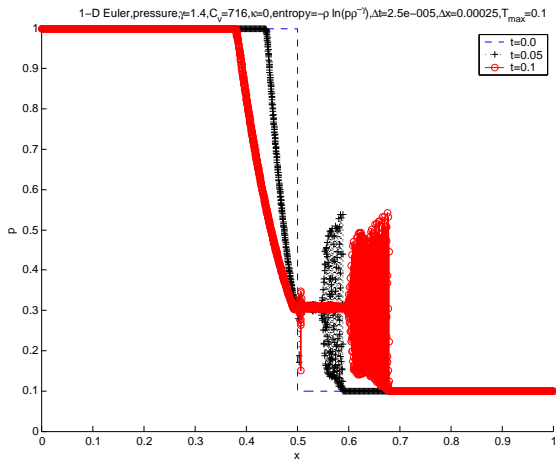
(b) Velocity
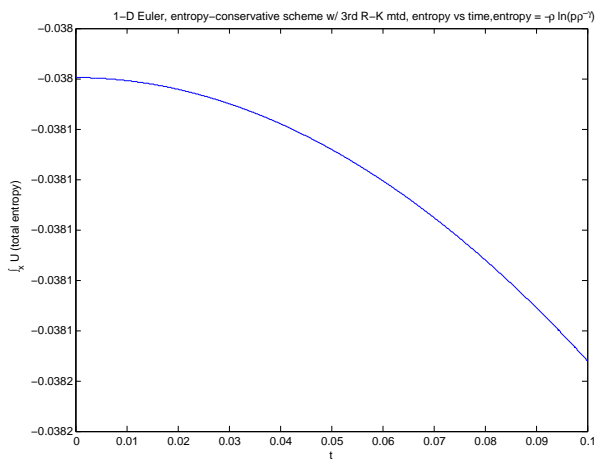
(c) Pressure

(d) Total entropy v.s. time

Figure 4.5.4: Euler equations with 4000 spatial gridpoints, $U(\mathbf{u}) = -\rho \ln \left(p \rho^{-\gamma} \right)$ and same Δt and Δx as Figure 4.5.3
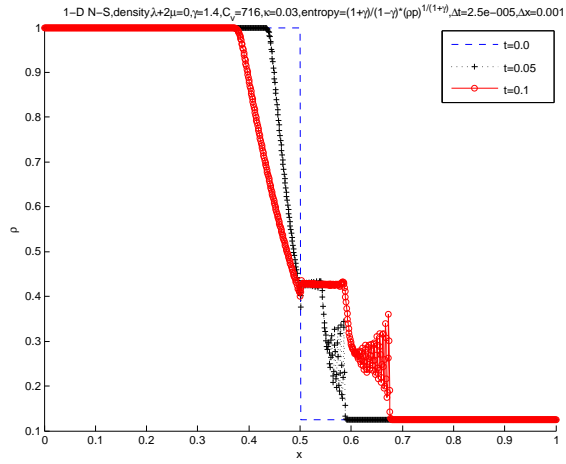
(a) Density
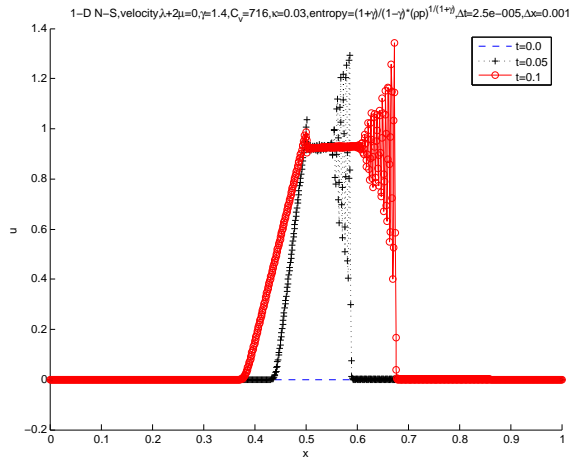
(b) Velocity
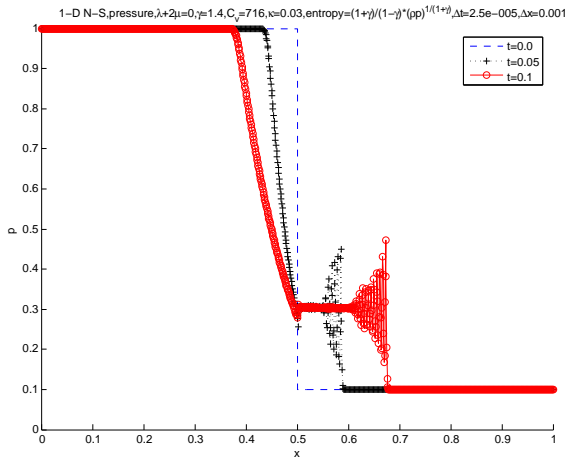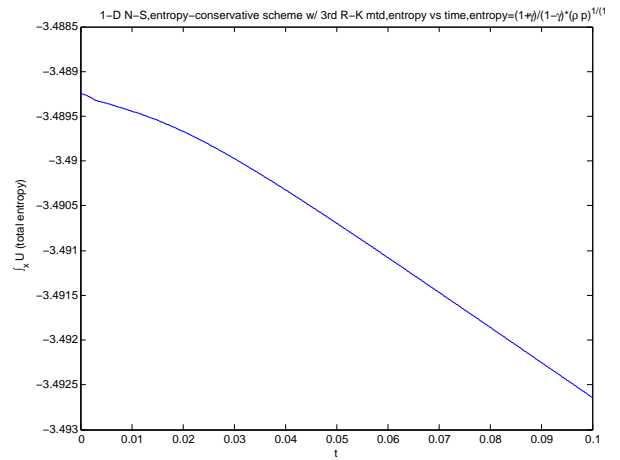
(c) Pressure

(d) Total entropy v.s. time

Figure 4.5.5: Navier-Stokes equations with heat conduction and no viscous term. 1000 spatial gridpoints, $U(\mathbf{u}) = \frac{1+\gamma}{1-\gamma} \cdot (p\rho)^{\frac{1}{1+\gamma}}$, $\Delta t = 2.5 \times 10^{-5}$, $\Delta x = 10^{-3}$
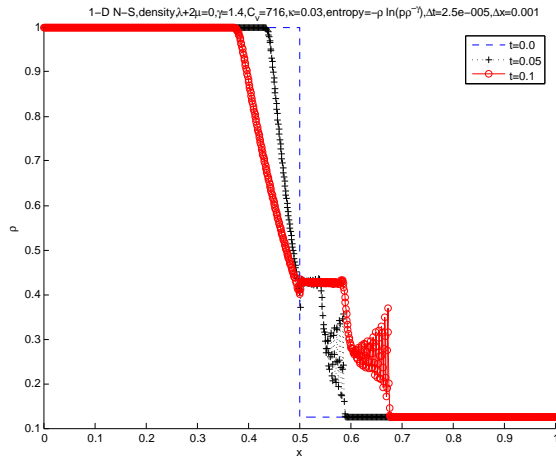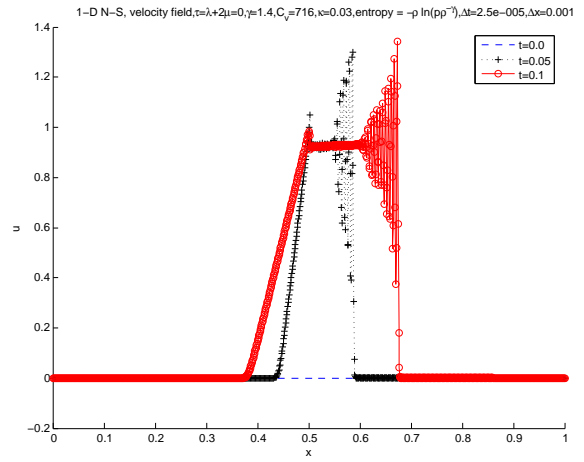
(a) Density
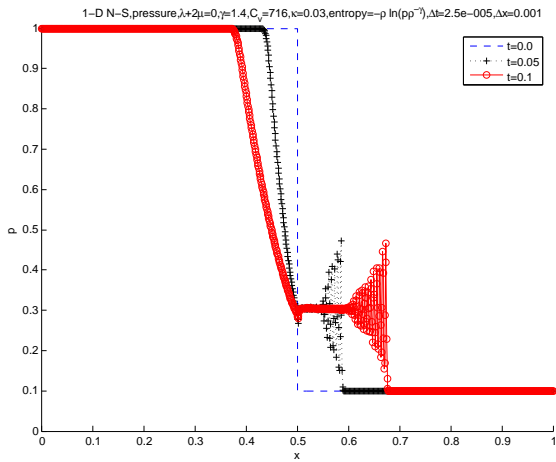
(b) Velocity
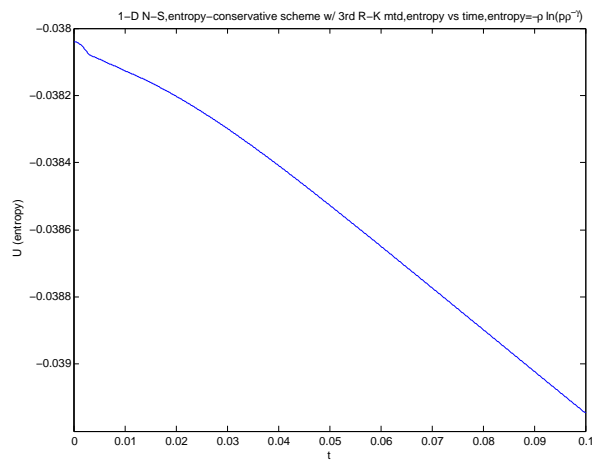
(c) Pressure

(d) Total entropy v.s. time

Figure 4.5.6: Navier-Stokes equations with heat conduction and no viscous terms. 1000 spatial gridpoints, $U(\mathbf{u}) = -\rho \ln\left(p\rho^{-\gamma}\right)$ and same Δt and Δx as Figure 4.5.5
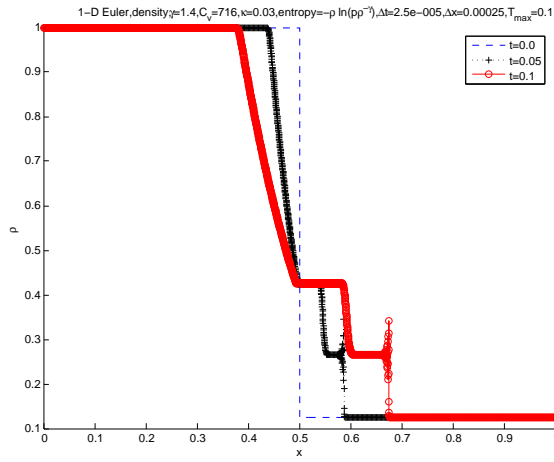
(a) Density
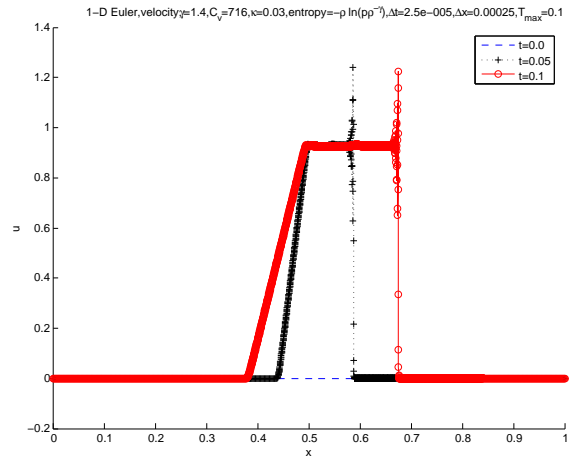
(b) Velocity
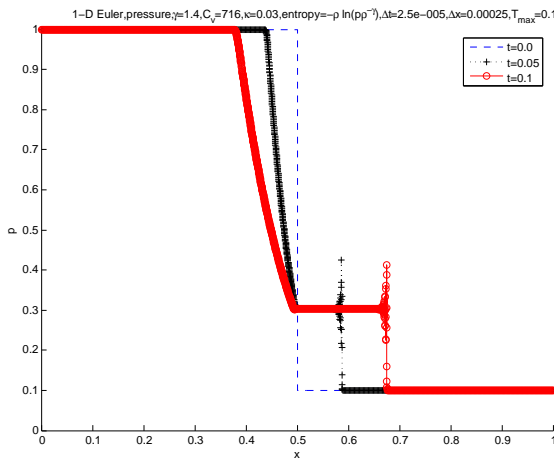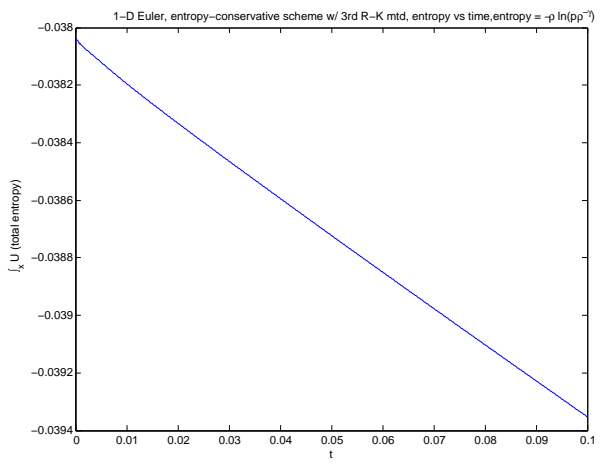
(c) Pressure

(d) Total entropy v.s. time

Figure 4.5.7: Navier-Stokes equations with heat conduction and no viscous terms.

4000 spatial grids, $U(\mathbf{u}) = -\rho \ln\left(p\rho^{-\gamma}\right)$, $\Delta t = 2.5 \times 10^{-5}$, $\Delta x = 2.5 \times 10^{-4}$
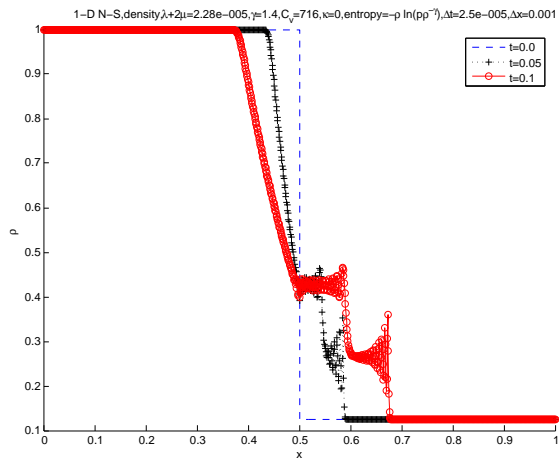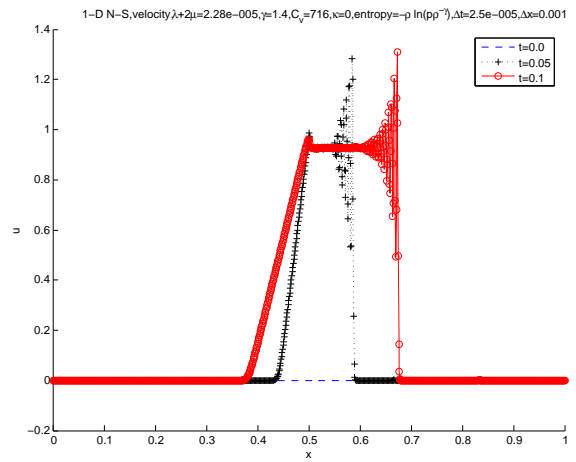
(a) Density
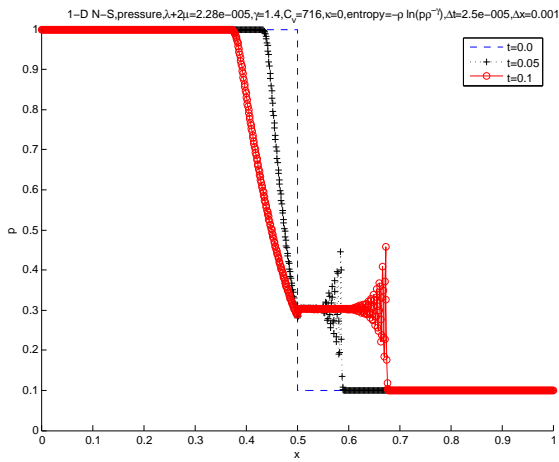
(b) Velocity
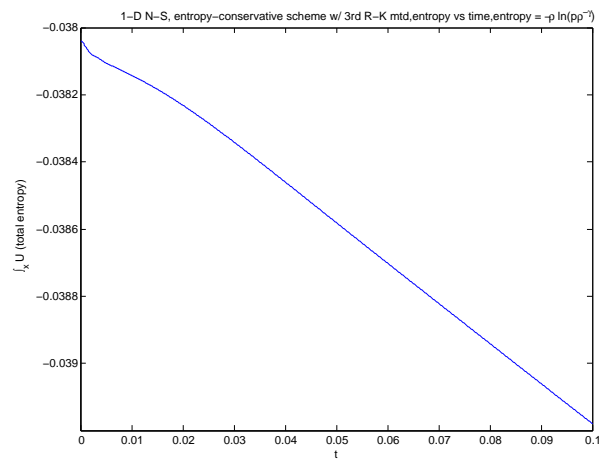
(c) Pressure

(d) Total entropy v.s. time

Figure 4.5.8: Navier-Stokes equations with viscous terms and no heat conduction. 1000 spatial gridpoints, $U(\mathbf{u}) = -\rho \ln\left(p\rho^{-\gamma}\right)$, $\Delta t = 2.5 \times 10^{-5}$, $\Delta x = 10^{-3}$
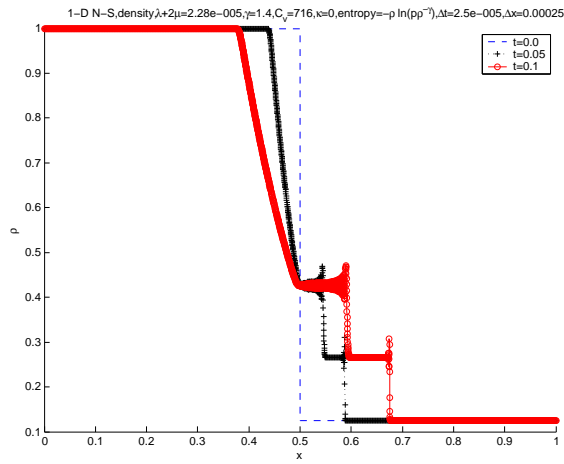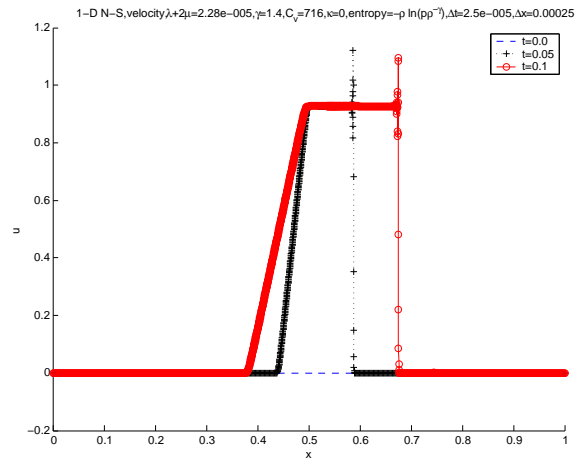
(a) Density
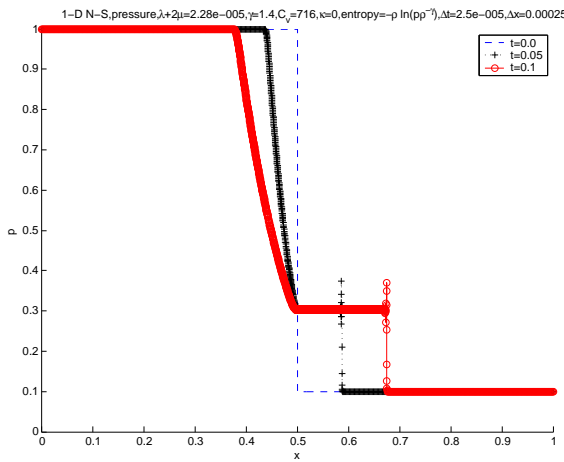
(b) Velocity
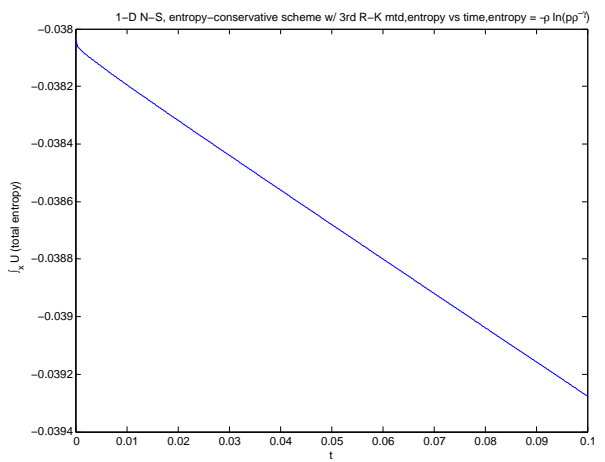
(c) Pressure

(d) Total entropy v.s. time

Figure 4.5.9: Navier-Stokes equations with viscous terms and no heat conduction. 4000 spatial grids, $U(\mathbf{u}) = -\rho \ln\left(p\rho^{-\gamma}\right)$, $\Delta t = 2.5 \times 10^{-5}$, $\Delta x = 2.5 \times 10^{-4}$
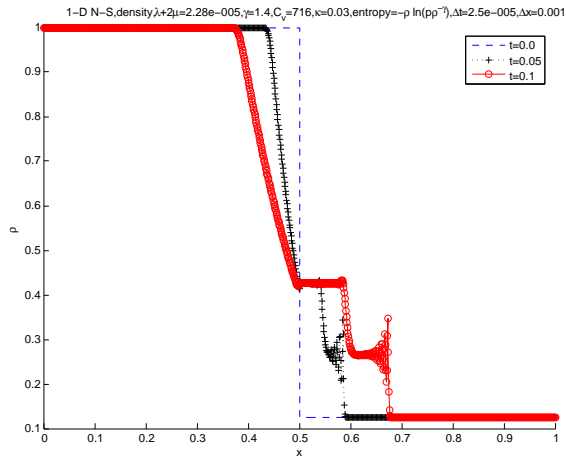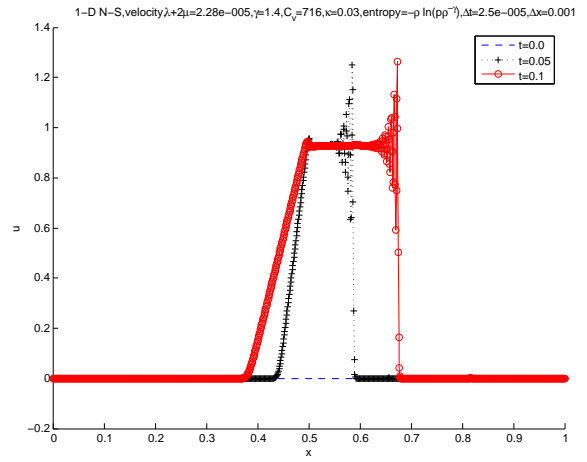
(a) Density
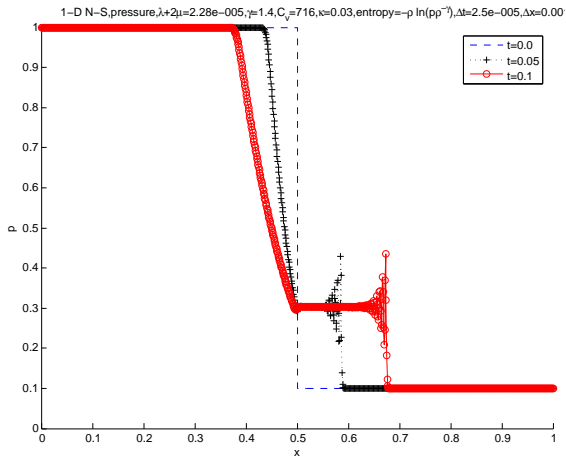
(b) Velocity
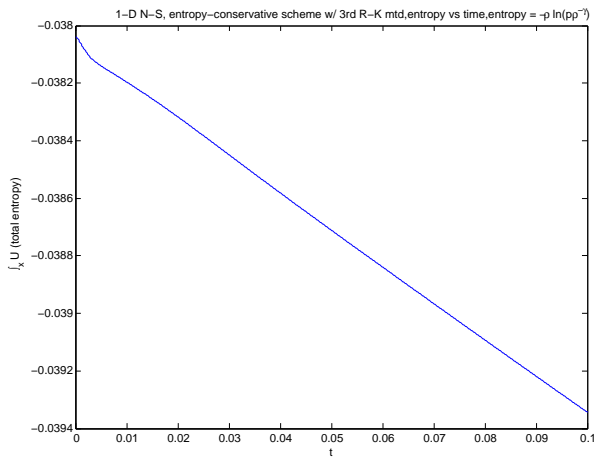
(c) Pressure

(d) Total entropy v.s. time

Figure 4.5.10: Navier-Stokes equations with viscosity and heat conduction. 1000 spatial gridpoints, $U(\mathbf{u}) = -\rho \ln \left(p\rho^{-\gamma} \right)$, $\Delta t = 2.5 \times 10^{-5}$, $\Delta x = 10^{-3}$
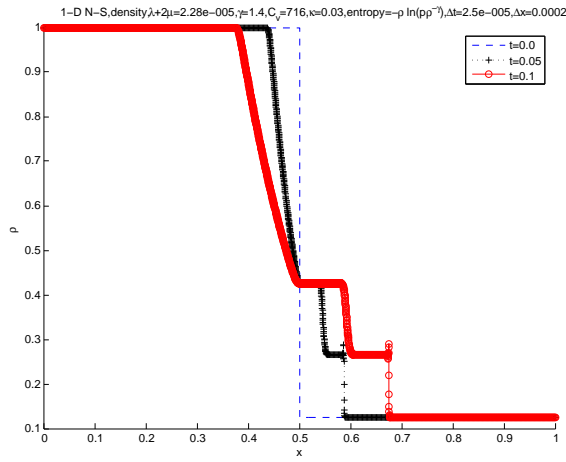
(a) Density
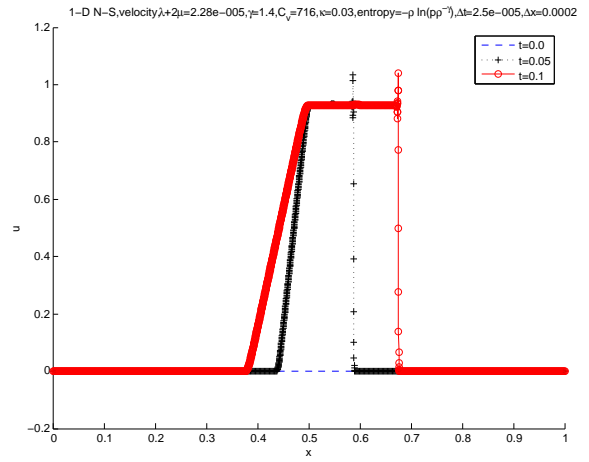
(b) Velocity
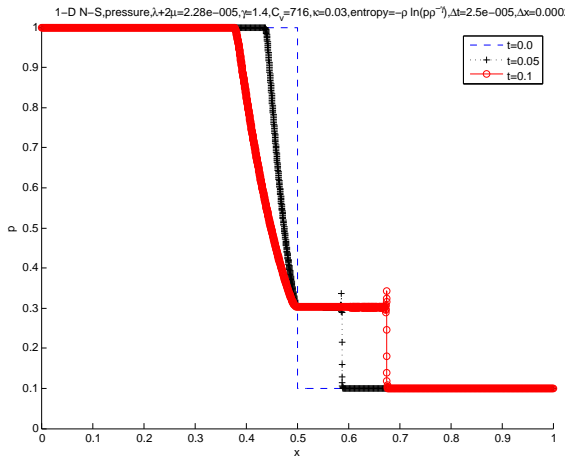
(c) Pressure
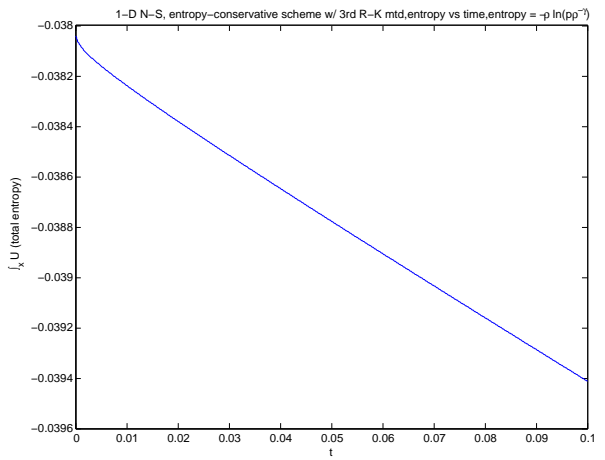
(d) Total entropy v.s. time

Figure 4.5.11: Navier-Stokes equations with viscosity and heat conduction. 4000 spatial gridpoints, $U(\mathbf{u}) = -\rho \ln\left(p\rho^{-\gamma}\right),\ \Delta t = 2.5 \times 10^{-5},\ \Delta x = 2.5 \times 10^{-4}$

67

Chapter 5

Two-Dimensional Shallow Water Equations

5.1 Governing equations

Consider a three-dimensional domain in which the homogenous fluid flows with a free surface under the influence of gravity. One of the widely used approaches for the description of such unsteady free-surface flows is that of shallow water. Under the shallow-water approximation that refers to the fact that a horizontal scale is in excess of the depth of the fluid, the 3D Navier-Stokes equations can be simplified to the shallow water equations with the depth-averaged continuity equation and momentum equations. The motions of the fluid are driven by the variations of the height of the free surface while the density is assumed to be constant. In general, the shallow water equations describe the time and space evolutions of the depth-averaged horizontal velocity components and the fluid elevation. Wide applications of the shallow water equations can be found in modeling the wave propagation in atmosphere and ocean as well as gravity waves in the smaller domain.

Neglecting diffusion of momentum due to wind effects and Coriolis terms, we consider two-dimensional shallow water equations in the conservative form for free-surface compressible flow with flat frictionless bottom on two dimensional x-y plane,

$$\frac{\partial}{\partial t}\mathbf{u} + \frac{\partial}{\partial x}\mathbf{f}(\mathbf{u}) + \frac{\partial}{\partial y}\mathbf{g}(\mathbf{u}) = \varsigma\frac{\partial}{\partial x}\left(h\frac{\partial}{\partial x}\mathbf{d}(\mathbf{u})\right) + \varsigma\frac{\partial}{\partial y}\left(h\frac{\partial}{\partial y}\mathbf{d}(\mathbf{u})\right), \qquad \text{(5.1.1a)}$$

with $\mathbf{u}$ being the vector of conserved variables,

$$\mathbf{u} = [h, \, uh, \, vh]^\top, \tag{5.1.1b}$$

balanced by the flux vectors

$$\mathbf{f} = [uh, \, u^2h + gh^2/2, \, uvh]^\top, \quad \mathbf{g} = [vh, \, uvh, \, v^2h + gh^2/2]^\top, \tag{5.1.1c}$$

and the viscous flux vector

$$\mathbf{d} = [0, \, u, \, v]^\top. \tag{5.1.1d}$$

The system (5.1.1a) represents the mass and momentum conservation. Here, $h = h(x, y, t)$ is the total water depth which plays the role of density, and $(u(x, y, t), v(x, y, t))$ are the depth-averaged velocity components along x and y direction. Finally, g is the constant acceleration due to the gravity, and $\varsigma > 0$ is the constant eddy viscosity. By ignoring the small scale vortices in the motion, we calculate a large-scale flow motion with eddy viscosity ς that characterizes the transport and dissipation of energy in the smaller scale flow.

If we turn off the eddy viscosity ($\varsigma = 0$), the system (5.1.1a) is reduced to the homogeneous inviscid shallow water equations,

$$\frac{\partial}{\partial t}\mathbf{u} + \frac{\partial}{\partial x}\mathbf{f}(\mathbf{u}) + \frac{\partial}{\partial y}\mathbf{g}(\mathbf{u}) = 0. \tag{5.1.2}$$

The shallow water equations constitute a hyperbolic or incompletely parabolic system, solutions to which can exhibit discontinuities associated with hydraulic jumps and bores in flow or the propagation of sharp fronts. In the numerical simulations of shallow water flows, the conservation of energy guarantees the numerical schemes are nonlinearly stable and free of artificial numerical viscosity, which

may dramatically change the profiles of the solutions in long time integration. In this chapter, we are concerned with the energy-stable numerical methods for simulating flow situations in which discontinuities are present initially. Specifically, we apply entropy-stable schemes to solve the two dimensional partial-dam-break problem. In our computation, energy conservation will be enforced through the conservation of entropy by choosing the sum of the potential and kinetic energies $U = (gh^2 + u^2h + v^2h)/2$ as a generalized entropy function. The resulting numerical scheme is energy-stable with no artificial numerical viscosity in the sense that energy dissipation is driven solely by the eddy viscous fluxes. In the particular case that eddy viscosity is absent, $\varsigma = 0$, our scheme *precisely* preserves the total energy U.

5.2 Energy balance

5.2.1 Entropy/energy conservation and dissipation

We consider the inviscid shallow water equations (5.1.2),

$$\mathbf{u}_x + \mathbf{f}(\mathbf{u})_x + \mathbf{g}(\mathbf{u})_y = 0.$$

Any smooth solution $\mathbf{u}$ satisfies the additional conservation laws of an admissible entropy $U(\mathbf{u})$, which is balanced by entropy fluxes $F(\mathbf{u})$ and $G(\mathbf{u})$,

$$\frac{\partial}{\partial t} U(\mathbf{u}) + \frac{\partial}{\partial x} F(\mathbf{u}) + \frac{\partial}{\partial y} G(\mathbf{u}) = 0. \tag{5.2.1}$$

(5.2.1) indeed is the case if the entropy function $U(\mathbf{u})$ is linked to the entropy fluxes $F(\mathbf{u})$ and $G(\mathbf{u})$ through the compatibility relations,

$$U_{\mathbf{u}}^\top \mathbf{f_u} = F_{\mathbf{u}}^\top, \quad U_{\mathbf{u}}^\top \mathbf{g_u} = G_{\mathbf{u}}^\top. \tag{5.2.2}$$

In fact, multiplying (5.1.2) by $U_{\mathbf{u}}^{\top}$ on the left, one recovers the equivalence between (5.1.2) and (5.2.2) for all classical solutions $\mathbf{u}$'s of (5.1.2).

In the presence of shock discontinuities, (5.1.2) is realized by appropriate vanishing viscosity limits. To this end, we turn to the viscous shallow water equations (5.1.1a),

$$\mathbf{u}_t + \mathbf{f}(\mathbf{u})_x + \mathbf{g}(\mathbf{u})_y = \varsigma \left[(h\mathbf{d}(\mathbf{u})_x)_x + (h\mathbf{d}(\mathbf{u})_y)_y \right].$$

We integrate (5.1.1a) against the entropy variable $\mathbf{v} := U_{\mathbf{u}}$, employ the compatibility relations (5.2.2) and use 'differentiation by parts' on the dissipation terms on the RHS to find the following entropy balance statement,

$$\frac{\partial}{\partial t} U(\mathbf{u}) + \frac{\partial}{\partial x} (F(\mathbf{u}) - \varsigma \langle \mathbf{v}, h\mathbf{d}(\mathbf{u})_x \rangle) + \frac{\partial}{\partial y} (G(\mathbf{u}) - \varsigma \langle \mathbf{v}, h\mathbf{d}(\mathbf{u})_y \rangle) =$$

$$- \varsigma \left[\langle \mathbf{v}_x, h\mathbf{d}_{\mathbf{v}}\mathbf{v}_x \rangle + \langle \mathbf{v}_y, h\mathbf{d}_{\mathbf{v}}\mathbf{v}_y \rangle \right] \le 0. \quad (5.2.3)$$

Spatial integration of (5.2.3) yields

$$\frac{d}{dt} \int_y \int_x U(\mathbf{u}) \, dxdy = -\varsigma \int_y \int_x \left[\langle \mathbf{v}_x, h\mathbf{d}_{\mathbf{v}}\mathbf{v}_x \rangle + \langle \mathbf{v}_y, h\mathbf{d}_{\mathbf{v}}\mathbf{v}_y \rangle \right] \, dxdy \le 0. \quad (5.2.4)$$

For the inviscid shallow water equation ($\varsigma = 0$), the global entropy conservation is satisfied,

$$\int_y \int_x U(\mathbf{u}(x, t)) \, dxdy = \int_y \int_x U(\mathbf{u}(x, 0)) \, dxdy.$$

5.2.2 Entropy variables for shallow water equations

As I mentioned above, we apply the entropy-stable discretization constructed in Chapter 2 to guarantee the *energy stability* in our numerical approximations. To

this end, we employ the depth-averaged sum of the potential and kinetic energies as a generalized entropy function,

$$U(\mathbf{u}) = \frac{gh^2 + u^2h + v^2h}{2}. \tag{5.2.5}$$

Straightforward computation gives us the following entropy fluxes, entropy variables and potentials.

- Entropy fluxes

$$F(\mathbf{u}) = guh^2 + \frac{u^3h + uv^2h}{2}, \quad G(\mathbf{u}) = gvh^2 + \frac{u^2vh + v^3h}{2}; \tag{5.2.6}$$

- Entropy variable

$$\mathbf{v}(\mathbf{u}) = \begin{bmatrix} gh - \dfrac{u^2 + v^2}{2} \\ u \\ v \end{bmatrix} \tag{5.2.7}$$

with the Jacobian matrices

$$H(\mathbf{v}) := \mathbf{u}_{\mathbf{v}} = \frac{1}{g} \begin{bmatrix} 1 & u & v \\ u & c^2 + u^2 & uv \\ v & uv & c^2 + v^2 \end{bmatrix}, \tag{5.2.8}$$

$$(H(\mathbf{v}))^{-1} = \mathbf{v}_{\mathbf{u}} = \frac{1}{h} \begin{bmatrix} c^2 + u^2 + v^2 & -u & -v \\ -u & 1 & 0 \\ -v & 0 & 1 \end{bmatrix}, \tag{5.2.9}$$

where $c := \sqrt{gh}$ is the 'sound' speed, or wave celerity.

- Potential of $\mathbf{u}(\mathbf{v})$

$$\phi(\mathbf{v}) = \frac{gh^2}{2}, \tag{5.2.10}$$

72

and potentials of $\mathbf{f}(\mathbf{u}(\mathbf{v}))$ and $\mathbf{g}(\mathbf{u}(\mathbf{v}))$, respectively,

$$\psi^x(\mathbf{v}) = \frac{guh^2}{2}, \quad \psi^y(\mathbf{v}) = \frac{gvh^2}{2}. \tag{5.2.11}$$

In this case, the general statement of entropy/energy balance of shallow water equations in (5.2.4) with the entropy function and fluxes

$$(U, F, G) = \left(\frac{gh^2 + u^2h + v^2h}{2}, guh^2 + \frac{u^3h + uv^2h}{2}, gvh^2 + \frac{u^2vh + v^3h}{2} \right)$$

amounts to

$$\frac{d}{dt} \int_y \int_x U(\mathbf{u})\, dxdy = -\varsigma \int_y \int_x h(u_x^2 + u_y^2 + v_x^2 + v_y^2)\, dxdy \leq 0. \tag{5.2.12}$$

Due to the negativity of the expression on the RHS, we conclude that the total entropy/energy $\int_y \int_x \frac{gh^2 + u^2h + v^2h}{2}\, dxdy$ is decreasing in time, thus recovering the energy stability. In fact, the expression on the RHS specifies the precise decay rate, which is dictated solely by the viscous fluxes through their dependence on the nonnegative eddy viscosity ς.

5.3   Energy stable schemes

5.3.1   Entropy/energy-stable semi-discrete schemes for shallow water equations

The second-order semi-discrete entropy conservative schemes (2.2.10), (2.2.11) can be extended to two dimensional problems in a straightforward manner. The construction of the piece-wise constant intermediate path in $\mathbf{u}$ and $\mathbf{v}$-spaces can be carried out separately in x and y directions as indicated in (2.2.9).

73

Let (U, F, G) be the admissible entropy function (5.2.5) and entropy fluxes (5.2.6) associated with the two dimensional shallow water equations, $\mathbf{v} := U_{\mathbf{v}}$ be the corresponding entropy variable outlined in (5.2.7), and (ψ^x, ψ^y) be the potential pair (5.2.11). In order to conserve the total entropy/energy $\int_y \int_x U(\mathbf{u}(x, y, t)) \, dx dy$ in our numerical approximation, we argue along the same line as one dimensinoal Navier-Stokes equations dimension by dimension. We discretize the convective parts on the LHS by the entropy/energy differencing. For the dissipative terms on the RHS, we employ the centered differences, while the intermediate h-values are taken to be the arithmetic mean of two neighboring grid-points, $\widehat{h_{\nu+\frac{1}{2},\mu}} := (h_{\nu+1,\mu}+h_{\nu,\mu})/2$. We then obtain the entropy/energy stable semi-discrete schemes

$$\frac{d}{dt}\mathbf{u}_{\nu,\mu}(t) + \frac{1}{\Delta x}(\mathbf{f}^*_{\nu+\frac{1}{2},\mu} - \mathbf{f}^*_{\nu-\frac{1}{2},\mu}) + \frac{1}{\Delta y}(\mathbf{g}^*_{\nu,\mu+\frac{1}{2}} - \mathbf{g}^*_{\nu,\mu-\frac{1}{2}})$$

$$= \frac{\varsigma}{\Delta x}(\widehat{h_{\nu+\frac{1}{2},\mu}}\frac{\mathbf{d}_{\nu+1,\mu} - \mathbf{d}_{\nu,\mu}}{\Delta x} - \widehat{h_{\nu-\frac{1}{2},\mu}}\frac{\mathbf{d}_{\nu,\mu} - \mathbf{d}_{\nu-1,\mu}}{\Delta x})$$

$$+ \frac{\varsigma}{\Delta y}(\widehat{h_{\nu,\mu+\frac{1}{2}}}\frac{\mathbf{d}_{\nu,\mu+1} - \mathbf{d}_{\nu,\mu}}{\Delta x} - \widehat{h_{\nu,\mu-\frac{1}{2}}}\frac{\mathbf{d}_{\nu,\mu} - \mathbf{d}_{\nu,\mu-1}}{\Delta x}), \quad (5.3.1a)$$

with the entropy-conservative fluxes $\mathbf{f}^*_{\nu+\frac{1}{2},\mu}$ and $\mathbf{g}^*_{\nu,\mu+\frac{1}{2}}$ outlined in (2.2.11) along x and y direction, respectively,

$$\mathbf{f}^*_{\nu+\frac{1}{2},\mu} = \sum_{j=1}^{3} \frac{\psi^x\left(\mathbf{v}^{j+1}_{\nu+\frac{1}{2},\mu}\right) - \psi^x\left(\mathbf{v}^j_{\nu+\frac{1}{2},\mu}\right)}{\left\langle \boldsymbol{\ell}^{xj}_{\nu+\frac{1}{2},\mu}, \Delta\mathbf{v}_{\nu+\frac{1}{2},\mu}\right\rangle}\boldsymbol{\ell}^{xj}_{\nu+\frac{1}{2},\mu}$$

$$= \frac{g}{2}\sum_{j=1}^{3} \frac{(h^{j+1}_{\nu+\frac{1}{2},\mu})^2 u^{j+1}_{\nu+\frac{1}{2},\mu} - (h^j_{\nu+\frac{1}{2},\mu})^2 u^j_{\nu+\frac{1}{2},\mu}}{\left\langle \boldsymbol{\ell}^{xj}_{\nu+\frac{1}{2},\mu}, \Delta\mathbf{v}_{\nu+\frac{1}{2},\mu}\right\rangle}\boldsymbol{\ell}^{xj}_{\nu+\frac{1}{2},\mu}, \quad (5.3.1b)$$

$$\mathbf{g}^*_{\nu,\mu+\frac{1}{2}} = \sum_{j=1}^{3} \frac{\psi^y\left(\mathbf{v}^{j+1}_{\nu,\mu+\frac{1}{2}}\right) - \psi^y\left(\mathbf{v}^j_{\nu,\mu+\frac{1}{2}}\right)}{\left\langle \boldsymbol{\ell}^{yj}_{\nu,\mu+\frac{1}{2}}, \Delta\mathbf{v}_{\nu,\mu+\frac{1}{2}}\right\rangle}\boldsymbol{\ell}^{yj}_{\nu,\mu+\frac{1}{2}}$$

$$= \frac{g}{2}\sum_{j=1}^{3} \frac{(h^{j+1}_{\nu,\mu+\frac{1}{2}})^2 v^{j+1}_{\nu,\mu+\frac{1}{2}} - (h^j_{\nu,\mu+\frac{1}{2}})^2 v^j_{\nu,\mu+\frac{1}{2}}}{\left\langle \boldsymbol{\ell}^{yj}_{\nu,\mu+\frac{1}{2}}, \Delta\mathbf{v}_{\nu,\mu+\frac{1}{2}}\right\rangle}\boldsymbol{\ell}^{yj}_{\nu,\mu+\frac{1}{2}}, \quad (5.3.1c)$$

74

Here, $\mathbf{u}_{\nu,\mu}(t)$ denotes the discrete solution at the grid point (x_ν, y_μ, t) with $x_\nu :=$ $\nu \Delta x$, $y_\mu := \mu \Delta y$, Δx and Δy being the uniform mesh sizes, and $\mathbf{d}_{\nu,\mu} := \mathbf{d}(\mathbf{u}_{\nu,\mu})$. Numerical flux $\mathbf{f}^*_{\nu+\frac{1}{2},\mu}$ and $\mathbf{g}^*_{\nu,\mu+\frac{1}{2}}$ are constructed separately along two different phase pathes dictated by two sets of vectors $\{\boldsymbol{\ell}^{x^j}\}$ and $\{\boldsymbol{\ell}^{y^j}\}$. $\{u^j\}$, $\{v^j\}$, and $\{h^j\}$ are intermediate values of height and velocities along pathes. Here in (5.3.1b) and (5.3.1c), $\Delta \mathbf{v}_{\nu+\frac{1}{2},\mu} := \mathbf{v}_{\nu+1,\mu} - \mathbf{v}_{\nu,\mu}$ and $\Delta \mathbf{v}_{\nu,\mu+\frac{1}{2}} := \mathbf{v}_{\nu,\mu+1} - \mathbf{v}_{\nu,\mu}$. The physical relevance of the intermediate solutions along the path needs to be maintained. To this end, we choose to work along the pathes which are determined by (approximate) Riemann solvers. Specifically, we use the eigensystems of the Roe matrix in x direction, [Roe81, Gla87],

$$
\begin{bmatrix}
0 & 1 & 0 \\
\bar{c}^2_{\nu+\frac{1}{2},\mu} - \bar{u}^2_{\nu+\frac{1}{2},\mu} & 2\bar{u}_{\nu+\frac{1}{2},\mu} & 0 \\
-\bar{u}_{\nu+\frac{1}{2},\mu}\bar{v}_{\nu+\frac{1}{2},\mu} & \bar{v}_{\nu+\frac{1}{2},\mu} & \bar{u}_{\nu+\frac{1}{2},\mu}
\end{bmatrix},
\tag{5.3.2a}
$$

and the Roe matrix in y direction,

$$
\begin{bmatrix}
0 & 0 & 1 \\
-\bar{u}_{\nu,\mu+\frac{1}{2}}\bar{v}_{\nu,\mu+\frac{1}{2}} & \bar{v}_{\nu,\mu+\frac{1}{2}} & \bar{u}_{\nu,\mu+\frac{1}{2}} \\
\bar{c}^2_{\nu,\mu+\frac{1}{2}} - \bar{v}^2_{\nu,\mu+\frac{1}{2}} & 0 & 2\bar{v}_{\nu,\mu+\frac{1}{2}}
\end{bmatrix}.
\tag{5.3.2b}
$$

Here $\bar{u}$, $\bar{v}$, and $\bar{c}$ are the average values of the velocities u, v and the sound speed $c := \sqrt{gh}$ at Roe-average state,

$$
\bar{u} = \frac{u_R\sqrt{h_R} + u_L\sqrt{h_L}}{\sqrt{h_R} + \sqrt{h_L}}, \quad \bar{v} = \frac{v_R\sqrt{h_R} + v_L\sqrt{h_L}}{\sqrt{h_R} + \sqrt{h_L}}
\tag{5.3.2c}
$$

$$
\bar{c} = \sqrt{\frac{g(h_R + h_L)}{2}},
\tag{5.3.2d}
$$

75

where the subscripts $(\cdot)_R$ and $(\cdot)_L$ represent two neighboring spatial grid-points. The vector sets $\{\widehat{\mathbf{r}}^{x^j}\}_{j=1}^3$ and $\{\widehat{\mathbf{r}}^{y^j}\}_{j=1}^3$ are chosen to be the right eigenvectors of the x-Roe matrix (5.3.2a) and the y-Roe matrix (5.3.2b), respectively, (omitting the sub/superscripts of all averaged variables)

$$\widehat{\mathbf{r}}^{x^1} = \begin{bmatrix} 1 \\ \bar{u} - \bar{c} \\ \bar{v} \end{bmatrix}, \quad \widehat{\mathbf{r}}^{x^2} = \begin{bmatrix} 0 \\ 0 \\ \bar{c} \end{bmatrix}, \quad \widehat{\mathbf{r}}^{x^3} = \begin{bmatrix} 1 \\ \bar{u} + \bar{c} \\ \bar{v} \end{bmatrix}, \tag{5.3.2e}$$

$$\widehat{\mathbf{r}}^{y^1} = \begin{bmatrix} 1 \\ \bar{u} \\ \bar{v} - \bar{c} \end{bmatrix}, \quad \widehat{\mathbf{r}}^{y^2} = \begin{bmatrix} 0 \\ -\bar{c} \\ 0 \end{bmatrix}, \quad \widehat{\mathbf{r}}^{y^3} = \begin{bmatrix} 1 \\ \bar{u} \\ \bar{v} + \bar{c} \end{bmatrix}, \tag{5.3.2f}$$

with the corresponding left eigenvector sets $\{\widehat{\boldsymbol{\ell}}^{x^j}\}_{j=1}^3$ and $\{\widehat{\boldsymbol{\ell}}^{y^j}\}_{j=1}^3$ given by

$$\widehat{\boldsymbol{\ell}}^{x^1} = \begin{bmatrix} \dfrac{\bar{u} + \bar{c}}{2\bar{c}} \\ -\dfrac{1}{2\bar{c}} \\ 0 \end{bmatrix}, \quad \widehat{\boldsymbol{\ell}}^{x^2} = \begin{bmatrix} -\dfrac{\bar{v}}{\bar{c}} \\ 0 \\ \dfrac{1}{\bar{c}} \end{bmatrix}, \quad \widehat{\boldsymbol{\ell}}^{x^3} = \begin{bmatrix} \dfrac{-\bar{u} + \bar{c}}{2\bar{c}} \\ \dfrac{1}{2\bar{c}} \\ 0 \end{bmatrix}, \tag{5.3.2g}$$

$$\widehat{\boldsymbol{\ell}}^{y^1} = \begin{bmatrix} \dfrac{\bar{v} + \bar{c}}{2\bar{c}} \\ 0 \\ -\dfrac{1}{2\bar{c}} \end{bmatrix}, \quad \widehat{\boldsymbol{\ell}}^{y^2} = \begin{bmatrix} \dfrac{\bar{u}}{\bar{c}} \\ -\dfrac{1}{\bar{c}} \\ 0 \end{bmatrix}, \quad \widehat{\boldsymbol{\ell}}^{y^3} = \begin{bmatrix} \dfrac{-\bar{v} + \bar{c}}{2\bar{c}} \\ 0 \\ \dfrac{1}{2\bar{c}} \end{bmatrix}. \tag{5.3.2h}$$

We now are able to form the intermediate pathes along x and y directions in $\mathbf{u}$-space as in (2.2.9),

$$\mathbf{u}^{j+1}_{\nu+\frac{1}{2},\mu} = \mathbf{u}^{j}_{\nu+\frac{1}{2},\mu} + \left\langle \widehat{\boldsymbol{\ell}}^{x^j}, \Delta\mathbf{u}_{\nu+\frac{1}{2},\mu} \right\rangle \widehat{\mathbf{r}}^{x^j}, \quad j = 1, 2, 3,$$

$$\mathbf{u}^{j+1}_{\nu,\mu+\frac{1}{2}} = \mathbf{u}^{j}_{\nu,\mu+\frac{1}{2}} + \left\langle \widehat{\boldsymbol{\ell}}^{y^j}, \Delta\mathbf{u}_{\nu,\mu+\frac{1}{2}} \right\rangle \widehat{\mathbf{r}}^{y^j}, \quad j = 1, 2, 3.$$

Then the construction of the entropy/energy conservative numerical fluxes $\mathbf{f}^*_{\nu+\frac{1}{2},\mu}$

and $\mathbf{g}^*_{\nu,\mu+\frac{1}{2}}$ follows the algorithm indicated in Algorithm 4.4.1.

Remark 5.3.1. We want to point out that in the case $\left\langle \widehat{\boldsymbol{\ell}}^j, \Delta \mathbf{u} \right\rangle = 0$ for certain

j's in $\mathbf{u}$-space, which may cause $\left\langle \boldsymbol{\ell}^j, \Delta \mathbf{v} \right\rangle = 0$ in $\mathbf{v}$-space, hence fail Algorithm

4.4.1. Arguing along the same line as Remark 4.4.1, we compute the corresponding

entropy/energy numerical fluxes in the alternate formulas,

$$\mathbf{f}^*_{\nu+\frac{1}{2},\mu} = \sum_{\{j|\xi^{xj}\neq 0\}} \frac{\psi^x(\mathbf{v}^j_{\nu+\frac{1}{2},\mu} + \xi^{xj}\mathbf{r}^j_{\nu+\frac{1}{2},\mu}) - \psi^x(\mathbf{v}^j_{\nu+\frac{1}{2},\mu})}{\xi^{xj}} \boldsymbol{\ell}^{xj}_{\nu+\frac{1}{2},\mu}, \quad \xi^{xj} = \left\langle \boldsymbol{\ell}^{xj}_{\nu+\frac{1}{2},\mu}, \Delta\mathbf{v}_{\nu+\frac{1}{2},\mu} \right\rangle,$$

$$\mathbf{g}^*_{\nu,\mu+\frac{1}{2}} = \sum_{\{j|\xi^{yj}\neq 0\}} \frac{\psi^y(\mathbf{v}^j_{\nu,\mu+\frac{1}{2}} + \xi^{yj}\mathbf{r}^j_{\nu,\mu+\frac{1}{2}}) - \psi^y(\mathbf{v}^j_{\nu,\mu+\frac{1}{2}})}{\xi^{yj}} \boldsymbol{\ell}^{yj}_{\nu,\mu+\frac{1}{2}}, \quad \xi^{yj} = \left\langle \boldsymbol{\ell}^{yj}_{\nu,\mu+\frac{1}{2}}, \Delta\mathbf{v}_{\nu,\mu+\frac{1}{2}} \right\rangle,$$

where the right and left eigensystems $\{\mathbf{r}^{xj}\}^3_{j=1}$ $\{\mathbf{r}^{yj}\}^3_{j=1}$ and $\{\boldsymbol{\ell}^{xj}\}^3_{j=1}$ $\{\boldsymbol{\ell}^{yj}\}^3_{j=1}$ are

constructed as the precise mirror images of the Roe-pathes in $\mathbf{v}$-space,

$$\mathbf{r}^{xj}_{\nu+\frac{1}{2},\mu} := [H]^{-1}_{\nu+\frac{1}{2},\mu} \widehat{\mathbf{r}}^{xj}_{\nu+\frac{1}{2},\mu}, \quad \boldsymbol{\ell}^{xj}_{\nu+\frac{1}{2},\mu} := [H]_{\nu+\frac{1}{2},\mu} \widehat{\boldsymbol{\ell}}^{xj}_{\nu+\frac{1}{2},\mu}, \qquad j = 1,2,3$$

$$\mathbf{r}^{yj}_{\nu,\mu+\frac{1}{2}} := [H]^{-1}_{\nu,\mu+\frac{1}{2}} \widehat{\mathbf{r}}^{yj}_{\nu,\mu+\frac{1}{2}}, \quad \boldsymbol{\ell}^{yj}_{\nu,\mu+\frac{1}{2}} := [H]_{\nu,\mu+\frac{1}{2}} \widehat{\boldsymbol{\ell}}^{yj}_{\nu,\mu+\frac{1}{2}}, \qquad j = 1,2,3$$

where $[H]_{\nu+\frac{1}{2},\mu}$ and $[H]_{\nu,\mu+\frac{1}{2}}$ denote the averaged symmetrizers such that

$\Delta\mathbf{u}_{\nu+\frac{1}{2},\mu} = [H]_{\nu+\frac{1}{2},\mu}\Delta\mathbf{v}_{\nu+\frac{1}{2},\mu}$ and $\Delta\mathbf{u}_{\nu,\mu+\frac{1}{2}} = [H]_{\nu,\mu+\frac{1}{2}}\Delta\mathbf{v}_{\nu,\mu+\frac{1}{2}}$.

Here we conclude our main result of two dimensional shallow water equations

in the following theorem.

Theorem 5.3.1. *Let U be a given entropy function, and (F,G) be corresponding*

entropy flux pair of the shallow water equations (5.1.1a)-(5.1.1d), which respect the

entropy inequality (5.2.3). Consider the semi-discrete approximation (5.3.1a),

$$\frac{d}{dt}\mathbf{u}_{\nu,\mu}(t) + \frac{1}{\Delta x}(\mathbf{f}^*_{\nu+\frac{1}{2},\mu} - \mathbf{f}^*_{\nu-\frac{1}{2},\mu}) + \frac{1}{\Delta y}(\mathbf{g}^*_{\nu,\mu+\frac{1}{2}} - \mathbf{g}^*_{\nu,\mu-\frac{1}{2}})$$

$$= \frac{\varsigma}{\Delta x}(\widehat{h_{\nu+\frac{1}{2},\mu}}\frac{\mathbf{d}_{\nu+1,\mu} - \mathbf{d}_{\nu,\mu}}{\Delta x} - \widehat{h_{\nu-\frac{1}{2},\mu}}\frac{\mathbf{d}_{\nu,\mu} - \mathbf{d}_{\nu-1,\mu}}{\Delta x})$$

$$+ \frac{\varsigma}{\Delta y}(\widehat{h_{\nu,\mu+\frac{1}{2}}}\frac{\mathbf{d}_{\nu,\mu+1} - \mathbf{d}_{\nu,\mu}}{\Delta x} - \widehat{h_{\nu,\mu-\frac{1}{2}}}\frac{\mathbf{d}_{\nu,\mu} - \mathbf{d}_{\nu,\mu-1}}{\Delta x}), \quad (5.3.3a)$$

Here $\mathbf{f}^*_{\nu+\frac{1}{2},\mu}$ and $\mathbf{g}^*_{\nu,\mu+\frac{1}{2}}$ are entropy-conservative numerical fluxes (5.3.1b) and (5.3.1c),

$$\mathbf{f}^*_{\nu+\frac{1}{2},\mu} = \frac{g}{2}\sum_{j=1}^{3}\frac{(h^{j+1}_{\nu+\frac{1}{2},\mu})^2 u^{j+1}_{\nu+\frac{1}{2},\mu} - (h^j_{\nu+\frac{1}{2},\mu})^2 u^j_{\nu+\frac{1}{2},\mu}}{\left\langle \boldsymbol{\ell}^{xj}_{\nu+\frac{1}{2},\mu}, \Delta \mathbf{v}_{\nu+\frac{1}{2},\mu}\right\rangle}\boldsymbol{\ell}^{xj}_{\nu+\frac{1}{2},\mu}, \quad (5.3.3b)$$

$$\mathbf{g}^*_{\nu,\mu+\frac{1}{2}} = \frac{g}{2}\sum_{j=1}^{3}\frac{(h^{j+1}_{\nu,\mu+\frac{1}{2}})^2 v^{j+1}_{\nu,\mu+\frac{1}{2}} - (h^j_{\nu,\mu+\frac{1}{2}})^2 v^j_{\nu,\mu+\frac{1}{2}}}{\left\langle \boldsymbol{\ell}^{yj}_{\nu,\mu+\frac{1}{2}}, \Delta \mathbf{v}_{\nu,\mu+\frac{1}{2}}\right\rangle}\boldsymbol{\ell}^{yj}_{\nu,\mu+\frac{1}{2}}, \quad (5.3.3c)$$

{i} The resulting difference scheme (5.3.3a)-(5.3.3c) is entropy stable with no

artificial viscosity in the sense that the following discrete entropy balance is satisfied,

$$\frac{d}{dt}\sum_{\nu,\mu} U(\mathbf{u}_{\nu,\mu}(t))\Delta x\Delta y = -\varsigma\sum_{\nu,\mu}\left[\frac{1}{\Delta x^2}\left\langle \Delta\mathbf{v}_{\nu+\frac{1}{2},\mu}, \widehat{h_{\nu+\frac{1}{2},\mu}}\frac{\Delta\mathbf{d}_{\nu+\frac{1}{2},\mu}}{\Delta\mathbf{v}_{\nu+\frac{1}{2},\mu}}\Delta\mathbf{v}_{\nu+\frac{1}{2},\mu}\right\rangle\right.$$

$$\left. +\frac{1}{\Delta y^2}\left\langle \Delta\mathbf{v}_{\nu,\mu+\frac{1}{2}}, \widehat{h_{\nu,\mu+\frac{1}{2}}}\frac{\Delta\mathbf{d}_{\nu,\mu+\frac{1}{2}}}{\Delta\mathbf{v}_{\nu,\mu+\frac{1}{2}}}\Delta\mathbf{v}_{\nu,\mu+\frac{1}{2}}\right\rangle\right]\Delta x\Delta y. \quad (5.3.4)$$

The entropy balance (5.3.4) is a discrete analogue of the entropy balance state-

ment (5.2.4).

{ii} In the specific case of the generalized entropy function $U = (gh^2 + u^2h + v^2h)/2$ being the sum of potential and kinetic energy, and the corresponding flux pair $(F, G) = \left(guh^2 + \frac{u^3h+uv^2h}{2}, gvh^2 + \frac{u^2vh+v^3h}{2}\right)$, the entropy decay (5.3.4) amounts to

the energy dissipation statement,

$$\frac{d}{dt}\sum_{\nu,\mu} U(\mathbf{u}_{\nu,\mu}(t))\Delta x \Delta y = -\varsigma \sum_{\nu,\mu}\left\{ \widehat{h_{\nu+\frac{1}{2},\mu}}\left[\left(\frac{\Delta u_{\nu+\frac{1}{2},\mu}}{\Delta x}\right)^2 + \left(\frac{\Delta v_{\nu+\frac{1}{2},\mu}}{\Delta x}\right)^2\right]\right.$$

$$\left.+\widehat{h_{\nu,\mu+\frac{1}{2}}}\left[\left(\frac{\Delta u_{\nu,\mu+\frac{1}{2}}}{\Delta y}\right)^2 + \left(\frac{\Delta v_{\nu,\mu+\frac{1}{2}}}{\Delta y}\right)^2\right]\right\}\Delta x \Delta y. \quad (5.3.5)$$

Proof. We multiply (5.3.3a) by $[U_{\mathbf{u}}]^\top_{\nu,\mu} = \mathbf{v}^\top_{\nu,\mu}$, then sum up all spatial cells to get the balance of the total entropy,

$$\frac{d}{dt}\sum_{\nu,\mu} U_{\nu,\mu}(t)\Delta x \Delta y + \sum_{\nu,\mu}\left\langle \mathbf{v}_{\nu,\mu}, \mathbf{f}^*_{\nu+\frac{1}{2},\mu} - \mathbf{f}^*_{\nu-\frac{1}{2},\mu}\right\rangle \Delta y + \sum_{\nu,\mu}\left\langle \mathbf{v}_{\nu,\mu}, \mathbf{g}^*_{\nu,\mu+\frac{1}{2}} - \mathbf{g}^*_{\nu,\mu-\frac{1}{2}}\right\rangle \Delta x$$

$$= \varsigma \sum_{\nu,\mu}\left\langle \mathbf{v}_{\nu,\mu}, \widehat{h_{\nu+\frac{1}{2},\mu}}\Delta \mathbf{d}_{\nu+\frac{1}{2},\mu} - \widehat{h_{\nu-\frac{1}{2},\mu}}\Delta \mathbf{d}_{\nu-\frac{1}{2},\mu}\right\rangle \frac{\Delta y}{\Delta x}$$

$$+ \varsigma \sum_{\nu,\mu}\left\langle \mathbf{v}_{\nu,\mu}, \widehat{h_{\nu,\mu+\frac{1}{2}}}\Delta \mathbf{d}_{\nu,\mu+\frac{1}{2}} - \widehat{h_{\nu,\mu-\frac{1}{2}}}\Delta \mathbf{d}_{\nu,\mu-\frac{1}{2}}\right\rangle \frac{\Delta x}{\Delta y} \quad (5.3.6)$$

Since numerical fluxes $\mathbf{f}^*_{\nu+\frac{1}{2},\mu}$ and $\mathbf{g}^*_{\nu,\mu+\frac{1}{2}}$ are chosen as the entropy conservative fluxes in x and y direction respectively, they must satisfy the entropy conservative requirement in (2.2.7),

$$\left\langle \Delta\mathbf{v}_{\nu+\frac{1}{2},\mu}, \mathbf{f}^*_{\nu+\frac{1}{2},\mu}\right\rangle = \Delta\psi^x_{\nu+\frac{1}{2},\mu}, \quad \left\langle \Delta\mathbf{v}_{\nu,\mu+\frac{1}{2}}, \mathbf{g}^*_{\nu,\mu+\frac{1}{2}}\right\rangle = \Delta\psi^y_{\nu,\mu+\frac{1}{2}}.$$

A straightforward manipulation on the above requirements yields the perfect conservative differences,

$$\left\langle \mathbf{v}_{\nu,\mu}, \mathbf{f}^*_{\nu+\frac{1}{2},\mu} - \mathbf{f}^*_{\nu-\frac{1}{2},\mu}\right\rangle = F_{\nu+\frac{1}{2},\mu} - F_{\nu-\frac{1}{2},\mu}, \quad (5.3.7a)$$

$$\left\langle \mathbf{v}_{\nu,\mu}, \mathbf{g}^*_{\nu,\mu+\frac{1}{2}} - \mathbf{g}^*_{\nu,\mu-\frac{1}{2}}\right\rangle = G_{\nu,\mu+\frac{1}{2}} - G_{\nu,\mu-\frac{1}{2}}, \quad (5.3.7b)$$

where the discrete entropy fluxes are given by

$$2F_{\nu+\frac{1}{2},\mu} = \left\langle (\mathbf{v}_{\nu,\mu} + \mathbf{v}_{\nu+1,\mu}), \mathbf{f}^*_{\nu+\frac{1}{2},\mu}\right\rangle - (\psi(\mathbf{v}_{\nu,\mu})) + \psi(\mathbf{v}_{\nu+1,\mu})$$

$$2G_{\nu,\mu+\frac{1}{2}} = \left\langle (\mathbf{v}_{\nu,\mu} + \mathbf{v}_{\nu,\mu+1}), \mathbf{g}^*_{\nu,\mu+\frac{1}{2}}\right\rangle - (\psi(\mathbf{v}_{\nu,\mu})) + \psi(\mathbf{v}_{\nu,\mu+1}).$$

On the other hand, summation by parts on the RHS of (5.3.6) yields

$$\varsigma \sum_{\nu,\mu} \left\langle \mathbf{v}_{\nu,\mu}, \widehat{h_{\nu+\frac{1}{2},\mu}}\Delta\mathbf{d}_{\nu+\frac{1}{2},\mu} - \widehat{h_{\nu-\frac{1}{2},\mu}}\Delta\mathbf{d}_{\nu-\frac{1}{2},\mu}\right\rangle \frac{\Delta y}{\Delta x}$$

$$= -\varsigma \sum_{\nu,\mu}\left\langle \Delta\mathbf{v}_{\nu+\frac{1}{2},\mu}, \widehat{h_{\nu+\frac{1}{2},\mu}}\Delta\mathbf{d}_{\nu+\frac{1}{2},\mu}\right\rangle \frac{\Delta y}{\Delta x}$$

$$= -\varsigma \sum_{\nu,\mu}\left\langle \Delta\mathbf{v}_{\nu+\frac{1}{2},\mu}, \widehat{h_{\nu+\frac{1}{2},\mu}}\frac{\Delta\mathbf{d}_{\nu+\frac{1}{2},\mu}}{\Delta\mathbf{v}_{\nu+\frac{1}{2},\mu}}\Delta\mathbf{v}_{\nu+\frac{1}{2},\mu}\right\rangle \frac{\Delta y}{\Delta x}$$

$$(5.3.8a)$$

$$\varsigma \sum_{\nu,\mu} \left\langle \mathbf{v}_{\nu,\mu}, \widehat{h_{\nu,\mu+\frac{1}{2}}}\Delta\mathbf{d}_{\nu,\mu+\frac{1}{2}} - \widehat{h_{\nu,\mu-\frac{1}{2}}}\Delta\mathbf{d}_{\nu,\mu-\frac{1}{2}}\right\rangle \frac{\Delta x}{\Delta y}$$

$$= -\varsigma \sum_{\nu,\mu}\left\langle \Delta\mathbf{v}_{\nu,\mu+\frac{1}{2}}, \widehat{h_{\nu,\mu+\frac{1}{2}}}\Delta\mathbf{d}_{\nu,\mu+\frac{1}{2}}\right\rangle \frac{\Delta x}{\Delta y}$$

$$= -\varsigma \sum_{\nu,\mu}\left\langle \Delta\mathbf{v}_{\nu,\mu+\frac{1}{2}}, \widehat{h_{\nu,\mu+\frac{1}{2}}}\frac{\Delta\mathbf{d}_{\nu,\mu+\frac{1}{2}}}{\Delta\mathbf{v}_{\nu,\mu+\frac{1}{2}}}\Delta\mathbf{v}_{\nu+\frac{1}{2},\mu}\right\rangle \frac{\Delta x}{\Delta y}$$

$$(5.3.8b)$$

By (5.3.8a)-(5.3.8b), and (5.3.7a)-(5.3.7b), the semi-discrete entropy balance of two dimensional shallow water equations (5.3.6) amounts to

$$\frac{d}{dt}\sum_{\nu,\mu}U_{\nu,\mu}(t)\Delta x\Delta y = -\varsigma\sum_{\nu,\mu}\left[\frac{1}{\Delta x^2}\left\langle \Delta\mathbf{v}_{\nu+\frac{1}{2},\mu}, \widehat{h_{\nu+\frac{1}{2},\mu}}\frac{\Delta\mathbf{d}_{\nu+\frac{1}{2},\mu}}{\Delta\mathbf{v}_{\nu+\frac{1}{2},\mu}}\Delta\mathbf{v}_{\nu+\frac{1}{2},\mu}\right\rangle\right.$$

$$\left.+\frac{1}{\Delta y^2}\left\langle \Delta\mathbf{v}_{\nu,\mu+\frac{1}{2}}, \widehat{h_{\nu,\mu+\frac{1}{2}}}\frac{\Delta\mathbf{d}_{\nu,\mu+\frac{1}{2}}}{\Delta\mathbf{v}_{\nu,\mu+\frac{1}{2}}}\Delta\mathbf{v}_{\nu+\frac{1}{2},\mu}\right\rangle\right]\Delta x\Delta y. \quad (5.3.9)$$

Here,

$$\frac{\Delta\mathbf{d}_{\nu+\frac{1}{2},\mu}}{\Delta\mathbf{v}_{\nu+\frac{1}{2},\mu}} = \int_{\xi=-\frac{1}{2}}^{\frac{1}{2}}\mathbf{d_v}(\mathbf{v}_{\nu+\frac{1}{2},\mu}(\xi))\,d\xi, \quad \mathbf{v}_{\nu+\frac{1}{2},\mu}(\xi) := \frac{1}{2}(\mathbf{v}_{\nu,\mu}+\mathbf{v}_{\nu+1,\mu})+\xi\Delta\mathbf{v}_{\nu+\frac{1}{2},\mu}$$

$$\frac{\Delta\mathbf{d}_{\nu,\mu+\frac{1}{2}}}{\Delta\mathbf{v}_{\nu,\mu+\frac{1}{2}}} = \int_{\xi=-\frac{1}{2}}^{\frac{1}{2}}\mathbf{d_v}(\mathbf{v}_{\nu,\mu+\frac{1}{2}}(\xi))\,d\xi, \quad \mathbf{v}_{\nu,\mu+\frac{1}{2}}(\xi) := \frac{1}{2}(\mathbf{v}_{\nu,\mu}+\mathbf{v}_{\nu,\mu+1})+\xi\Delta\mathbf{v}_{\nu,\mu+\frac{1}{2}}$$

By admissibility of the viscous flux, $\mathbf{d_v} \geq 0$, the RHS of (5.3.3a) guarantees the total entropy dissipation in the sense of satisfying (5.3.9).

80

When the sum of potential and kinetic energy serves as a generalized entropy function, $U = (gh^2 + u^2 h + v^2 h)/2$, the corresponding entropy fluxes and entropy variables are found in (5.2.6)and (5.2.7). We then explicitly compute the RHS of (5.3.9) to obtain the following,

$$
\begin{aligned}
-\varsigma \sum_{\nu,\mu} & \left[\frac{1}{\Delta x^2} \left\langle \Delta \mathbf{v}_{\nu+\frac{1}{2},\mu}, \widehat{h}_{\nu+\frac{1}{2},\mu} \frac{\Delta \mathbf{d}_{\nu+\frac{1}{2},\mu}}{\Delta \mathbf{v}_{\nu+\frac{1}{2},\mu}} \Delta \mathbf{v}_{\nu+\frac{1}{2},\mu} \right\rangle \right. \\
& \left. + \frac{1}{\Delta y^2} \left\langle \Delta \mathbf{v}_{\nu,\mu+\frac{1}{2}}, \widehat{h}_{\nu,\mu+\frac{1}{2}} \frac{\Delta \mathbf{d}_{\nu,\mu+\frac{1}{2}}}{\Delta \mathbf{v}_{\nu,\mu+\frac{1}{2}}} \Delta \mathbf{v}_{\nu+\frac{1}{2},\mu} \right\rangle \right] \Delta x \Delta y \\
= -\varsigma \sum_{\nu,\mu} & \left[\frac{1}{\Delta x^2} \widehat{h}_{\nu+\frac{1}{2},\mu} \left(\Delta u_{\nu+\frac{1}{2},\mu}^2 + \Delta v_{\nu+\frac{1}{2},\mu}^2 \right) \right. \\
& \left. + \frac{1}{\Delta y^2} \widehat{h}_{\nu,\mu+\frac{1}{2}} \left(\Delta u_{\nu,\mu+\frac{1}{2}}^2 + \Delta v_{\nu,\mu+\frac{1}{2}}^2 \right) \right] \Delta x \Delta y
\end{aligned}
$$

The semi-discrete entropy/energy balance statement (5.3.5) now follows.□

Remark 5.3.2. It should be pointed out that even though the semi-discrete scheme (5.3.3a)-(5.3.3c) conserves the sum of total potential and kinetic energy, the potential enstrophy $\frac{1}{2}\overline{\eta^2/h}$ may increase considerably, especially for the flow over steep topography, due to spurious energy cascade into smaller scales, consult [AL77, AL81]. Here, η is the absolute vorticity expressed as the sum of the relative vorticity $\frac{\partial v}{\partial x} - \frac{\partial u}{\partial y}$ and the Coriolis parameter at that latitude, and the overbar $\overline{(\cdot)}$ denotes a horizontal average. After time integrations of sufficient length, a significant amount of energy exists in the smallest resolvable scales, where truncation error is large. Under such circumstances, the smoothness of numerical solutions highly depends on the grid size.

As shown in [Ara97], a finite-difference Jacobian was designed to maintain important integral constraints on the continuous Jacobian $J(a, b) := a_x b_y - a_y b_x$.

Specifically, the absolute potential vorticity η/h and kinetic energy are conserved in the discretization. When this discrete Jacobian is applied to the vorticity equation governing two dimensional incompressible inviscid flow, the total energy and the absolute potential enstrophy in the discrete system shall be conserved. These potential enstrophy and energy conserving schemes for the shallow water equations make more sense for the problems in atmospheric sciences, in which flow over and near mountains (steep topography) is governed during advective processes by the conservation of absolute potential vorticity. See more details of these schemes in [AL81].

In this dissertation, we are interested in extension of the entropy stable schemes without artificial numerical viscosity in two dimensional problems. As I will show you in the next section, we still obtain satisfying numerical solutions of two dimensional shallow water equations with the choice of not very complicated topography and relatively fine computational mesh in the absence of enstrophy-conserving mechanism. It remains to be an open problem that our entropy/energy stable discretization can be incorporated with the enstrophy-conserving schemes.

5.3.2 Boundary condition

The numerical treatment of boundaries is intended to be as physically relevant as possible. We describe two basic types of boundary conditions that are applicable to the two dimensional shallow water problems: the first type simulates a boundary at infinity or a transmissive boundary; the second type applies in the presence of

solid fixed walls.

5.3.2.1 Transmissive boundaries

These are cases in which boundaries are supposed to be transparent in the sense that waves are allowed to pass through. The inflow and outflow conditions need to be described, hence the method of characteristics in two dimension follows. The local value of the Froude number $Fr := V/\sqrt{gH}$ determines the flow regime and, accordingly, the number of boundary conditions to apply. Here V and H denote the characteristic velocity and length scales of the phenomenon, respectively. For subcritical flow, two external boundary conditions are required at inflow boundaries, whereas only one boundary condition is required at outflow boundaries. Two dimensional supercritical flow requires three inflow boundary conditions and no boundary condition at outflow boundaries where the flow is only influenced by the information coming from the interior nodes.

5.3.2.2 Reflective boundaries

This is a particular case in which the flow is confined in a fixed field by the solid walls. We simply impose the reflective boundary conditions. Since our testing problems in next section are concern with the flow in a square basin, we consider the solid boundaries along x and y-direction with the computational domain in the lower-left corner without losing generality, as shown in Figure 5.3.2.2. By the three-point stencil used in our semi-discrete scheme, we try to impose the value of one

computational grid point added outside boundary.
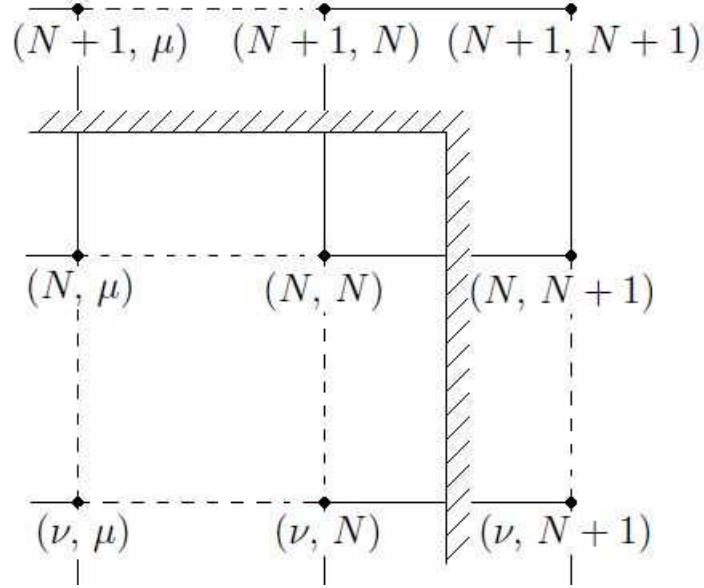
Figure 5.3.1: Right-hand boundary

The reflection is incorporated by changing the sign of the normal component of the velocity, while the water depth is unaltered. The values at all the $(\nu,\, N+1)$ points on the right-hand side of the wall are replaced by the values at interior $(\nu,\, N)$ points and sign of the normal velocity component u is switched,

$$h_{\nu,\, N+1} = h_{\nu,\, N}, \quad u_{\nu,\, N+1} = -u_{\nu,\, N}, \quad v_{\nu,\, N+1} = v_{\nu,\, N};$$

the values at all the $(N+1,\, \mu)$ points on the top of the wall are replaced by the values at interior $(N,\, \mu)$ points and sign of the normal velocity component v is switched

$$h_{N+1,\, \mu} = h_{N,\, \mu}, \quad u_{N+1,\, \mu} = u_{N,\, \mu}, \quad v_{N+1,\, \mu} = -v_{N,\, \mu};$$

the values at all the $(N+1,\, N+1)$ point in the upper-right corner are given by

$$h_{\nu+1,\, N+1} = h_{\nu,\, \mu}, \quad u_{\nu+1,\, N+1} = -u_{\nu,\, \mu}, \quad v_{\nu+1,\, N+1} = -v_{\nu,\, \mu}.$$

5.3.3 Time discretization

Similar to the time discretizations of the Burgers equation and one dimensional Navier-Stokes equations, we integrate the entropy stable scheme (5.3.3a)-(5.3.3c) with the explicit three-stage Runge-Kutta method (3.2.1) by its high-order accuracy, large stability region and simplicity. Consult [GST01] for more detail of its strong stability-preserving property.

$$
\begin{cases}
\mathbf{u}^{(1)} &= \mathbf{u}^n + \Delta t L(\mathbf{u}^n) \\[2mm]
\mathbf{u}^{(2)} &= \dfrac{3}{4}\mathbf{u}^n + \dfrac{1}{4}\mathbf{u}^{(1)} + \dfrac{1}{4}\Delta t L(\mathbf{u}^{(1)}) \\[2mm]
\mathbf{u}^{n+1} &= \dfrac{1}{3}\mathbf{u}^n + \dfrac{2}{3}\mathbf{u}^{(2)} + \dfrac{2}{3}\Delta t L(\mathbf{u}^{(2)})
\end{cases}
$$

where

$$
\begin{aligned}
[L(\mathbf{u})]_{\nu,\mu} = &-\frac{1}{\Delta x}(\mathbf{f}_{\nu+\frac{1}{2},\mu} - \mathbf{f}_{\nu-\frac{1}{2},\mu}) - \frac{1}{\Delta y}(\mathbf{g}_{\nu,\mu+\frac{1}{2}} - \mathbf{g}_{\nu,\mu-\frac{1}{2}}) \\
&+ \frac{\varsigma}{\Delta x}(\widehat{h_{\nu+\frac{1}{2},\mu}}\frac{\mathbf{d}_{\nu+1,\mu} - \mathbf{d}_{\nu,\mu}}{\Delta x} - \widehat{h_{\nu-\frac{1}{2},\mu}}\frac{\mathbf{d}_{\nu,\mu} - \mathbf{d}_{\nu-1,\mu}}{\Delta x}) \\
&+ \frac{\varsigma}{\Delta y}(\widehat{h_{\nu,\mu+\frac{1}{2}}}\frac{\mathbf{d}_{\nu,\mu+1} - \mathbf{d}_{\nu,\mu}}{\Delta x} - \widehat{h_{\nu,\mu-\frac{1}{2}}}\frac{\mathbf{d}_{\nu,\mu} - \mathbf{d}_{\nu,\mu-1}}{\Delta x}). \quad (5.3.10a)
\end{aligned}
$$

5.4 Numerical experiments

We test our entropy-stable schemes with the two dimensional frictionless partial-dam-break problem originally studied by Fennema and Chaudhry in [FC90]. It imposes computational difficulties due to the discontinuous initial conditions. It also involves other computational issues like boundary treatments and positive-water-depth preserving solver.

As shown in Figure 5.4, the simplified geometry of the problem consists of a
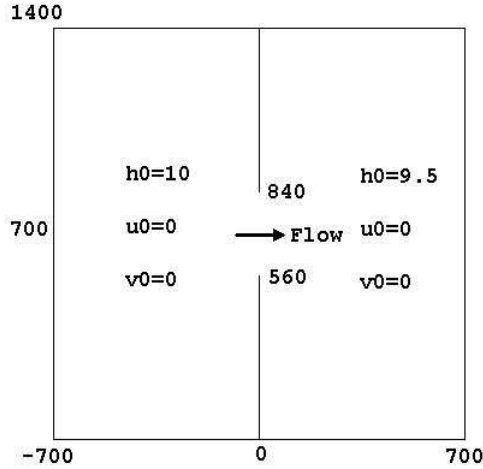
Figure 5.4.1: Geometry configuration and initial setting of 2D Partial-Dam-Break problem

$1400 \times 1400 \, m^2$ basin with a idealized dam in the middle. Water is confined by the fixed, solid, frictionless walls in this square basin. To prevent any damping by the source terms, a frictionless, horizontal bottom is used. All walls are assumed to be reflective. The initial water level of the dam is $10 \, m$ and the tail water is $9.5 \, m$ high. The central part of the dam is assumed to fail instantaneously or the gate in the middle of the dam is opened instantly. Water is released into the downstream side through a breach $280 \, m$ wide, located between $y = 560$ and $y = 840$, forming a wave that propagates while spreading laterally. A negative wave propagates upstream at the same time. For simplicity, the Coriolis force is ignored in the computation. The acceleration due to gravity is taken to be $9.8 \, m/s^2$. Although there is no analytical reference solution for this test problem, but other numerical results of similar problems are available in [FC90, CK04].

All the numerical tests are done by a C++ program run on P4 3.0 GHz

computer. In the following figures, we display the numerical solutions for the fully discrete scheme (5.3.10a)-(5.3.10a) with the numerical fluxes (5.3.3b)-(5.3.3c). The sum of potential and kinetic energy serves as the generalized entropy function in the design of our numerical schemes,

$$U(\mathbf{u}) = \frac{gh^2 + u^2h + v^2h}{2}.$$

Uniform space and time grid sizes, $\Delta x = \Delta y$ and Δt are used. The computational model is run for up to $50\,s$ after the dam broke when the water waves haven't reached the boundaries. Both inviscid and viscous cases are explored. For the viscous cases, the eddy viscosity is taken to be $10\,m^2 \cdot s^{-1}$. We use different spatial resolutions for the same problem, and adjust time step according to the CFL condition. We group our results into two sets.

1. Inviscid shallow water equations. The first two sets of six figures are devoted to the two dimensional shallow water equations (5.1.1a) with zero eddy viscosity $\varsigma = 0$.

Firstly, we use a 50×50 cell square grid with $\Delta x = \Delta y = 28m$. Figure 5.4.2(a) and 5.4.2(b) depict the perspective plots of water surface profiles at $t = 25s$ and $t = 50s$ respectively. Figure 5.4.2(c) and 5.4.2(d) depict the contour lines of water surface elevation at the same moments. The velocity field at time $t = 50\,s$ is shown in Figure 5.4.2(e). In the perspective plots Figure 5.4.2(a) and 5.4.2(b), remnants of the dam are represented by jumps near the middle of the plot. The vertical scale is exaggerated with respect to the horizontal scales. In the velocity field Figure 5.4.2(e), the velocity is indicated by an arrow with the magnitude represented by

the length of the arrow.

We see that the numerical solutions of the water depth in Figures 5.4.2(a) and 5.4.2(b) successfully simulate both the circular shock water wave propagations and the vortices formed on the both sides of the breach. The undershoots are also developed near sharp corners of the remanent dam. These steep degressions in the water surface are noticeable downstream of the breach at $t = 50\,s$. Similar numerical tests were done in [CK04] by the second-order central-upwind schemes, which were originally proposed in [ST92]. Due to the absence of any dissipative mechanism in the numerical schemes, dispersive errors of the numerical schemes, in the form of spurious oscillations in the mesh scale, are noticeable near the breach. Figure 5.4.2(f) demonstrates the conservation of the total entropy.

We display the numerical solutions of the same problem in the refined spatial mesh, taking $\Delta x = \Delta y = 7m$. Following the same pattern as Figure 5.4.2, Figure 5.4.3 presents the perspective plots and contour plots of water surface, velocity fields, and total entropy conservation. The profiles of the water elevation in Figure 5.4.3(a) and 5.4.3(b) demonstrate smoother numerical solutions due to the decrease of the grid size, while the spurious oscillations in the mesh scale are still detectable near the breach because of the entropy-conservative shallow water solver with the increase of the total enstrophy.

2 Viscous shallow water equations. We solve the shallow water equations (5.1.1a) with the eddy viscosity $\varsigma = 10m^2 \cdot s^{-1}$. The results are summarized in the next three sets of figures Figure 5.4.4, Figure 5.4.5 and Figure 5.4.6. We follow

the same pattern of plotting the perspective plots and contour plots of water surface, velocity fields, and total entropy. As before, both the coarse mesh (50×50) and the fine mesh $(100 \times 100)/(200 \times 200)$ are tested.

As shown in Figure 5.4.4(a) and 5.4.4(b), the presence of the eddy viscosity causes the oscillations to be dramatically reduced around the breach. In addition to eliminating the wiggles, the eddy viscosity terms also single out the undershoot near sharp corners of the remanents of dam without damping it, see Figure 5.4.4(c) and 5.4.4(d). The plot of the total entropy/energy in Figure 5.4.4(f) demonstrates the total entropy/energy dissipation due to the presence of the eddy viscosity.

When the mesh is refined, Figure 5.4.5 shows that the solution is better smoothed due to the decrease in the grid size. The amplitude of those wiggles near the breach are significantly reduced though they are still detectable. Further refinement of the mesh from (100×100) to (200×200) generates very smooth solutions of the water depth h in Figure 5.4.6(a) and 5.4.6(b), when the oscillations are limited in the very small mesh scale.
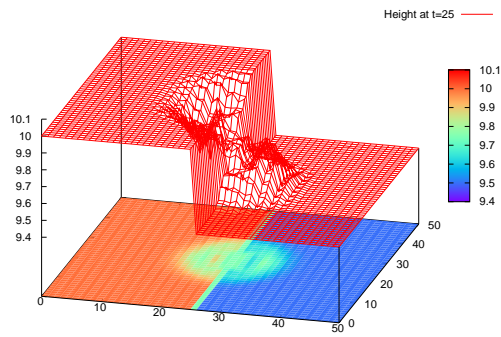
(a) Water depth at t=25
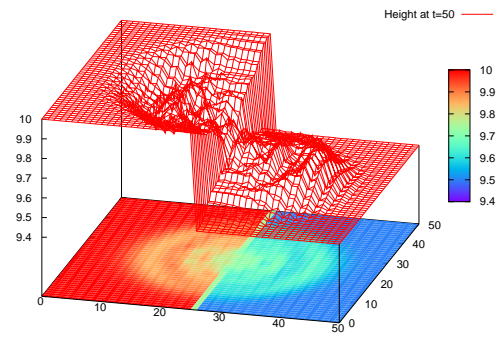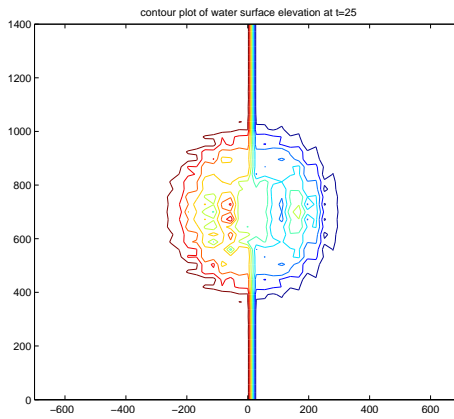
(b) Water depth at t=50

(c) Contour plot of water depth at t=25
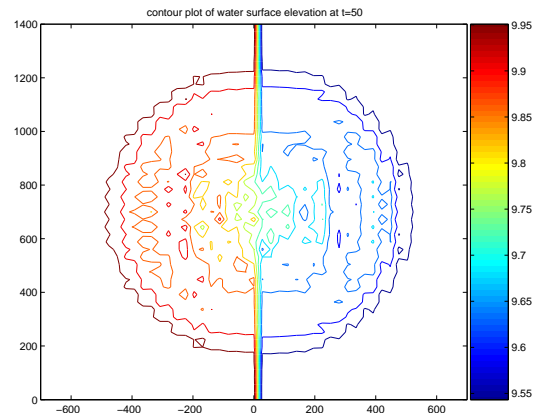
(d) Contour plot of water depth at t=50
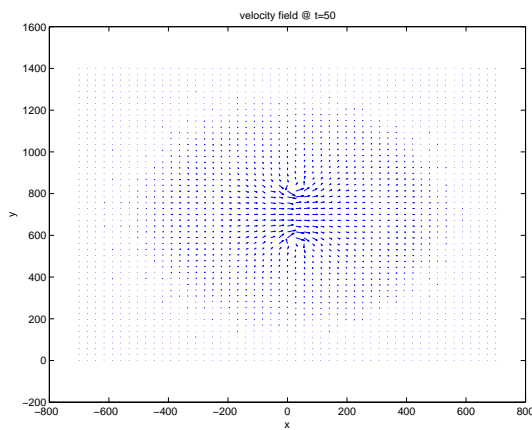
(e) Velocity field at t=50
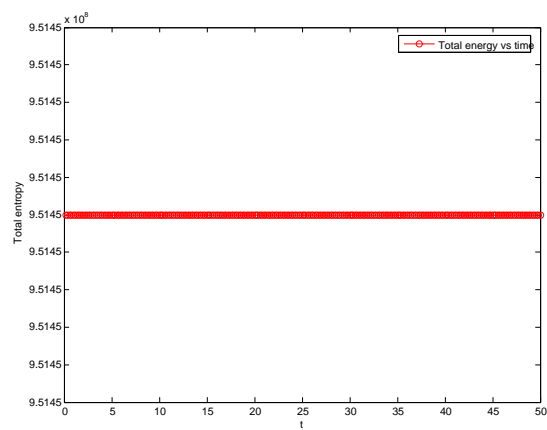
(f) Total energy v.s. time

Figure 5.4.2: Shallow water equations, $\varsigma = 0$, Dam-Break, $1400 \times 1400 \, m^2$ basin, reflective-slip boundary, $\Delta x = \Delta y = 28 \, m$, $\Delta t = 0.2 \, s$
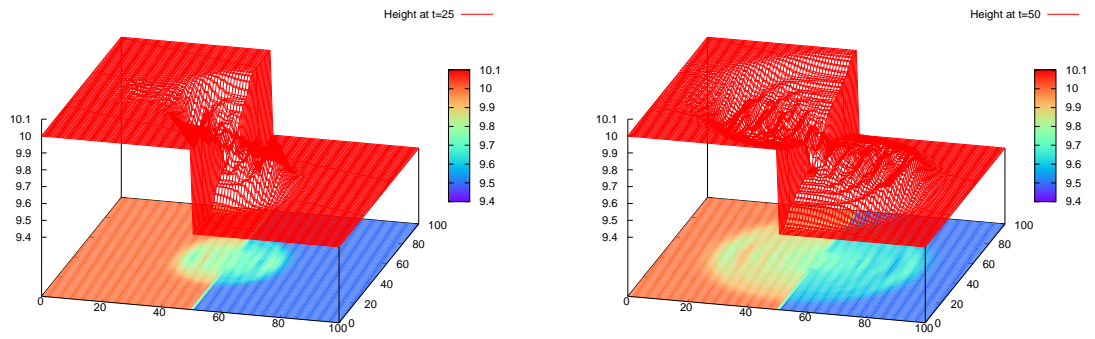
(a) Water depth at t=25
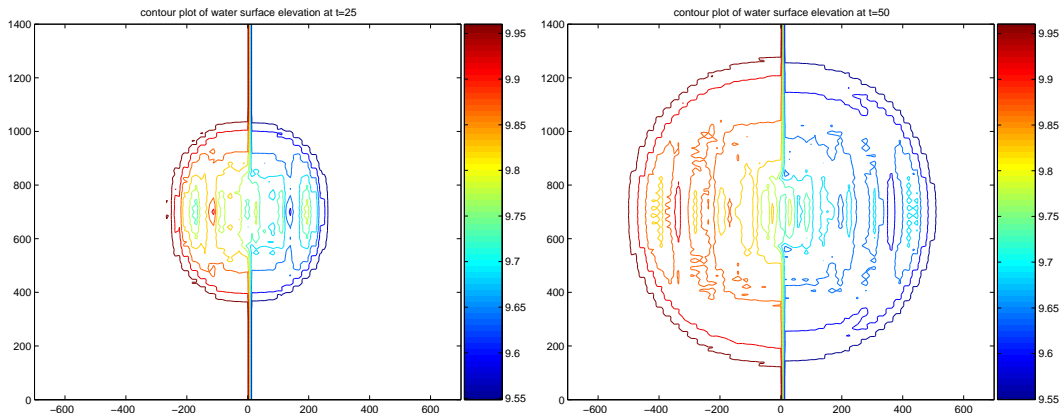
(b) Water depth at t=50

(c) Contour plot of water depth at t=25

(d) Contour plot of water depth at t=50
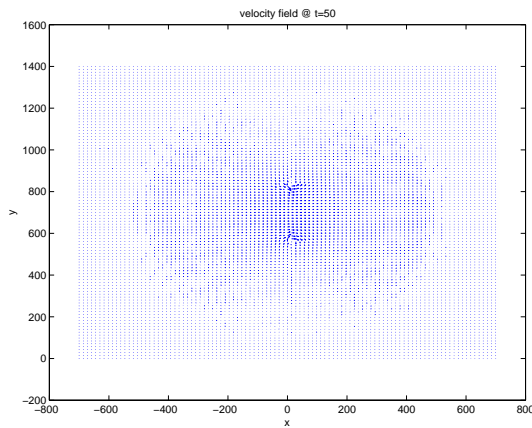
(e) Velocity field at t=50
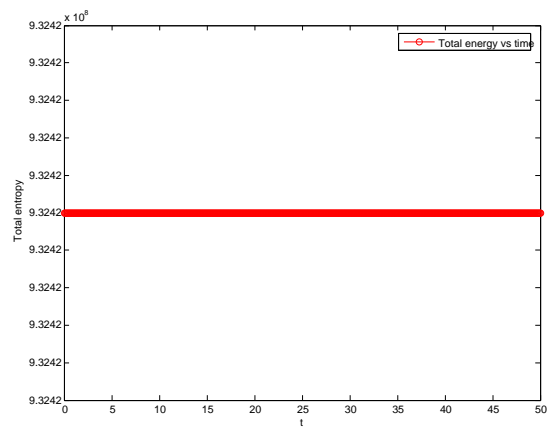
(f) Total energy v.s. time

Figure 5.4.3: Shallow water equations, $\varsigma = 0$, Dam-Break, $1400 \times 1400\,m^2$ basin, reflective-slip boundary, $\Delta x = \Delta y = 14\,m$, $\Delta t = 0.01\,s$
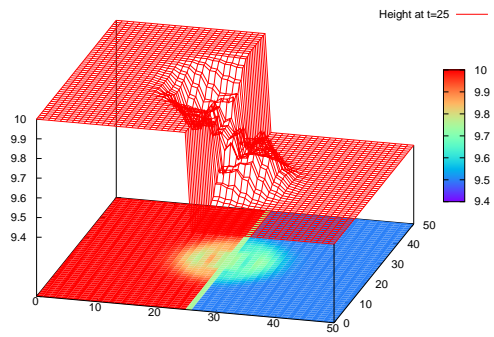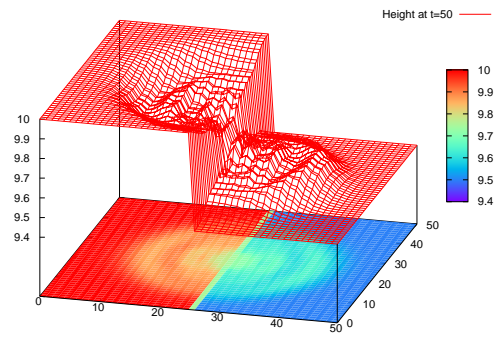
(a) Water depth at t=25
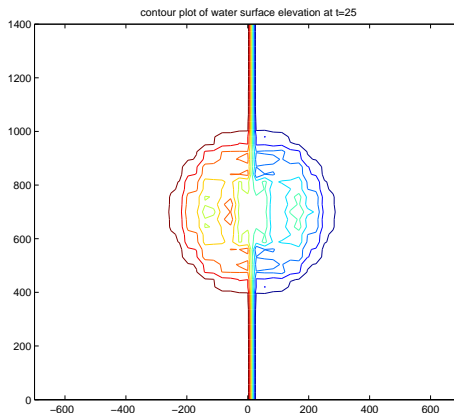
(b) Water depth at t=50

(c) Contour plot of water depth at t=25
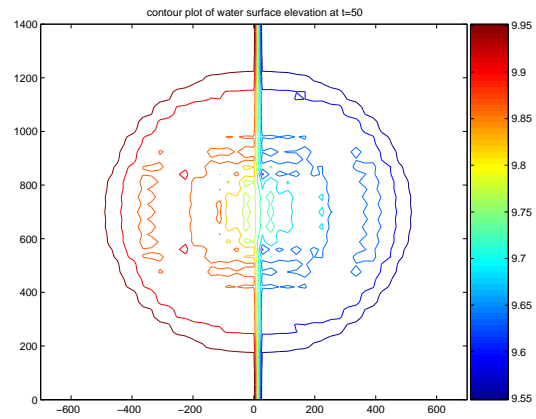
(d) Contour plot of water depth at t=50
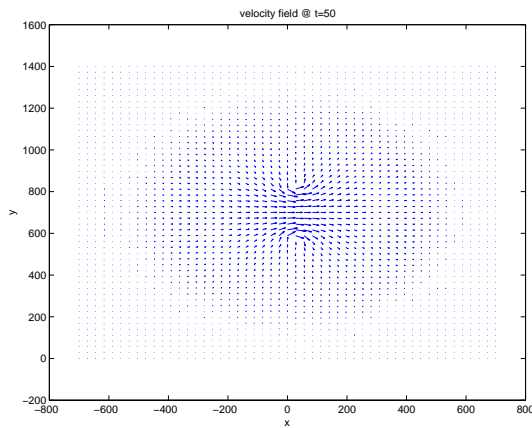
(e) Velocity field at t=50
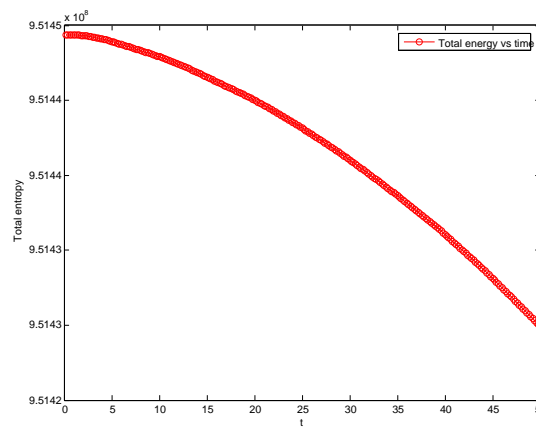
(f) Total energy v.s. time

Figure 5.4.4: Shallow water equations, $\varsigma = 10\,m^2 \cdot s^{-1}$, Dam-Break, $1400 \times 1400\,m^2$ basin, reflective-slip boundary, $\Delta x = \Delta y = 28\,m$, $\Delta t = 0.2\,s$
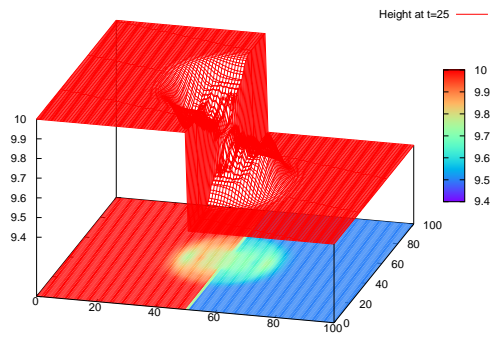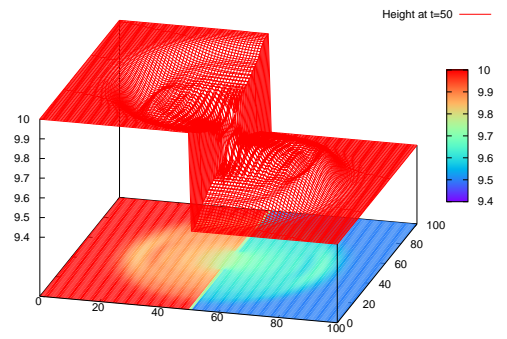
(a) Water depth at t=25
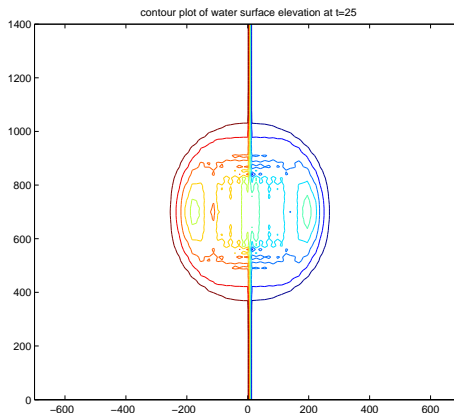
(b) Water depth at t=50

(c) Contour plot of water depth at t=25
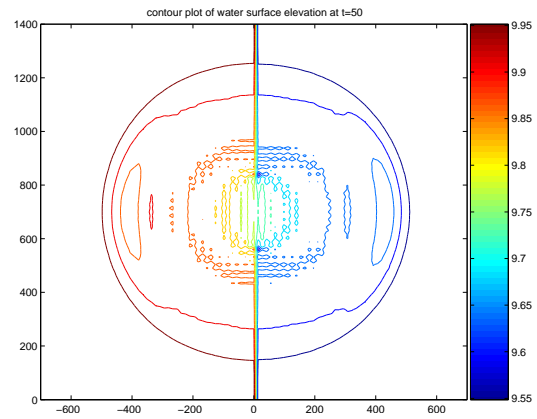
(d) Contour plot of water depth at t=50
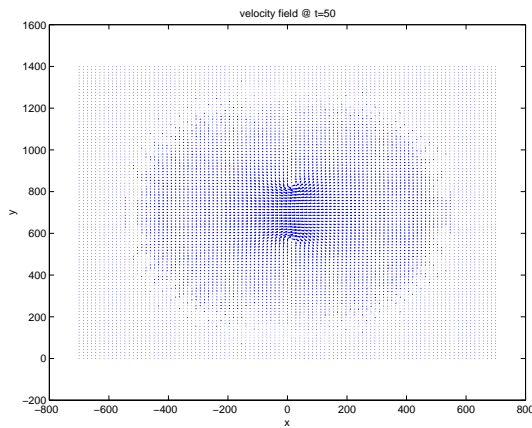
(e) Velocity field at t=50
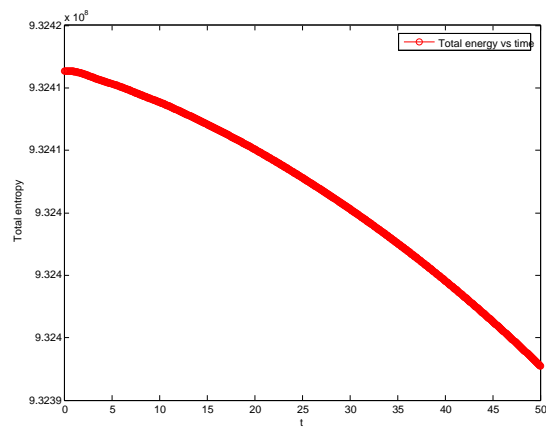
(f) Total energy v.s. time

Figure 5.4.5: Shallow water equations, $\varsigma = 10 \, m^2 \cdot s^{-1}$, Dam-Break, $1400 \times 1400 \, m^2$ basin, reflective-slip boundary, $\Delta x = \Delta y = 14 \, m$, $\Delta t = 0.01 \, s$
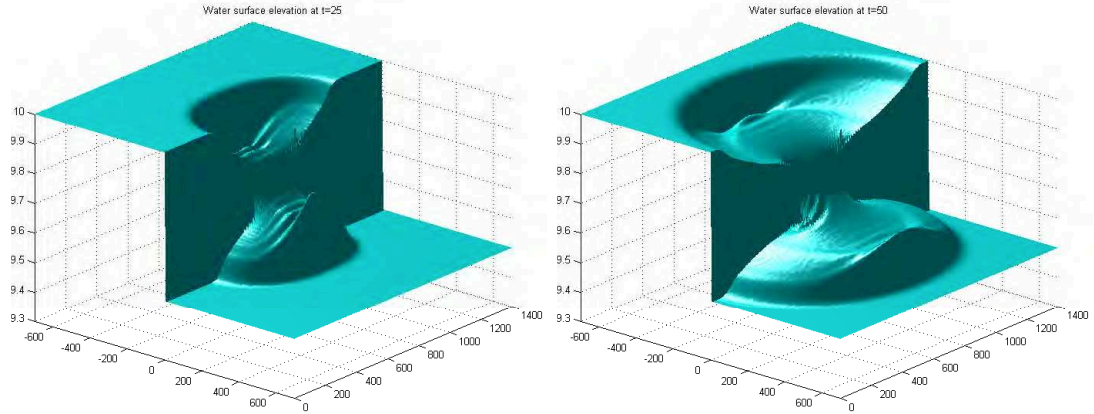
(a) Water depth at t=25
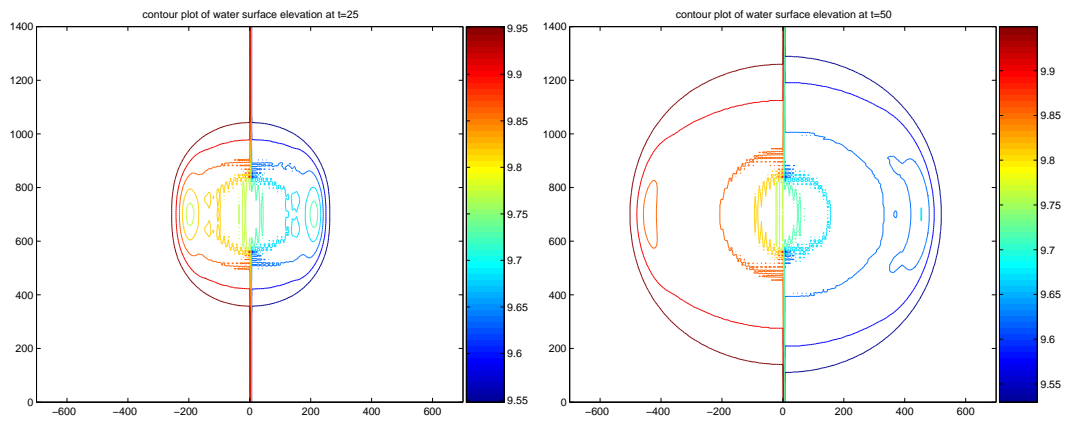
(b) Water depth at t=50

(c) Contour plot of water depth at t=25

(d) Contour plot of water depth at t=50
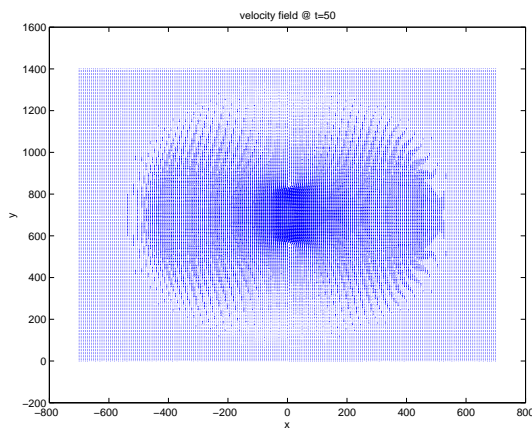
(e) Velocity field at t=50
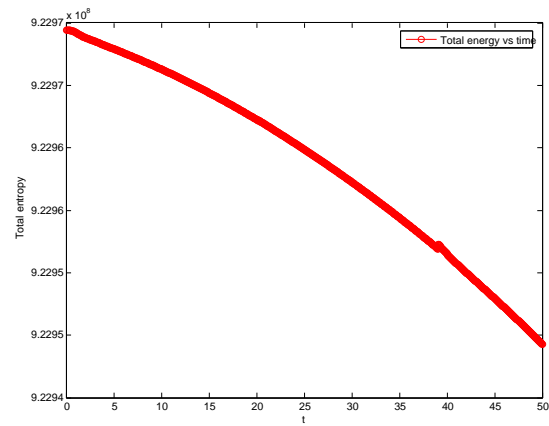
(f) Total energy v.s. time

Figure 5.4.6: Shallow water equations, $\varsigma = 10\,m^2 \cdot s^{-1}$, Dam-Break, $1400 \times 1400\,m^2$ basin, reflective-slip boundary, $\Delta x = \Delta y = 7\,m$, $\Delta t = 0.002\,s$

Bibliography

[AL77]   Akio Arakawa and Vivian R. Lamb. Computational design of the basic
          dynamical process of the ucla general circulation model. *Meth. Comput.
          Phys.*, 17:173–265, 1977.

[AL81]   Akio Arakawa and Vivian R. Lamb. A potential enstrophy and energy
          conserving scheme for the shallow water equations. *Mont. Weat. Rev.*,
          109:18–36, 1981.

[Ara97]   Akio Arakawa. Computational design for long-term numerical integra-
          tion of the equations of fluid motion: two-dimensional incompressible
          flow. I [J. Comput. Phys. **1** (1966), no. 1, 119–143]. *J. Comput. Phys.*,
          135(2):101–114, 1997. With an introduction by Douglas K. Lilly, Com-
          memoration of the 30th anniversary {of J. Comput. Phys.}.

[Bur48]   J. M. Burgers. A mathematical model illustrating the theory of tur-
          bulence. In *Advances in Applied Mechanics*, pages 171–199. Academic
          Press Inc., New York, N. Y., 1948. edited by Richard von Mises and
          Theodore von Kármán,.

[CK04]   Alina Chertock and Alexander Kurganov. On a hybrid finite-volume-
          particle method. *M2AN Math. Model. Numer. Anal.*, 38(6):1071–1091,
          2004.

[Daf00]   Constantine M. Dafermos. *Hyperbolic conservation laws in continuum
          physics*, volume 325 of *Grundlehren der Mathematischen Wissenschaften
          [Fundamental Principles of Mathematical Sciences]*. Springer-Verlag,
          Berlin, 2000.

[dGM84]   S. R. de Groot and P. Mazur. *Nonequilibrium thermodynamics.* Dover
          Publications Inc., New York, 1984. Reprint of the 1962 original.

[EO80]   Bjorn Engquist and Stanley Osher. Stable and entropy satisfying approx-
          imations for transonic flow calculations. *Math. Comp.*, 34(149):45–75,
          1980.

[FC90]   Robert J. Fennema and M. Hanif Chaudhry. Explicit methods for 2d
          transient free-surface flows. *J. Hydraul. Eng. ASCE*, 116(8):1013–1034,
          1990.

[FL71]   K. O. Friedrichs and P. D. Lax. Systems of conservation equations with
          a convex extension. *Proc. Nat. Acad. Sci. U.S.A.*, 68:1686–1688, 1971.

[Gla87]   P. Glaister. Difference schemes for the shallow water equations. Nu-
          merical Analysis Report 9/87, University of Reading, Department of
          Mathematics, 1987.

[God61]   S. K. Godunov. An interesting class of quasi-linear systems. *Dokl. Akad. Nauk SSSR*, 139:521–523, 1961.

[GR96]   Edwige Godlewski and Pierre-Arnaud Raviart. *Numerical approximation of hyperbolic systems of conservation laws*, volume 118 of *Applied Mathematical Sciences*. Springer-Verlag, New York, 1996.

[GST01]   Sigal Gottlieb, Chi-Wang Shu, and Eitan Tadmor. Strong stability-preserving high-order time discretization methods. *SIAM Rev.*, 43(1):89–112 (electronic), 2001.

[Har83]   Amiram Harten. On the symmetric form of systems of conservation laws with entropy. *J. Comput. Phys.*, 49(1):151–164, 1983.

[HFM86]   T. J. R. Hughes, L. P. Franca, and M. Mallet. A new finite element formulation for computational fluid dynamics. I. Symmetric forms of the compressible Euler and Navier-Stokes equations and the second law of thermodynamics. *Comput. Methods Appl. Mech. Engrg.*, 54(2):223–234, 1986.

[HLLM98] Ami Harten, Peter D. Lax, C. David Levermore, and William J. Morokoff. Convex entropies and hyperbolicity for general Euler equations. *SIAM J. Numer. Anal.*, 35(6):2117–2127 (electronic), 1998.

[HM86a]   Thomas J. R. Hughes and Michel Mallet. A new finite element formulation for computational fluid dynamics. III. The generalized streamline operator for multidimensional advective-diffusive systems. *Comput. Methods Appl. Mech. Engrg.*, 58(3):305–328, 1986.

[HM86b]   Thomas J. R. Hughes and Michel Mallet. A new finite element formulation for computational fluid dynamics. IV. A discontinuity-capturing operator for multidimensional advective-diffusive systems. *Comput. Methods Appl. Mech. Engrg.*, 58(3):329–336, 1986.

[HMM86]   Thomas J. R. Hughes, Michel Mallet, and Akira Mizukami. A new finite element formulation for computational fluid dynamics. II. Beyond SUPG. *Comput. Methods Appl. Mech. Engrg.*, 54(3):341–355, 1986.

[Lax73]   Peter D. Lax. *Hyperbolic systems of conservation laws and the mathematical theory of shock waves*. Society for Industrial and Applied Mathematics, Philadelphia, Pa., 1973. Conference Board of the Mathematical Sciences Regional Conference Series in Applied Mathematics, No. 11.

[Lax86]   Peter D. Lax. On dispersive difference schemes. *Phys. D*, 18(1-3):250–254, 1986. Solitons and coherent structures (Santa Barbara, Calif., 1985).

[Liu91]   Tai-Ping Liu. On the viscosity criterion for hyperbolic conservation laws. In *Viscous profiles and numerical methods for shock waves (Raleigh, NC, 1990)*, pages 105–114. SIAM, Philadelphia, PA, 1991.

[LL96]   C. David Levermore and Jian-Guo Liu. Large oscillations arising in a dispersive numerical scheme. *Phys. D*, 99(2-3):191–216, 1996.

[LLV93]   P. D. Lax, C. D. Levermore, and S. Venakides. The generation and propagation of oscillations in dispersive initial value problems and their limiting behavior. In *Important developments in soliton theory*, Springer Ser. Nonlinear Dynam., pages 205–241. Springer, Berlin, 1993.

[LMR02]   P. G. Lefloch, J. M. Mercier, and C. Rohde. Fully discrete, entropy conservative schemes of arbitrary order. *SIAM J. Numer. Anal.*, 40(5):1968–1992 (electronic), 2002.

[LR00]   Philippe G. Lefloch and Christian Rohde. High-order schemes, entropy inequalities, and nonclassical shocks. *SIAM J. Numer. Anal.*, 37(6):2023–2060 (electronic), 2000.

[LW60]   Peter Lax and Burton Wendroff. Systems of conservation laws. *Comm. Pure Appl. Math.*, 13:217–237, 1960.

[Moc80]   M. S. Mock. Systems of conservation laws of mixed type. *J. Differential Equations*, 37(1):70–88, 1980.

[Ole63]   O. A. Oleĭnik. Discontinuous solutions of non-linear differential equations. *Amer. Math. Soc. Transl. (2)*, 26:95–172, 1963.

[Roe81]   P. L. Roe. Approximate Riemann solvers, parameter vectors, and difference schemes. *J. Comput. Phys.*, 43(2):357–372, 1981.

[Sod78]   Gary A. Sod. A survey of several finite difference methods for systems of nonlinear hyperbolic conservation laws. *J. Computational Phys.*, 27(1):1–31, 1978.

[ST92]   Steven Schochet and Eitan Tadmor. The regularized Chapman-Enskog expansion for scalar conservation laws. *Arch. Rational Mech. Anal.*, 119(2):95–107, 1992.

[Tad84a] Eitan Tadmor. Numerical viscosity and the entropy condition for conservative difference schemes. *Math. Comp.*, 43(168):369–381, 1984.

[Tad84b] Eitan Tadmor. Skew-selfadjoint form for systems of conservation laws. *J. Math. Anal. Appl.*, 103(2):428–442, 1984.

[Tad86]   Eitan Tadmor. Entropy conservative finite element schemes. In T. E. Tezduyar and T.J.R. Hughes, editors, *Numerical Methods for Compressible Flows - Finite Difference Element and Volume Techniques*, pages 149–158. Proc. winter annual meeting of the ASME AMD, AMD, 1986.

[Tad87]   Eitan Tadmor. The numerical viscosity of entropy stable schemes for systems of conservation laws. I. *Math. Comp.*, 49(179):91–103, 1987.

[Tad03]   Eitan Tadmor. Entropy stability theory for difference approximations of nonlinear conservation laws and related time-dependent problems. *Acta Numer.*, 12:451–512, 2003.

[TT61]   J. G. Trulio and K. R. Trigger. Numerical solution of one dimensional hydrodynamical shock problem. *UCRL Report 6522*, 1961.

[TZ06]   Eitan Tadmor and Weigang Zhong. Entropy stable approximations of Navier-Stokes equations with no artificial numerical viscosity. *J. Hyperbolic Differ. Equ.*, 3(3):529–559, 2006.

[TZ07]   Eitan Tadmor and Weigang Zhong. Novel entropy stable schemes for 1d and 2d fluid equations. In *Hyperbolic Problems: Theory, Numerics, Applications*, page in press. Proc. of 11th. Inte. Conf. on Hype. Prob. Theo. Nume. Appl., Springer, 2007.